SOLVENT-FREE EXTRUSION EMULSIFICATION INSIDE TWIN SCREW EXTRUDER

SOLVENT-FREE EXTRUSION EMULSIFICATION INSIDE TWIN SCREW EXTRUDER

By Ali Göğer, B.Eng, M.ASc

A Thesis

Submitted to the School of Graduate Studies

in Partial Fulfillment of the Requirements

for the Degree

Doctor of Philosophy

McMaster University

DOCTOR OF PHILOSOPHY (2017) McMaster University

(Chemical Engineering) Hamilton, Ontario

TITLE: Solvent-Free Extrusion Emulsification inside Twin Screw Extruder

AUTHOR: Ali Göğer, B.Eng. (Yıldız Technical University), M.ASc. (McMaster University)

SUPERVISOR: Professor M.R. Thompson

NUMBER OF PAGES: XVII, 120

Dedicated to my lovely wife,

son and daughter…

Abstract

Solvent-free extrusion emulsification (SFEE) is new top-down technique specially suited to high viscosity polymers (100-1000 Pa.s) for producing sub-micron (100-500 nm) particles inside a twin screw extruder (TSE) without the use of hazardous solvents. SFEE has been difficult to implement in industry due to process sensitivities and a lack of mechanistic knowledge on how the polymer-water morphology must develop prior to inversion. To devise a mechanistic explanation of the critical stages of the process, an inline orifice-plate type viscometer was developed to monitor rheological changes previously witnessed in early batch studies. The general variables of study throughout the thesis included the manner by which sodium hydroxide (NaOH) can be added as well as the NaOH content necessary, resin-to-water (R/W) ratio, and surfactant content. The last study in the thesis explores the influence of matrix viscosity, which was accomplished by crosslinking the polyester. The striated lamellae morphology of the polyester-water system, critically controlling the final particle size, depended on two factors, specifically surface energy (determined by endgroup conversion and added surfactant) and matrix viscosity. Analysis of the rheological response indicated that a higher polar surface energy contribution had the greatest influence on the morphological state, demonstrating a steeper viscosity transition due to more favourable and more rapid incorporation of water within the polyester matrix. A strong correlation was repeatedly found between particle size and this viscosity transition, which has been related to the thickness of striated lamellae through a theory of lamellae coarsening (or thinning as is more relevant to the current process). The reported lamellae coarsening model in the literature, which shows the predominant effects of interfacial energy and viscosity on lamellae thickness in a mixed phase system showed excellent correspondence to the results in this thesis.

Among the variables of study in this thesis, the dissolution of the sodium hydroxide species (when added as a solid particle) and the kinetics of end-groups conversion proved to be rate-limiting phenomena to generating thinner striated lamellae. The ionic strength of the system was notably important to the viscosity change occurring in the process as

water was added for the first time and subsequently influenced the particle size produced, particularly when additional surfactant was not added and the system relied exclusively on the carboxylate endgroups present. Finally, with mounting evidence that SFEE showed significant sensitivity to the matrix viscosity, a final study examined the effectiveness of SFEE in the face of ever increasing viscous force by blending a crosslinked polyester into the neat resin at different weight fractions. With higher viscosity there was a corresponding decrease in interfacial area growth between the polyester and water, resulting in increased particle size but even with a viscosity near 800 Pa.s, far above a traditional oil-in-water system, it was still found possible in this study to create nano-sized particles by SFEE.

Acknowledgments

I wish to express my sincere appreciation to those who have contributed to this thesis and supported me during all steps of my project. This thesis would not be possible without the guidance from my supervisor Prof. Michael Thompson. I would like to thank to him for his exceptional guidance and showing how to be critical thinker every day of my graduate student life.

I also would like to thank my supervisory committee members; Professor An-Chang Shi and Professor Todd Hoare for their brilliant suggestions on my research. I also would like to present my gratitude to Dr. John Pawlak in Xerox Corporation for the useful discussions and suggestions to improve myself. I would not be where I am today without his help. My many thanks go to David Lawton for the all help and motivations he provides. I wish to express my thanks to Mark Arnould at Xerox Corporation who conducted the countless numbers of GPC tests to determine the molecular weights of our polymer samples.

I also would like to thank everybody in polymer processing group at chemical engineering department of McMaster University. I am grateful to the entire Department of Chemical Engineering staffs at McMaster University for their assistance.

I owe special gratitude to my parents, Osman Goger and Havva Goger and my brothers Huseyin Goger and Dursun Goger who all guided and supported me my entire life. Finally, I can never finish this dissertation without thanking my wife; Aysenur Safa; my son; Yayha Goger and my daughter; Havva Goger; for their love and peaceful support.

Table of Contents

List of Figures

Chapter 1

Chapter 2

Chapter 3

Chapter 4

Chapter 5

List of Tables

Chapter 1

Chapter 2

Chapter 3

Chapter 4

Chapter 5

List of Abbreviations and Symbols

AN: Acid Number

C: Converted

Ca: Capillary Number

CPI: Catastrophic Phase Inversion

D: Diameter

D_{50}: Mean Particle Diameter

DR: Degradation Ratio

EP: Emulsion Polymerization

FA: Fumaric Acid

FIPI: Flow Induced Phase Inversion

g: Gram

GPC: Gel Permeation Chromatography

h: Hour

HMWSPs: Hydrophobically Modified Water Soluble Polymers

KOH: Potassium Hydroxide

L/D: Length to Diameter Ratio

LDPE: Low Density Polyethylene

MEK: Methylene Ethylene Ketone

min: Minute

mL: Milliliter

M_n: Number average molecular weight

MRT: Mean Residence Time

Na^+: Sodium Ion

NaCl: Sodium Chloride

NaOH: Sodium Hydroxide

NC: Non-converted

nm: Nano Meter

NR: Neutralization Ratio

O/W: Oil-in-Water

ºC: Degree Celsius

p: Viscosity ratio

pBPA: Dipropoxylated Bisphenol-A

PIT: Phase Inversion Temperature

PM: Processing Modifier

R/W_1: Resin-to-Water in dispersion zone of SFEE

R/W_T: Resin-to-Water in dilution zone of SFEE

R: Radius

RTD: Residence Time Distribution

SDBS: Sodium dodecylbenzenesulfonate

SEM: Scanning Electron Microscopy

SEPI: Solvent Emulsification by Phase Inversion

SFE: Solvent-Free Emulsification

SFEE:Solvent-Free Extrusion Emulsification

T_g: Glass Transition Temperature

TPI: Transitional Phase Inversion

TPU: Thermoplastic Polyurethane

TSE: Twin Screw Extruder

W/O: Water-in-Oil

W/O: Water-in-Oil

wt. %: Weight Percentage

δ_d: Dispersive Component

δ_p: Polar Component

ΔP: Pressure Drop

$\Delta\eta/\Delta t$: Slope of Viscosity Change

η_c: Continuous Phase Viscosity

η_d: Dispersed Phase Viscosity

λ: Relative Viscosity

σ: Interfacial Tension

$\dot{\gamma}$= Shear Rate

τ_w: Shear Stress

µm: Micron Meter

Chapter 1 Introduction and Literature View

1.1. Overview

Sub-micron sized polymer-water dispersions are used in many applications such as adhesives[1], coatings[2] and pharmaceutics[3]. There are numerous studies in polymer-liquid dispersion, but the focus of this discussion is specifically aqueous dispersion. Table 1-1 summarizes the two main approaches used to produce sub-micron particles: top-down and bottom-up. Emulsion polymerization (EP)[4,5] is a bottom-up approach that entails monomer polymerization but is not applicable for polymers like polyesters and olefins in the presence of water. Bottom-up approaches are therefore not of interest in this thesis. Mechanical agitation[6–8], a top-down approach, without the use of hazardous solvents presents challenges in achieving sub-micron particles. Solvent emulsification[9,10] is the most commonly used top-down approach for generating sub-micron sized polymer-liquid dispersions from polyesters or olefins and exhibits greater control over particle size compared to mechanical agitation. However, the high cost of background solvent recovery and tight environmental regulations ultimately inhibits the economic use of solvent emulsification. In solvent emulsification, the solvent is responsible for lowering the system viscosity by dissolving the polymer while acting as a surface-active agent. Solvent-free emulsification methods (SFE)[1,11–13] are reported as batch processes and show little robustness to phase inversion since the absence of organic solvents lend them to experiencing great difficulties in countering the high viscosities (1-1000 Pa·s) of most industry standard polymers. However, it is becoming increasingly apparent that solvent-free emulsification can be effective with several moderately viscous systems[11,12], albeit exhibiting extremely narrow processing windows.

Table 1-1 Summary of available methods to produce polymer-liquid dispersion

Methods	Energy Utilization	Solvent Required	Process Type
Emulsion Polymerization (EP) Bottom-up Approach	Moderate	Yes	Continuous/Batch
Mechanical Agitation Top-down Approach	High	No	Batch
Solvent Emulsification by phase inversion (SEPI) Top-down Approach	Moderate	Yes	Batch
Solvent-Free Emulsification (SFE) Top-down Approach	High	No	Batch
Solvent-Free Extrusion Emulsification (SFEE) Top-down Approach	Moderate	No	Continuous

1.2. Mechanical Top-Down Approach

This approach directly involves dispersing the polymer phase into the water phase in order to create an oil-in-water (O/W) emulsion (or other variants). The final particle size of the polymer droplet is a function of the amount of applied external energy and the interfacial energy between the polymer and water. High-shear mechanical devices are typically utilized and examples include a rotor-stator device, homogenizers and many different types of mills. The prerequisite shear forces for droplet break-up to occur by mechanical means increase as the desired final droplet size decreases. This approach poorly accommodates the preparation of aqueous dispersions. First, the mechanical top-down approach struggles to control particle size below the micron level. Secondly, agglomeration restricts the volume fraction of the dispersed phase. Therefore volume fraction of dispersed phase can be used in mechanical approach is generally lower than the chemical top-down approach.[11] Thirdly, phase inversion induced by chemical driving forces can better provide a sub-micron droplet and with a narrower size distribution than by mechanical approaches alone.[18] Finally, the intensive energy consumption of most mechanical approaches incur a high operating cost, making them unattractive if avoidable.

1.2.1. Droplet Break-Up

There are two main driving forces for the deformation of polymer droplets. The interfacial tension between a polymer and water tends to minimize droplet surface area and hence tend to reach the lowest energy state while externally applied shear forces increases the size of interface. The applied external force needs to overcome the interfacial force in order to break apart the polymer droplets.. Grace[19] built upon Taylor's[20] study and defines a critical capillary number, as shown in Eq. (1.1):

$$Ca = \frac{\eta_m \dot{\gamma} D}{\sigma} \tag{1.1}$$

where Ca is the capillary number, η_m is the viscosity of the matrix, D is the diameter of the matrix and σ is the interfacial tension. The viscosity ratio between the dispersed phase and the continuous phase versus capillary number, also known as a Grace plot, is depicted in Figure 1-1. The figure implies that droplet breakup cannot be accomplished when the viscosity ratio exceeds 4 for simple shear flow.

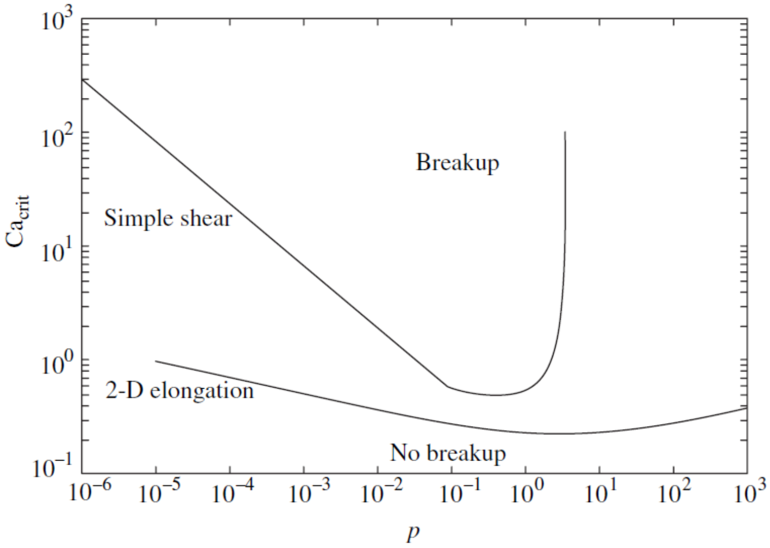

Figure 1-1 Critical capillary number for different viscosity ratios in simple shear and elongation flow.[19]

1.3. Chemical Top-Down Approach

The most common chemical top-down approach is known as solvent emulsification by phase inversion (SEPI). It has been increasingly adopted in the plastics industry since a broader range of polymers and products may be dispersed and sold in water respectively. SEPI typically involves dissolving a polymer in an organic solvent before water is added to carry out the inversion, yielding disperse polymer particles in a continuous aqueous phase.[35] In SEPI, the solvent is responsible for lowering the system viscosity by dissolving the polymer while acting as a surface-active agent. SEPI provides greater control over the particle size and the energy input is lower than the mechanical methods.[8,35,36] The cost of organic solvent, fire and/or explosion hazards of the solvent, carbon emission restrictions, toxicity, environmental regulations, as well as the cost of the solvent-recovery operation[37,38] all contribute to the decline in SEPI utilization within the wider plastics industry.

1.4. Solvent-Free Emulsification

Solvent-free emulsification (SFE) is a chemical process where the dispersed phase inverts to being the continuous phase by altering environmental conditions without use of organic solvent. SFE is frequently used in food, cosmetics, adhesive, and drug delivery applications due to three main features. First, it allows emulsions to be produced at higher dispersed phase volumes. Second, SFE is capable of processing exceptionally high viscosity ratios (i.e. up to 10^4) which far surpasses the capacity of a homogenizer or high shear mixers used in the dispersion industry. Grace[19] showed that the viscosity ratio between the continuous and dispersed phase cannot exceed a magnitude of four for a mechanical top down approach under simple shear flow of a non-viscoelastic Newtonian fluid. Finally, it avoids the use of harmful solvents.

There are two standard techniques to producing an oil-in-water (O/W) emulsion from initially water being dispersed into a continuous oil phase. These methods are known as *transitional phase inversion* (TPI) and *catastrophic phase inversion* (CPI). In Figure 1-2, the two phase inversion techniques are represented schematically by a two dimensional phase map of temperature versus water volume fraction.[10] It should be mentioned that the phase inversion locus (plotted with a solid black line in Figure 1-2) and optimal formulation in Figure 1-2 correspond to a minima for interfacial tension between the water and polymer. Figure 1-2 indicates that CPI is accomplished with the addition of water into the continuous phase while TPI relies on the physicochemical properties of the surfactant to change with temperature. Both are further described below.

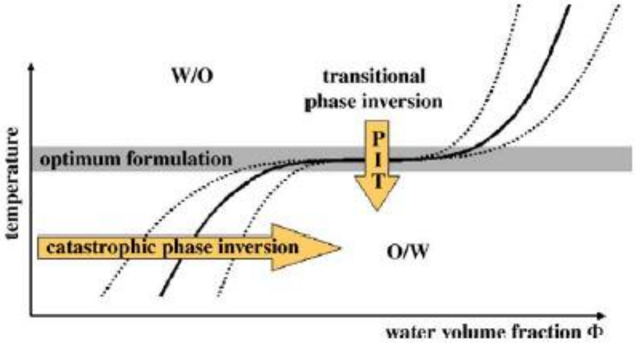

Figure 1-2 Schematic illustration of two phase inversion techniques (catastrophic and transitional phase inversion). Adopted by Fernandez et al.[10]

1.4.1. Transitional Phase Inversion

The transitional phase inversion technique (TPI) was introduced by Shinoda and Saito[39,40] using non-ionic surfactant. Although, a non-ionic surfactant tends to be more soluble in water at low temperatures, it becomes more soluble in oils with increasing temperature.[41] At a specific temperature (PIT), the solubility of non-ionic surfactant in both oil and water are theoretically equal. To add, a system prefers the W/O emulsion state at temperatures higher than PIT, while it favours the O/W emulsion state at temperatures lower than PIT. Submicron emulsions can be obtained when the system is cooled down from a temperature slightly above PIT to well below PIT[41], which is considered a thermodynamic response.[42] The Bancroft rule states that the phase in which an emulsifier is most soluble constitutes the continuous phase without depending on the continuous phase fraction.[43] It should be noted that the TPI method is not applied in this thesis.

1.4.2. Catastrophic Phase Inversion (CIP)

Becher[44] was the first to recognize the catastrophic phase inversion (CIP) technique where a system inverts to produce an aqueous dispersion by the gradual incorporation of water. Incorporation of water progressively negates the polymer-water interface and subsequently merges the polymer together into lamella-like bi-continuous structure. Eventually, a W/O emulsion is inverted into an O/W emulsion, as seen in Figure 1-3. It should be noted that the CIP method is used in this thesis.

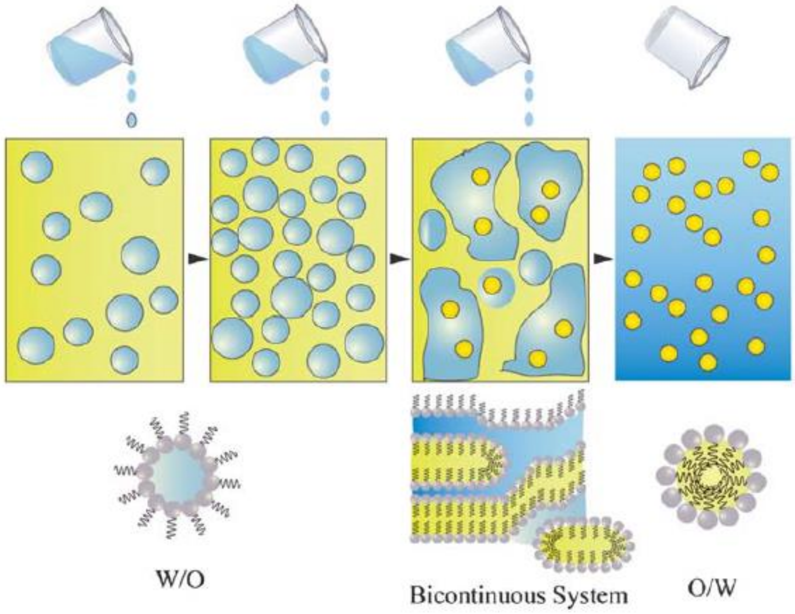

Figure 1-3 Schematic demonstration of catastrophic phase inversion (CPI). Adopted from McClements[45]

Among the physical properties, the oil phase viscosity plays one of the most important roles on both the phase inversion mechanism and final drop size due to the difficulty of dispersing high viscosity material into the water. Li et al.[46] found that sub-micron size (i.e. 0.04 to 0.2 µm) emulsion formation is especially influenced by the viscosity range, favouring values between 0.03 Pa.s and 0.4 Pa.s. In addition, Brooks and Richmond[9] observed that the droplet size increases from 40 µm to 181 µm when the oil phase viscosity increases from 0.0007 Pa.s to 0.2 Pa.s. Galindo-Alvarez et al.[47] studied the effect of oil viscosity on the phase inversion point (PIP) in the range of 1-12.5 Pa.s at room temperature by using a batch reactor. They reported that the PIP occurred at a volume ratio of 0.38 with an oil viscosity of 1 Pa.s and a volume ratio of 0.1 with an oil viscosity of 12.5 Pa.s. They[47] concluded that PIP may be enhanced by a very low viscosity ratio between the dispersed phase and the continuous phase ($\eta_d << \eta_c$). It should be mentioned that the influence of oil viscosity on final particle size was not studied while enhancing the PIP. Interestingly, Rondon-Gonzales et al.[48] performed a special procedure called a *statistic phase inversion* process by continuously stirring abnormal O/W emulsion.. They studied viscosities in the range between 0.001 Pa.s and 0.02 Pa.s. They noticed a tendency that the oil droplet breakup became less efficient with increasing oil viscosity, due to lower deformation under shear, which enhanced the formation of bi-continuous structure for phase inversion. Their qualitative microscopic observations also indicated that the emulsion prepared with a higher oil viscosity exhibited larger water droplets without giving any scientific explanation for the result. Salager et al.[49] reports that the stable W/O emulsion region tends to shrink while the viscosity increases from

0.001 Pa.s to 0.1 Pa.s and vanishes above viscosities of 0.5 Pa.s. However, the oil viscosities in these studies were outside of a practical industry viscosity range for polymers. A more appropriate viscosity range would include 1-1000 Pa.s.

Ashrafizadeh et al.[12] demonstrated emulsification of a relatively viscous (2.7 Pa.s) crude oil in water via the use of a homogenizer to produce an oil domain with a Sauter diameter varying between 8µm and 25µm. Evidently, the particle size is larger compared to a standard emulsion, which could be a result of increasing oil viscosity within this type of mechanical dispersion process.[50] In addition, Song et al.[1] created water-borne pressure adhesives with a mean particle size between 0.6µm to 1.5µm by using a multi-impeller system. Song et al.[1] found that a submicron emulsion of rosin can be obtained with a low water incorporation rate (i.e. 10 ml/min) and high inner/outer impellers speeds of 70/50 rpm. Conversely, they found that emulsion particles are larger than micron at a high water incorporation rate with low inner/outer impellers speeds of 30/20 rpm. It should be mentioned that a high water incorporation rate at high impeller speed is not very interesting from the industrial perspective because of the increased costs related to high energy mixing as well as the high foam content in the emulsion produced.

Akay[13] used a multiple-expansion contraction static mixer (MECSM) to promote droplet break-up by superimposing shear and extensional forces simultaneously to study what they referred to as *flow-induced phase inversion* (FIPI). The Sauter diameters of emulsion are 0.64µm and 0.68 µm for epoxy resins with a viscosity of 42 Pa.s and 2.1 Pa.s respectively. The final particle size differed by only 5%, one had an oil phase viscosity that was 20 times larger than the other. The high extension rate and large number of MECSM elements were primarily responsible for the similar particle sizes between the two resins. Akay[13] defined the mechanism of FIPI in MECSM where the water extends into cylindrical threads and is compressed into discs. Later, these discs trigger oil phase encapsulation by coalescing and aggregating. A more relevant example to this thesis, from the perspective of the polymer phase viscosity, was conducted by Akay et al.[11,51] who studied aqueous phase inversion in a batch mixer for different polymer melts including low density polyethylene (LDPE). The phase inversion point was determined with a slight increase in torque followed by a sharp drop in torque upon addition of the aqueous phase. The mean particle size was varied between 1.03-4.19µm for different concentrations of the hydrophobically modified water-soluble polymers (HMWSPs). They also concluded that phase inversion occurred when the water phase volume reaches approximately 20%. One of drawbacks to their method is the formation of a second and third phase inversion during the batch reactor cooling cycle, which can lead to uncontrolled particle size and span of its size distribution, as well as form multiple emulsions. Overall, it can be said that none of the studies in this section have used a continuous system, like the twin screw extruder (TSE), or conducted studies for highly viscous polymers over 200 Pa.s.

1.5. Solvent-Free Extrusion Emulsification (SFEE)

A twin screw extruder (TSE) is very popular in the plastics industry because of its ability to integrate different processes like melting, mixing, and devolatilization into a single piece of equipment with promising prospects for large scale production[21]. In the polymer processing field, the TSE is normally used to melt different polymers together, and uniformly mix in filler[22] and small quantities of liquids;[23] occasionally, the same machine has also been used for bulk polymerization[24]. Polymer emulsification is generally considered to lie outside the normal viscosity range of TSE usage in the industry. Despite a lack of fundamental understanding on the emulsification inside the extruder, some patens[17,25–28] show industrial interest in generating aqueous polymer dispersions by TSE.

Solvent-free extrusion emulsification (SFEE) is a green manufacturing process used to produce aqueous polymer dispersions with an unconventional use of a TSE. The SFEE process makes continuous products with stable emulsions and well-controlled particle sizes for a moderate energy expenditure whilst avoiding organic solvents. SFEE is a complicated process due to its sensitivity to a number of variables, as shown in Figure 1-4. Warner and Leng[52] were first known inventors to produce a continuous solvent free emulsification with a concentric rotating cylinder within a heated barrel. The quoted particle size ranged between 0.55-12.8μm with an epoxy resin and a polyvinyl alcohol emulsifier. The twin screw extruder was introduced to perform solvent-free extrusion emulsification for the dispersion of several resins such as ethylene vinyl acetate, maleic anhydride-grafter ethylene vinyl acetate, and low density polyethylene by Abe et al.[53]

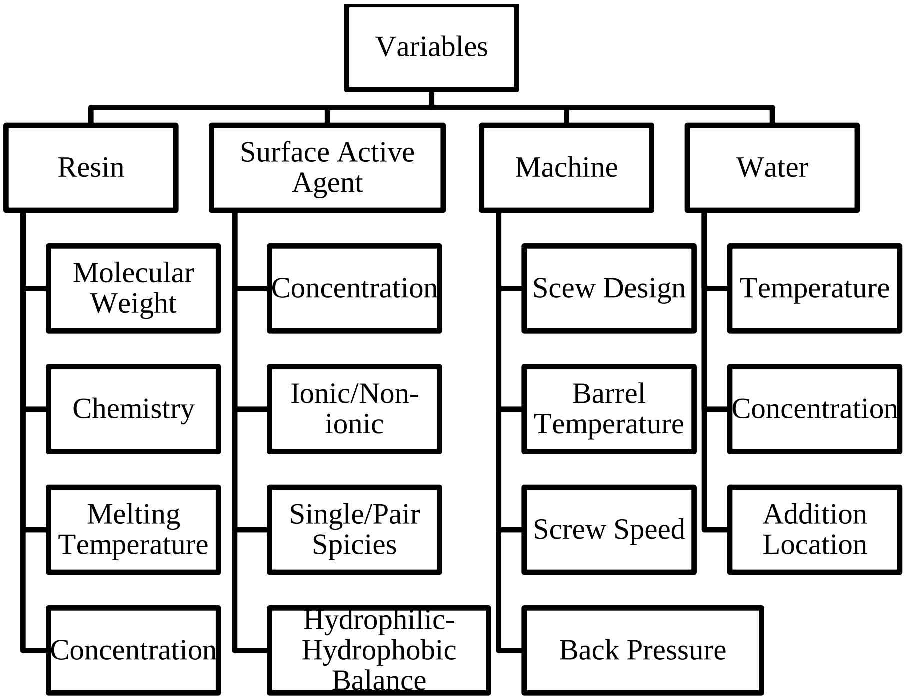

Figure 1-4 Parameters that affects the SFEE process.

SFEE takes place inside a TSE and its operations are divided into three processing zones[14,15,38] as shown in Figure 1-5. The first zone is the standard *melting zone*, where polymers, and possibly solid surface active agents, are mixed into a uniform molten phase. Other ingredients could be incorporated into the polymer phase in the melting zone such as colorants and fillers, but were not used in this thesis. The second extruder stage is the *dispersion zone* where a small weight fraction of water is initially injected and mixed into the molten polymer. Finally, the last zone of the extruder is for *dilution* where the final, and much higher, weight fraction of water is injected to create the desired oil-in water (O/W) type emulsion prior to the melt solidifying.

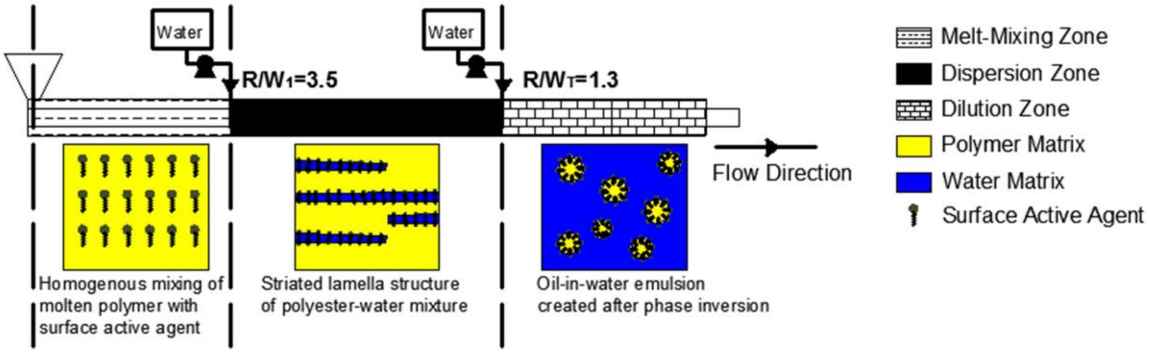

Figure 1-5 Schematic of a SFEE layout for preparing aqueous dispersions.

The SFEE process currently runs with a narrow window of stable operations, but that can be changed as the mechanism of this emulsification method is better understood.

1.2.3. Inline Rheometer

Extruders are commonly treated as black-boxes due to their combined high shear and extensional flow, high pressure and elevated temperature needed to perform their intended function. To ensure process-sensitive polymer systems maintain their morphological state during rheological characterization, inline rheometers have been demonstrated for different fields such as supercritical CO_2 foaming[29–31] , water dispersion inside the polymer and even thermoplastic polyurethane (TPU) to obtain real-time data. Inline viscosity measurements are usually done using designs based on flow through a capillary passage[32,33] due to the lower manufacturing cost, operational flexibility, and similarity to flow inside an extruder. The pressure drop across the capillary die is monitored for a known capillary geometry and viscosity, approximated by the following equations (1.2-1.4):

$$\tau_w = \left(-\frac{\Delta P}{L}\right)\left(\frac{R}{2}\right) \tag{1.2}$$

$$\dot{\gamma_{app}} = \left(\frac{4Q}{\pi R^3}\right) \tag{1.3}$$

$$\eta_{app} = \frac{\tau_w}{\dot{\gamma_{app}}} \tag{1.4}$$

where τ_w is the shear stress, $\dot{\gamma_{app}}$ is the apparent shear rate, η_{app} is the apparent viscosity, R is capillary die radius, L is the length of the die, and Q is the volumetric flow rate; the equations assume laminar flow of a Newtonian fluid exhibiting no-slip on the boundaries. There are two main drawbacks to the capillary die. Firstly, exit and entrance loses must be taken into account in order to obtain a true viscosity rather than apparent values. Secondly, only a single viscosity value can be obtained at a fixed flow rate. Lee et al.[29,30] used a slit die to determine the viscosity of polyethylene-polystyrene blends with supercritical CO_2 at various shear rates.

1.6. Objectives

Solvent-free extrusion emulsification (SFEE) is introduced for the first time in this thesis as a process sensitive to a number of variables. This has resulted in a very narrow operational window for the industries using the method, but understanding the process mechanism should permit improved processability. The research that was conducted aims to devise a mechanistic explanation for the SFEE process and advance the technology to accommodate the environment, public, and industry. The specific objectives of this study include:

1. To address the effect of chemical contents on the SFEE process, examining the process separately based on the three zones of SFEE: melt-mixing, dispersion, and the inversion zone.
2. To clarify the individual and combined effect of chemical contents such as resin-to-water (R/W) ratio, surfactant content, sodium hydroxide (NaOH) addition type, NaOH content on the polymer-water mixture methodology.
3. To develop an integrated inline viscometer to monitor the rheological behaviour of the polymer-water mixture.
4. To understand the influence of machinery design, such as different extruder configurations, on particle size and dispersion stability.
5. To examine the effect of polymer viscosity by varying the molecular weight on particle size and dispersion stability.
6. To create a continuous sub-micron level oil-in-water (O/W) emulsion inside the twin screw extruder with highly viscous polyester in the range of 200 Pa.s.

1.7. Thesis Outline

Chapter 1 Introduction and literature view. This chapter summarizes the literature related to produce oil-in-water (O/W) emulsions including the overview of mechanical top-down, chemical top-down and solvent-free emulsification approaches. Solvent-free extrusion emulsification (SFEE) is introduced. The research objectives and thesis outline are provided.

Chapter 2 In Situ Rheological Measurement of an Aqueous Polyester Dispersion during Emulsification. This chapter represents the first study on the complex rheological behaviour of aqueous polymer dispersion by applying the Metzner-Otto approach to monitor the process within a batch reactor. Transient, *in situ* rheological information while mixing water into the molten polymer was determined by monitoring torque changes during the addition of water at high pressure and elevated temperature. The result showed that a rapid torque drop occurring during water addition was related to a developing morphological state of mixing. It also revealed that chemical parameters like the content of surface active species and mechanical parameters such as shear forces were necessary to the polyester-water mixture. This chapter has been published in *Industrial & Engineering Chemistry Research*.

Chapter 3 Inline Rheological Behaviour of Dispersed Water in a Polyester Matrix with a Twin Screw Extruder. The new inline rheological measurement technique was developed with the validation of 3D numerical software, OpenFOAM, as well as conventional parallel plate and capillary rheometers. Rheological changes during polyester-water mixing was monitored by an custom built inline orifice type rheometer. The effect of polar group contributions on surface energy and viscosity, which have significant control over the final state of the dispersion, were examined separately. Analysis in this chapter indicated that higher polar surface energy had the greatest influence on the mixing state of the polymer-water system. This chapter was published *Polymer Engineering & Science.*

Chapter 4 Solvent-Free Polymer Emulsification inside a Twin Screw Extruder. The main objectives of this chapter was to gain the first detailed understanding of the dispersion zone of solvent-free extrusion emulsification (SFEE) by examining different chemical factors on the ability to create sub-micron sized emulsions inside the extruder. Particles as small as 100 nm were produced for a presented chemistry. It was revealed that a transient rheological change during the water addition, previously noted in the batch study in Chapter 2, can be a strong indicator of the striated lamella morphology developed in the dispersion zone of SFEE. It is shown that the dissolution kinetics of sodium hydroxide and end group conversions prove to be a rate-limiting phenomena to generate thinner lamella structure. This chapter is submitted *AIChE Journal.*

Chapter 5 The Effect of Polymer Viscosity on Solvent-Free Polymer Emulsification inside a Twin Screw Extruder Part I: Molecular Weight In this chapter, the aim was to examin the influence of matrix viscosity on its dispersion mechanism using crosslinked polyester as a viscosity modifier. The investigation used an inline rheometer for transient and steady state measurements of system viscosity, and offline characterizations including soxhlet extraction, colorimetric titration, and particle size analysis. Though it remained possible to produce particles close to their target size of 100-200 nm, particle size was notably increased by varying the matrix viscosity from 250 Pa.s for neat polyester up to 630 Pa.s with added modifier. The increasing viscous force with increasing polyester matrix viscosity with minimal impact on surface activity causes decreasing interfacial area growth between polyester and water which results with particle size increases. This manuscript is in the preparation for publication.

Chapter 6 Conclusion Remarks. The final chapter explores the conclusion remarks with key finding and future work.

1.8. References

1. Song D, Zhang W, Gupta RK, Melby EG. Role of operating conditions in determining droplet size and viscosity of tackifier emulsions formed via phase inversion. *AIChE J*. 2011;57(1):96-106.
2. Hall C. Polymer Materials and their Technology. In: *Polymer Materials*. Macmillan Education UK; 1981:141-183.
3. Felton LA, Porter SC. An update on pharmaceutical film coating for drug delivery. *Expert Opin Drug Deliv*. 2013;10(4):421-435.
4. Jönsson JB, Müllner M, Piculell L, Karlsson OJ. Emulsion Condensation Polymerization in Dispersed Aqueous Media. Interfacial Reactions and Nanoparticle Formation. *Macromolecules*. 2013;46(22):9104-9113.
5. Ma Z, Guan Y, Liu H. Synthesis and characterization of micron-sized monodisperse superparamagnetic polymer particles with amino groups. *J Polym Sci Part Polym Chem*. 2005;43(15):3433-3439.
6. Sundararaj U, Macosko CW, Rolando RJ, Chan HT. Morphology development in polymer blends. *Polym Eng Sci*. 1992;32(24):1814-1823.
7. Utracki L A. On the viscosity-concentration dependence of immiscible polymer blends. *J Rheol*. 1991;35(8):1615-1615.
8. Sani SN, Das NG, Das SK. Effect of microfluidization parameters on the physical properties of PEG-PLGA nanoparticles prepared using high pressure microfluidization. *J Microencapsul*. 2009;26(6):556-561.
9. Brooks BW, Richmond HN. Phase inversion in non-ionic surfactant—oil—water systems—III. The effect of the oil-phase viscosity on catastrophic inversion and the relationship between the drop sizes present before and after catastrophic inversion. *Chem Eng Sci*. 1994;49(11):1843-1853.

10. Fernandez P, André V, Rieger J, Kühnle A. Nano-emulsion formation by emulsion phase inversion. *Colloids Surf Physicochem Eng Asp*. 2004;251(1–3):53-58.

11. Akay G, Tong L. Preparation of Colloidal Low-Density Polyethylene Latexes by Flow-Induced Phase Inversion Emulsification of Polymer Melt in Water. *Journal of Colloid and Interface Science*. 2001;239:342-357.

12. Ashrafizadeh SN, Motaee E, Hoshyargar V. Emulsification of heavy crude oil in water by natural surfactants. *J Pet Sci Eng*. 2012;86-87:137-143.

13. Akay G. Flow-induced phase inversion in the intensive processing of concentrated emulsions. *Chem Eng Sci*. 1998;53(2):203-223.

14. Goger A, Thompson MR, Pawlak JL, Arnauld MA, Lawton DJW. Solvent-Free Polymer Emulsification Inside a Twin Screw Extruder. *AIChE J*. Submitted on 2017.

15. Lawton DJW, Thompson MR, Faucher S. Morphological Development of Latex Particles in a Solvent-Free Extrusion Process. *Society of Plastics Engineers (ANTEC)*.; 2014;1169-1174.

16. Zhou K, Qiu SS, Moffat KA, Sacripante GG, inventors; Xerox Corporation, assignee. Solvent-free phase inversion process for producing resin emulsions. US20090208864 A1 2009.

17. Chung JT, Cheng CM, Malachowski SM, Godshall ED, Pearson JL, inventors; Xerox Corporation, assignee. Method of continuously forming an aqueous colorant dispersion using a screw extruder. US9052625 B2 2015.

18. Watson DJ, Mackley MR. The rheology of aqueous emulsions prepared by direct emulsification and phase inversion from a high viscosity alkyd resin. *Colloids Surf Physicochem Eng Asp*. 2002;196(2–3):121-134.

19. GRACE† HP. Dispersion Phenomena in High Viscosity Immiscible Fluid Systems and Application of Static Mixers as Dispersion Devices in Such Systems. *Chem Eng Commun*. 1982;14(3-6):225-277.

20. Taylor GI. The Formation of Emulsions in Definable Fields of Flow. *Proc R Soc Lond Ser Contain Pap Math Phys Character*. 1934;146(858):501-523.
21. Utracki LA, Shi ZH. Development of polymer blend morphology during compounding in a twin-screw extruder. Part I: Droplet dispersion and coalescence—a review. *Polym Eng Sci*. 1992;32(24):1824-1833.
22. Migneault S, Koubaa A, Erchiqui F, Chaala A, Englund K, Wolcott MP. Effects of processing method and fiber size on the structure and properties of wood–plastic composites. *Compos Part Appl Sci Manuf*. 2009;40(1):80-85.
23. Thompson M r., Sun J. Wet granulation in a twin-screw extruder: Implications of screw design. *J Pharm Sci*. 2010;99(4):2090-2103.
24. Song Z, Baker WE. Basic functionalization of molten linear low-density polyethylene with 2-(dimethylamino)ethyl methacrylate in an intermeshing corotating twin-screw extruder. *J Appl Polym Sci*. 1990;41(5-6):1299-1313.
25. Lundgard RA, III JEP, Piechocki C, III PTK, Lutenske NE, Thumma I, inventors; Dow Chemical Company, assignee. Continuous process of extruding and mechanically dispersing a polymeric resin in an aqueous or non-aqueous medium. WO2000071609 A1 2003.
26. Inada J, Koshiro F, Shimizu R, Sato S, inventors; Tosoh Corporation, assignee. Method of emulsifying thermoplastic resin composition. US5354804 A 1994.
27. Shim AK, Tabler R, Tascarella D, inventors; Dow Corning Corporation, assignee. Mechanical inversion process for marking silicone oil-in-water emulsions. US7385001 2008.
28. Kmiecik-Lawrynowicz GE, Patel RD, Hopper MA, inventors; Xerox Corporation, assignee. Process of making toner compositions US5344738 A 1994.
29. Lee M, Tzoganakis C, Park CB. Extrusion of PE/PS blends with supercritical carbon dioxide. *Polym Eng Sci*. 1998;38(7):1112-1120.

30. Lee M, Tzoganakis C, Park CB. Effects of supercritical CO2 on the viscosity and morphology of polymer blends. *Adv Polym Technol*. 2000;19(4):300-311.
31. Xu X, Park CB, Xu D, Pop-Iliev R. Effects of die geometry on cell nucleation of PS foams blown with CO_2. *Polym Eng Sci*. 2003;43(7):1378-1390.
32. Maia JM, Covas JA, No JM. Rheological measurements along an extruder with an on-line capillary rheometer. *Polymer Testing* 2000;19:165-176.
33. Covas JA, Carneiro OS, Costa P, Machado AV, Maia JM. Online monitoring techniques for studying evolution of physical, rheological and chemical effects along the extruder. *Plast Rubber Compos*. 2004;33(1):55-61.
34. Goger A, Thompson MR, Pawlak JL, Lawton DJW. In situ rheological measurement of an aqueous polyester dispersion during emulsification. *Ind Eng Chem Res*. 2015;54(21):5820-5829.
35. Hamishehkar H, Emami J, Najafabadi AR, et al. The effect of formulation variables on the characteristics of insulin-loaded poly(lactic-co-glycolic acid) microspheres prepared by a single phase oil in oil solvent evaporation method. *Colloids Surf B Biointerfaces*. 2009;74(1):340-349.
36. Trotta M, Debernardi F, Caputo O. Preparation of solid lipid nanoparticles by a solvent emulsification-diffusion technique. *Int J Pharm*. 2003;257(1-2):153-160.
37. Song D, Virginia W. Phase Inversion in the Process for Making Tackifier Dispersions Used in Pressure Sensitive Adhesives. 2008.
38. Lawton DJW. Solvent Free Emulsification in Twin Screw Extruder. [Master of Applied Science Thesis], Hamilton, ON: McMaster University; 2013.
39. Shinoda K, Saito H. The Stability of O/W type emulsions as functions of temperature and the HLB of emulsifiers: The emulsification by PIT-method. *J Colloid Interface Sci*. 1969;30(2):258-263.

40. Shinoda K, Saito H. The effect of temperature on the phase equilibria and the types of dispersions of the ternary system composed of water, cyclohexane, and nonionic surfactant. *J Colloid Interface Sci*. 1968;26(1):70-74.

41. Anton N, Benoit J-P, Saulnier P. Design and production of nanoparticles formulated from nano-emulsion templates—A review. *J Controlled Release*. 2008;128(3):185-199.

42. Bouchama F, van Aken GA, Autin AJE, Koper GJM. On the mechanism of catastrophic phase inversion in emulsions. *Colloids Surf Physicochem Eng Asp*. 2003;231(1):11-17.

43. Bancroft WD. The Theory of Emulsification, V. *J Phys Chem*. 1912;17(6):501-519.

44. Becher P. Basic theory/measurement/applications. NewYork, NY: Marcel Dekker Inc; 1987.

45. McClements DJ. Edible nanoemulsions: fabrication, properties, and functional performance. *Soft Matter*. 2011;7(6):2297-2297.

46. Li Y, Zhang Z, Yuan Q, Liang H, Vriesekoop F. Process optimization and stability of d-limonene nanoemulsions prepared by catastrophic phase inversion method. *J Food Eng*. 2013;119(3):419-424.

47. Galindo-Alvarez J, Sadtler V, Choplin L, Salager J-L. Viscous Oil Emulsification by Catastrophic Phase Inversion: Influence of Oil Viscosity and Process Conditions. *Ind Eng Chem Res*. 2011;50(9):5575-5583.

48. Rondón-González M, Madariaga LF, Sadtler V, Choplin L, Márquez L, Salager J-L. Emulsion Catastrophic Inversion from Abnormal to Normal Morphology. 6. Effect of the Phase Viscosity on the Inversion Produced by Continuous Stirring. *Ind Eng Chem Res*. 2007;46(11):3595-3601.

49. Salager JL, Lopéz-Castellanos G, Miaña-Pérez M. Surfactant-Oil-Water Systems Near the Affinity Inversion: Part Vi: Emulsions Hith Viscous Hydrocarbons. *J Dispers Sci Technol*. 1990;11(4):397-407.

50. Pandolfe WD. Effect of Dispersed and Continuous Phase Viscosity on Droplet Size of Emulsions Generated by Homogenization. *J Dispers Sci Technol*. 1981;2(4):459-474.

51. Akay G, Tong L, Bakr H, Paints ICI, Sl S. Preparation of ethylene vinyl acetate copolymer latex by flow induced. 2002;7:4811-4818.

52. Warner GL, Leng DE, inventors; Dow Chemical Company, assignee. Continuous process for preparing aqueous polymer microsuspensions. US 4123403 A 1978.

53. Abe K, Tsuruoka M, Kiriyama S, Nakamori K, inventors; Mitsubishi Petrochemical Company, assignee. Aqueous dispersion of olefin resins and continuous process for preparing thereof. US432004 1982.

Chapter 2 In Situ Rheological Measurement of an Aqueous Polyester Dispersion during Emulsification

All experiments and data anlaysis in chapter 2 were conducted by the thesis author. M. Arnould at Xerox Webster conducted GPC test to determine molecular weights of the polymer samples. J. Pawlak and D. Lawton provided technical guidance on the project. This chapter is reprinted from Goger et al., Ind. Eng. Chem. Res. 2015, 54, 5820−5829 with the permission of ACS Publications © 2015 American Chemical Society.

I&EC research
Industrial & Engineering Chemistry Research
Article
pubs.acs.org/IECR

In Situ Rheological Measurement of an Aqueous Polyester Dispersion during Emulsification

A. Goger,[†] M. R. Thompson,*[,†] J. L. Pawlak,[‡] and D. J. W. Lawton[§]

[†]Department of Chemical Engineering, McMaster University, Hamilton, Ontario L8S 4L8, Canada
[‡]Xerox Corporation, Rochester, New York 14604, United States
[§]Xerox Research Center of Canada, Mississauga, Ontario L5K 2L1, Canada

ABSTRACT: Rheological analysis of a complex fluid system like an aqueous polymer dispersion can be challenging but can reveal mechanistic information as the viscous melt is emulsified. A pressurized vessel was used as a rheometer, based on the Metzner−Otto approach, to evaluate formulation variables where the developed morphology of a polyester/water mixture was shear-dependent. The parameters of the study were resin-to-water ratio (R/W), surfactant (type and concentration), and process variables of impeller speed and temperature. Transient in situ information on the system during the mixing of water into the molten polymer showed that a rapid, near-instantaneous decrease in the torque on the impeller occurred consistently around 2% water addition, related to the onset of the developed morphological state. It was observed to only demonstrate a drop in the torque for high shear rates and only with the appropriate content of surface-active species, revealing the chemical and physical parameters necessary to emulsify the polyester melt.

1. INTRODUCTION

Solvent-free emulsification of polymer presents numerous technological challenges to obtain a stable system yet provides an economical method of preparing aqueous latexes without the intermediate use of hazardous solvents. Few studies are currently found in the literature, although the process is receiving considerable industrial attention. Early demonstration of the technology showed the preparation of wax microparticles containing drugs,[1−3] while more recently an example was given for the preparation of a water-based pressure-sensitive adhesive from pine tree rosin.[4] In these processes, water is added gradually into a highly viscous fluid (on the order of 10^{-1}−10^{0} Pa·s) until phase inversion, presenting a difficult mixing environment because of its high viscosity ratio of components (approximately 10^{3}) and low compatibility of phases. In the case of the rosin study by Song et al.,[4] a multiimpeller batch reactor was converted into a rheometer by inclusion of a torque sensor, and it was found that the viscosity increased as the water fraction increased up until the point of inversion and then steadily decreased with further water addition. The torque sensor provided a dynamic means to gain information in situ of the emulsification process for the resin in regard to varied process variables like the impeller speed and system temperature. To make the process more broadly attractive to industry, it must be developed for more viscous polymers (100−1000 Pa·s) than just waxes, as demonstrated by Akay et al.,[5,6] and, most importantly, it mechanisms understood. A rheological study for this higher-viscosity process is necessary to provide new details of the mechanism and assist in the selection of surface-active agents based on in situ information rather than analysis of the final product.

Measurement of the rheological properties for complex fluid systems, such as the solvent-free emulsification process described above or the performance of deep-well drilling fluids[7] where the system response is determined by its morphological state, can be quite challenging. This is especially true when phase separation occurs rapidly for systems tested outside of their processing environment, for which there is a dependency upon the shear rate, temperature, or pressure. For such systems, commercial rheological instruments are often inadequate to appropriately replicate the needed process conditions, and in such cases, a batch mixing vessel may become a more desirable substitute to a rheometer if suitably modified to monitor the stress−strain relationship. Detailed reviews by both Carreau and Ulbrecht[8] and Tatterson[9] have summarized the efforts of researchers to study the mixing of non-Newtonian fluids based on rheological response by using different variants of impeller mixers. The common challenge among the studies they reviewed was always in regard to estimating the shear rate and viscosity from the impeller speed and torque data. The Metzner−Otto[10] approach was most often favored among those non-Newtonian studies for determination of the effective shear rate because it assumes a linear relationship to the impeller speed without requiring a mechanistic model of the system. Many authors[11−14] have proven the usefulness of the Metzner−Otto approximation to calculate the effective shear rate for both Newtonian and non-Newtonian fluids. Pressure can affect the accuracy of the approach but only significantly above 200 bar.[5] Conversely, Bousmina et al.[15] showed a complex mechanistic approach for estimating the shear rate based on a Couette analog and, subsequently, calculated the viscosity from the rotor speed and torque data for a double counter-rotating-type batch mixer characteristically used with shear-thinning polymers. Santi et al.[16] applied the Bousmina[15] approach to wood plastic

Received: February 25, 2015
Revised: April 24, 2015
Accepted: May 8, 2015
Published: May 8, 2015

DOI: 10.1021/acs.iecr.5b00765
Ind. Eng. Chem. Res. 2015, 54, 5820−5829

composites in that same type of mixer, whereas Carreau et al.[17] predicted the effective shear rate of a helical ribbon impeller by using the same approach. This Couette analog approach requires more detailed calculations and is not generally considered as robust as the Metzner−Otto approach.

The purpose of this paper is to understand the emulsification process of a high-viscosity polyester melt with near-Newtonian flow characteristics as it is blended at elevated temperatures above 100 °C with water based on in situ rheological analysis. A high-pressure reactor vessel fitted with a torque sensor was used as a tool in this study to measure the viscosity based on the Metzner−Otto approximation. The transient information collected from the process was used to understand the chemical and physical parameters that brought about morphological change for the polymer/water mixture.

2. EXPERIMENTAL SECTION

2.1. Materials. A proprietary amorphous polyester synthesized from fumaric acid and dipropoxylated bisphenol A was provided by Xerox Corporation (Webster, NY). The resin was a high flow grade (M_w = 20.1 kDa; M_w/M_n = 7.1) with an acid number of 16.2 mg/g KOH. Two different surfactants, which differed in their physical state during the trials, were used. Sodium dodecylbenzenesulfonate (surfactant A; Sigma-Aldrich, Toronto, Ontario, Canada) has a 300 °C melting temperature with a 348.48 g/mol molar mass and a 1 g/cm^3 solid density. On the other hand, Unicid 350, a long-chain, linear primary carboxylic acid (surfactant B; Baker Hughes, Houston, TX), has a 92 °C melting temperature with an acid number of 120 mg/g KOH and a viscosity of 0.004 Pa·s at 149 °C (according to the vendor datasheet). Sodium hydroxide (NaOH; Caledon Laboratories Ltd., Georgetown, Ontario, Canada) was ground for two testable particle sizes, i.e., 500−850 μm (size 1) or 850−1180 μm (size 2) (classified by a sieve shaker). Deionized water (>0.1 μS/cm^2) was used in the trials.

2.2. Procedures. The polymer/water system was mixed in a 2 L laboratory pressure reactor system (BEP 280; Buchiglas USA Corp., Farmingdale, NY) rated for 60 bar and fitted with an anchor-type impeller modified with three small turbine blades, as shown in Figure 1. The reactor was regulated to a headspace gas pressure of 1.72 MPa with nitrogen (99.999% purity; Air Liquide, Burlington, Ontario, Canada) for all conditions tested in this study as it maintained water, when present, well below its boiling point; the selected pressure was felt to have no impact on the viscosity of the polymer because all measurements in the batch vessel responded in the same manner to the shear rate, temperature, and composition as found with the offline rheometer. The reactor was heated using a 38 L circulating bath with a programmable controller (VWR International, Toronto, Ontario, Canada) filled with a heat-transfer oil (viscosity 0.15 Pa·s at 25 °C; Sigma-Aldrich, Toronto, Ontario, Canada). The stresses exerted on the anchor-type impeller were measured by a torque transducer (3 N·m capacity; Buchiglasuster Inc., Uster, Switzerland). A metal-sheathed, grounded K-type thermocouple was fitted to protrude into the melt within the reactor, and a pressure transducer (PX302-500gv; Omegadyne, Sunbury, OH) was installed to monitor the headspace gas pressure. The torque, temperature, and pressure data were sampled at 1 Hz using a 12-bit 10 kHz USB data acquisition system (NI USB-6008; National Instruments, Austin, TX) and monitored with a customized *LabVIEW* (National Instruments, Austin, TX) program. Water was metered into the reactor using an Optos metering pump (Eldex, Napa, CA) at 20 mL/min.

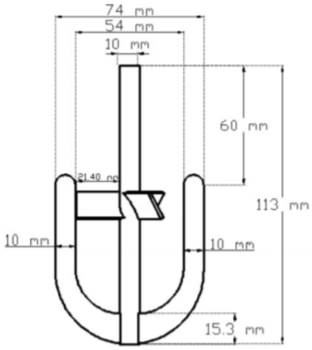

Figure 1. Dimensions of the anchor-type impeller.

For each experiment, the reactor was charged with a blended mixture consisting of 1.2 kg of polyester powder and appropriate amounts of the other dry components (i.e., surfactant, NaOH). The variables of the study for the mixture were the NaOH content (0, 0.5, and 1.5% w/w), NaOH particle size (500−850 and 850−1180 μm), surfactant content (0, 7.5, and 10% w/w), and surfactant type (A and B). After the melt reached 140 °C (within 30 min of heating), the batch reactor was pressurized to 1.72 MPa and the impeller started. System variables of the study were the impeller speed (50, 75, 100, and 150 rpm) and melt temperature (120, 130, and 140 °C). Deionized water was added at room temperature above the impeller at 20 mL/min. The final resin-to-water ratio (R/W) was varied from no water to R/W = 15 to R/W = 7. The torque was collected during the addition of the water, but its data were used in the viscosity calculation only after the system had stabilized for 20 min. The reported uncertainty was determined based on three repeats for 10 different experimental conditions, and the highest torque deviation was converted to shear viscosity (±8 Pa·s). Experimental factors in the trials were evaluated using *Design Expert 7.1* (State-Ease Inc., Mineapolis, MN) under a general factorial statistical design where the significance was determined for *P* values less than 0.05.

For validation purposes, shear viscosities were measured as a function of the shear rate by both parallel-plate (ARES; TA Instruments, New Castle, DE) and dual-capillary (ROSAND; Malvern Instruments, Malvern, U.K.) rheometers for the polyester as well as the polyester mixture with additional dry components. The offline calculated viscosity values were compared to the batch reactor results with the assumption that the Cox−Merz rule was valid for the cases where water had not been added. Parallel-plate measurements were performed in oscillating mode over a frequency range of 0.1−100 rad/s at a strain of 18% (based on a strain sweep test) at temperatures of 120, 130, and 140 °C. For the same temperature conditions, capillary measurements were carried out for 50−1000 s^{-1}.

2.3. Numerical Modeling. The anchor-type impeller with a three-blade turbine attachment presented a complicated geometry for determining the shear stress and shear rate based on torque and speed data. To use the Metzner−Otto approach for this system, it was felt that a numerical model was required to understand where shear stresses were localized around the

DOI: 10.1021/acs.iecr.5b00765
Ind. Eng. Chem. Res. 2015, 54, 5820−5829

impeller and how they could be correlated with the torque as it rotated. A computational simulation was developed using open-source numerical software *OpenFOAM 2.0.1* (OpenCFD Ltd., Bracknell, U.K.). Conservations of mass and momentum equations were solved by the *SIMPLE* algorithm. A power-law constitutive model was used to solve the momentum equations, with an index value of 0.96, which was obtained from the parallel-plate and capillary rheometers. The computational mesh for the fluid inside the reactor was composed of 2.5×10^6 tetrahedral elements, generated with a commercial mesh generator, GAMBIT (Fluent Inc., Canonsburg, PA). The no-slip boundary condition was considered valid for the simulations because of the low shear rates being tested and from the fact that no discontinuity was observed in the stress–strain measurements made on the rheometers or in the batch vessel. At the vessel wall and its bottom surface, a null velocity was assumed. The fluid at the impeller surface moved according to the local impeller rotation speed. Zero velocity was assumed in the normal direction, and zero-shear stresses were assumed in both normal and tangential directions at the free surface. Tanguy and co-workers[14] applied similar boundary conditions in their simulations of a reactor mixed by an anchor-type impeller.

Creeping-flow conditions were met based on the high melt viscosity, and a very low Reynolds number ($Re < 10^{-2}$) was calculated based on 0.28 m/s of velocity and 21.4 mm corresponding to the horizontal length across the impeller blade, for tested process conditions, which allowed the transient terms of the conservation equations to be neglected in the model solution. A quasi-steady-state solution was considered valid in the study because of the low Reynolds number, which meant that the rotating flow can be reasonably approximated as a sequence of steady-state solutions as the impeller moves from one position to another. Bravo et al.[18] and Li and Manas-Zloczower[19] demonstrated the validity of the quasi-steady-state approximation for a kneading block in corotating and counter-rotating twin screw extruders, respectively. The steady-state torque of the simulated system was calculated using eq 1 for each nodal element by the simulation software, and then it was integrated for all elements of the impeller:

$$\Gamma = \tau A r \tag{1}$$

where Γ is the torque, A is the area of the each nodal element, and r is the distance from the rotational axis for each nodal element.

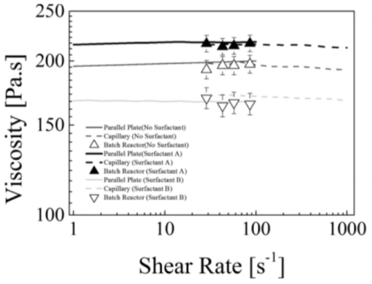

Figure 2. Comparison of the viscosity curves with different rheometers for 1.5% w/w NaOH, with/without surfactant A or B with error bars based on the largest torque deviation in the batch reactor.

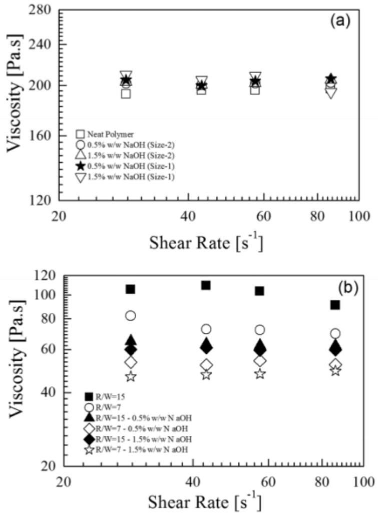

Figure 3. (a) Effect of NaOH on the viscosity without water and surfactant at 120 °C and 1.72 MPa. (b) Effect of the NaOH content on the viscosity when water is present for different R/W ratios at 120 °C and 1.72 MPa.

3. RESULTS AND DISCUSSION

3.1. Validation and Numerical Analysis. The difference between the calculated torque and measured values by the torque sensor of the reactor was less than 3% for the polymer/surface-active species mixtures (without water) at 120, 130, and 140 °C, providing confidence that the numerical results would be useful for determination of the Metzner–Otto fitted variables. The most intense shear stresses were found to be highly localized at the periphery of the impeller,. Therefore, shear stresses around the periphery of the impeller were averaged to obtain a system-averaged shear stress. The approach is similar to that of Anne-Archard et al.,[20] who used numerical simulations to solve for the Metzner–Otto fitted variables in their studies of fluids exhibiting a yield stress in a stirred vessel with either anchor-type or double-helical impellers. They reported findings similar to those of the present study, with the highest shear stresses along the edges of their anchor-type impeller.

An empirical model was derived from the simulation results for different shear rates and temperatures matching those intended for study in the experimental mixer. Equations 2–4 estimate the shear rate and shear stress at the impeller periphery, where the torque was predominantly determined for the polyester system for the specific geometry of the anchor-type impeller, with a best fit yielding $R^2 = 0.99$ and 0.97 for the empirical expressions of shear rate and K_{stress}, respectively:

$$\dot{\gamma} = 34.37\omega \tag{2}$$

$$\tau = K_{\text{stress}}\Gamma^n \tag{3}$$

$$K_{\text{stress}} = 6421\text{e}^{\Delta T} \tag{4}$$

where $\dot{\gamma}$ is the shear rate, ω is the angular velocity, τ is the shear stress, K_{stress} is the constant, Γ is the torque, n is the power law

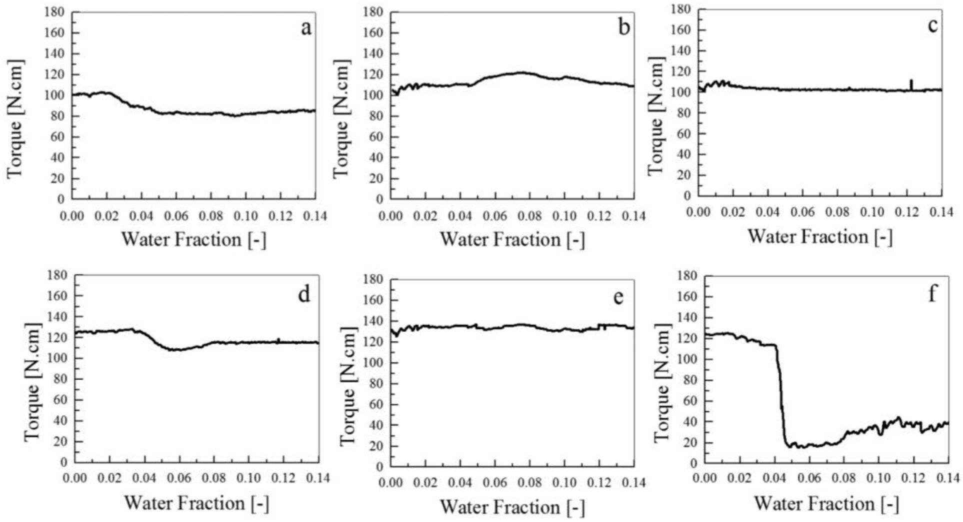

Figure 4. NaOH content effect on torque reduction without surfactant for different impeller speeds at 1.72 MPa: (a) 0% w/w NaOH at 100 rpm; (b) 0.5% w/w NaOH at 100 rpm; (c) 1.5% w/w at 100 rpm; (d) 0% w/w NaOH at 150 rpm; (e) 0.5% w/w NaOH at 150 rpm; (f) 1.5% w/w NaOH at 150 rpm.

Table 1. Discrete Derivatives of Torque Data of Different Contents for 100 and 150 rpm

sample	dT/dt at 100 rpm [N·m/s]	dT/dt at 150 rpm [N·m/s]
0% w/w NaOH	−0.0016	−0.0021
0.5% w/w NaOH	−0.0012	−0.0035
1.5% w/w NaOH	−0.0063	−0.1900
0% w/w NaOH/7.5% w/w surfactant A	−0.0037	−0.145/−0.452
0% w/w NaOH/10% w/w surfactant A	−0.0045	−0.051/−0.380
0.5% w/w NaOH/7.5% w/w surfactant A	−0.210	−0.191
0.5% w/w NaOH/10% w/w surfactant A	−0.170	−0.220
1.5% w/w NaOH/7.5% w/w surfactant A	−0.250	−0.230
1.5% w/w NaOH/10% w/w surfactant A	−0.290	−0.200
0% w/w NaOH/0.5% w/w surfactant B	−0.023	−0.074
0% w/w NaOH/10% w/w surfactant B	−0.015	−0.055
0.5% w/w NaOH/7.5% w/w surfactant B	−0.042	−0.103
0.5% w/w NaOH/10% w/w surfactant B	−0.051	−0.106
1.5% w/w NaOH/7.5% w/w surfactant B	−0.012	−0.033
1.5% w/w NaOH/10% w/w surfactant B	−0.011	−0.029

Table 2. Comparison of the Molecular Weight Moments of Samples Based on Whether a Sharp Torque Drop Was Experienced during Mixing at 150 rpm and 120 °C

sample	M_n (kDa)	M_w (kDa)	sharp drop
neat polyester	5.355	20.990	
R/W = 7	5.196	18.907	no
R/W = 7, 0.5% w/w NaOH	3.689	7.768	no
R/W = 7, 0.5% w/w NaOH, 7.5% w/w SDBS (surfactant A)	5.394	12.35	yes
R/W = 7, 0.5% w/w NaOH, 7.5% w/w Unicid 350 (surfactant B)	5.339	21.882	yes

index, and ΔT is the temperature difference based on the system temperature and a reference temperature of 120 °C.

The empirical model was verified based on a comparison of the viscosity measurements from the offline rheometers and the calculated results with the batch reactor. Figure 2 shows plots of selected viscosity data from the two rheometers, with curves closely matching the results from the batch reactor with error bars based on conversion of the largest torque deviation into shear stress for molten polyester as well as molten polyester blended with dry components (NaOH, surfactant A, or surfactant B). Observing comparable results from three different rheometers with respect to the shear rate provided some assurance that the type of shear field did not have a strong influence on the measurement; namely, that the Cox−Merz rule was valid. There was no statistical difference between the estimated results based on the empirical model and the offline rheometry data for these different polymer systems within the specified limits of 50−150 rpm impeller speed and melt temperatures of 120−140 °C. Studying different temperatures was important in validating the model because it showed that the calculated values would be accurate over large differences in the system viscosity. The model was concluded to be adequately reflecting the changes in rheological behavior for the polyester that it would be suitable to study the polymer/water system. Torque data are often reported as well in some of the following sections for discussion when the system was highly dynamic, and it was felt that the findings should be broadly considered without being limited to the polyester-specific Metzner−Otto fitted variables.

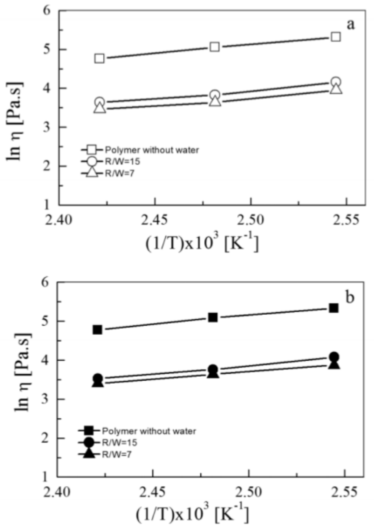

Figure 5. Temperature dependencies for (a) 0.5% w/w NaOH and (b) 1.5% w/w NaOH for different R/W ratios.

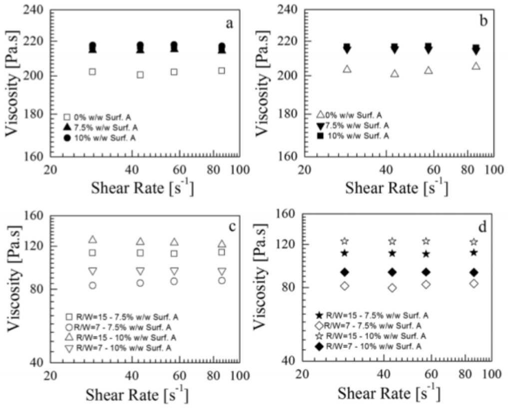

Figure 6. (a) Effect of the surfactant A content with 0.5% w/w NaOH without water at 120 °C at 1.72 MPa. (b) Effect of the surfactant A content with 1.5% w/w NaOH without water at 120 °C at 1.72 MPa. (c) Effect of the surfactant A content with 0.5% w/w NaOH for different R/W ratios at 120 °C at 1.72 MPa. (d) Effect of the surfactant A content with 1.5% w/w NaOH for different R/W ratios at 120 °C at 1.72 MPa.

3.2. Rheology of the Polymer/Water System without Surfactant.

The viscosity curves of the polymer matrix mixed with either 0.5% or 1.5% w/w NaOH are shown in Figure 3 in comparison to the neat polyester (i.e., 0% w/w) for the four tested values of the shear rate. The condition shown corresponded to a melt temperature of 120 °C. First, it was seen that the NaOH concentration had no effect on the viscosity in the absence of water. The consistency in the viscosity (195−206 Pa·s) indicated that any neutralization of the polyester chains by NaOH in the absence of water had no influence on the flow behavior of the polymer. NaOH was added to ultimately convert acidic end groups on the polyester chains into carboxylates so as to improve their interfacial association with water, but according to midrange IR analysis of the polymer samples (using an Nicolet 6700 IR spectrometer at 2 cm^{-1} resolution), no evidence of reaction was found in the absence of water even after 30 min of mixing. Because both Munari et al.[21] and Weiss et al.[22] had reported that the addition of ionic groups along the backbone of linear polymers significantly changes their rheological characteristics, it is assumed here that the concentration of ionic end groups created prior to water addition was too small to produce sufficient chain-to-chain interactions to influence flow, if any neutralization occurred at all. Both particle sizes of ground NaOH added into the polyester without water or surfactant did not significantly change the viscosity of the system, at either concentration. Because of the similarity in the rheological responses between the two particle sizes of NaOH, only the size 2 particles are commented upon for the rest of the study.

With the inclusion of water, the viscosity data presented in Figure 3 showed a significant decrease as the concentration of NaOH increased ($P = 0.0003$) at least for the tested R/W of 15 and 7. The viscosity of the polymer system was also noted to decrease as the water content increased from R/W = 15 to 7 ($P < 0.0001$). These results correspond to steady-state conditions where the temperature of the system had returned to the set point value of 120 °C once the water was added and viscous heat attributed to the impeller speed was dissipated. To understand if these changes in the viscosity were related to morphological change, i.e., preparation of a polymer/water dispersion rather than simple demonstrations of polymer degradation (alkaline hydrolysis[23,24]) or a poorly mixed polymer/water system, the transient rheological response of each condition was examined while water was being added.

Figure 4 showed torque versus water mass fraction plots for conditions with varying NaOH content (0, 0.5, and 1.0%) at 100 and 150 rpm. Figure 4 highlights the two common behaviors seen in the study: one where the decline in the torque (i.e., shear stress) was negligible (or arguably minor) and the second where a rapid substantial drop in the torque was experienced. To quantify the information, the discrete derivative of the torque data (dT/dt) was analyzed and the most significant change in the value was attributed to that mixing condition; the dT/dt values for different contents and different impeller speeds are shown in Table 1. Reduction in the torque at 150 rpm was gradual without NaOH ($dT/dt = -0.0021$ N·m/s) and with 0.5% w/w NaOH ($dT/dt = -0.0035$ N·m/s) but exhibited a severe decline when the NaOH content reached 1.5% w/w ($dT/dt = -0.19$ N·m/s). The sudden torque reduction seen at 1.5% w/w (Figure 4f) was impeller-speed-dependent and did not occur at any lower speed, as demonstrated in Figure 4c for 100 rpm ($dT/dt = -0.0063$ N·m/s). It appeared that the phenomenon related to this sudden torque reduction was shear-dependent. Therefore, unless otherwise stated, all conditions examined for their transient behavior were restricted to speeds of 150 rpm, with the focus of analysis then being on the chemical properties. It is impossible to conclude from this data so far that the torque drop was a response to morphological development related to mixing versus degradation. Certainly, hydrolytic degradation occurred in most samples, as is demonstrated by the gel permeation chromatography (GPC) results in Table 2. However, the extent of chain scission was often less in samples demonstrating the torque drop, suggesting that degradation was

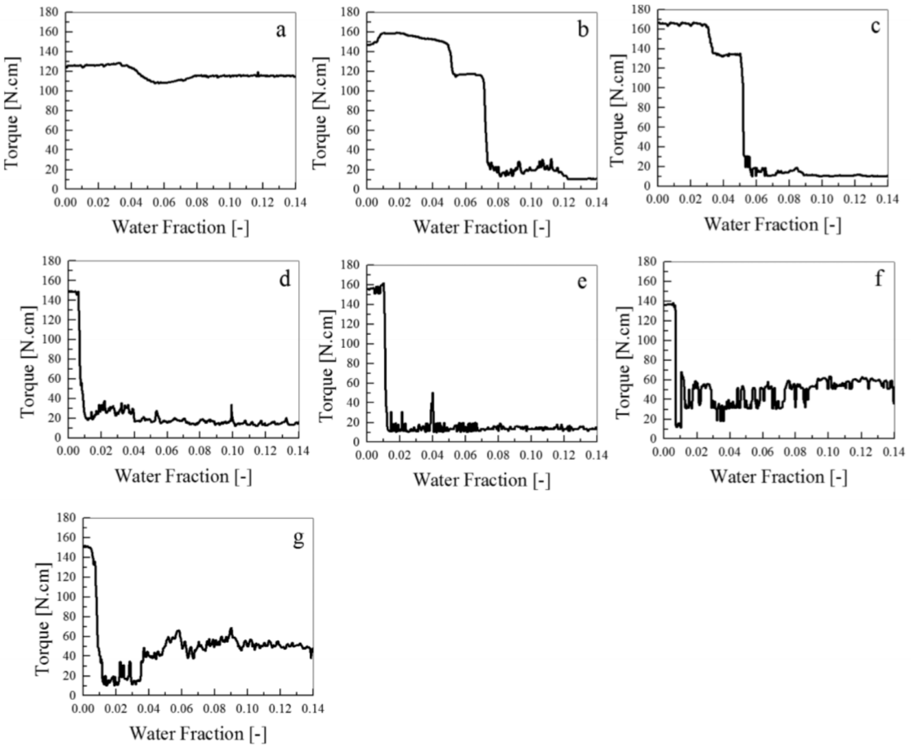

Figure 7. Surfactant A content effect on the torque reduction with/without NaOH at 150 rpm at 1.72 MPa with addition of water: (a) 0% w/w NaOH/0% w/w surfactant A; (b) 0% w/w NaOH/7.5% w/w surfactant A; (c) 0% w/w NaOH/10% w/w surfactant A; (d) 0.5% w/w NaOH/7.5% w/w surfactant A; (e) 0.5% w/w NaOH/10% w/w surfactant A; (f) 1.5% w/w NaOH/7.5% w/w surfactant A; (g) 1.5% w/w NaOH/10% w/w surfactant A.

unlikely the cause. The subsequent results with surface-active ingredients in the following sections were therefore beneficial in making this determination.

The influence of the temperature on the viscosity of the system is demonstrated in Figure 5 by plotting data at 150 rpm for the polyester with 0.5% w/w NaOH (Figure 5a) and 1.5% w/w NaOH (Figure 5b) for conditions without and with water addition. The temperature dependency in these rheological measurements is represented by the flow activation energy (E) which is assumed to follow an Arrhenius relationship:

$$\eta(T_1) = \eta_0(T_0)\exp\left[-\frac{E}{R}\left(\frac{1}{T_1} - \frac{1}{T_0}\right)\right] \tag{5}$$

where η is the viscosity (Pa·s), E is the flow activation energy (J/mol), R is the gas constant, 8.314 J/mol·K, and T is the melt temperature (K). Considering the evidence of alkaline hydrolysis given above, it should be realized that this activation energy term includes the effect of the temperature on the degradation reaction as well. Although the contribution by degradation is considered minor based on the fact that the energy values were similar for cases with no surfactant and surfactant B, the degradation was much less in the presence of the surface-active species, as demonstrated in Table 2. The plot of viscosity is reciprocal to the temperature used because the system temperature was below T_g + 100, as mentioned by Wang and Porter.[25] The activation energies were 37.0 ± 1.8, 35.1 ± 1.8, and 32.7 ± 1.8 kJ/mol for no water and R/W = 15 and 7 conditions with 0.5% w/w NaOH, respectively. On the other hand, the activation energies were 37.24 ± 1.8, 33.1 ± 1.8, and 31.7 ± 1.8 kJ/mol for no water and R/W = 15 and 7 conditions with 1.5% w/w NaOH, respectively. These values were similar in magnitude to those reported by Greener et al.[26] and Hsieh et al.[27] for different types of polyesters, being between 65 and 95 kJ/mol for different shear rates. Because the activation energies were similar for 0.5 and 1.5% w/w NaOH, it was decided to present the results only for 1.5% w/w NaOH for rest of the study. These activation energies indicated that the barrier to flow decreased in the presence of water, which was expected from the increase in the free volume. The NaOH concentration showed no significant sensitivity to the temperature, indicating that any effect it had on the system was insufficient to affect the free volume of the polyester.

3.3. Rheology of the Polymer/Water System with Surfactant A.

From the viscosity curves shown in Figure 6a at 0.5% w/w NaOH and in Figure 6b at 1.5% w/w NaOH for 120 °C, it can be seen that when no water was present the inclusion of surfactant A had a positive influence on the resistance to flow ($P = 0.048$), but increasing its concentration from 7.5% to 10% w/w had no observable effect. The fact that this surfactant did

DOI: 10.1021/acs.iecr.5b00765
Ind. Eng. Chem. Res. 2015, 54, 5820−5829

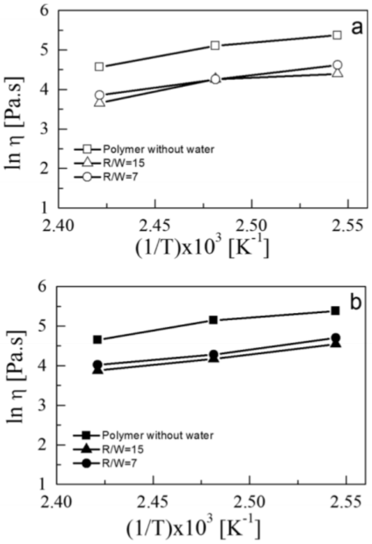

Figure 8. Temperature dependencies for (a) 7.5% w/w surfactant A and 1.5% w/w NaOH and (b) 10% w/w surfactant A and 1.5% w/w NaOH for different R/W ratios.

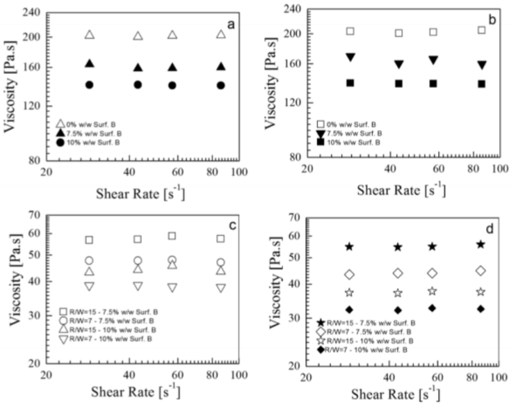

Figure 9. (a) Effect of the surfactant B content with 0.5% w/w NaOH without water at 120 °C at 1.72 MPa. (b) Effect of the surfactant B content with 1.5% w/w NaOH without water at 120 °C at 1.72 MPa. (c) Effect of the surfactant B content with 0.5% w/w NaOH for different R/W ratios at 120 °C at 1.72 MPa. (d) Effect of the surfactant B content with 1.5% w/w NaOH for different R/W ratios at 120 °C at 1.72 MPa.

not totally dissolve (based on the observations of samples after the tests) indicated that its particle size of 973 ± 45 μm (d_{50}) was sufficient to act as a reinforcement filler, yet the two concentrations did not differ adequately to see a concentration effect. The NaOH content had no effect on the viscosity without water ($P = 0.182$), which was the same outcome as noted in the previous section without surfactant present. However, unlike in the previous section, the influence of NaOH remained insignificant ($P = 0.544$) on the viscosity in the presence of water (Figure 6c at 0.5% w/w NaOH and Figure 6d at 1.5% w/w NaOH). This could be evidence of a retarding influence by the surfactant on the alkaline hydrolysis reaction. That is to say, the rate of neutralization increases in the presence of surfactant because of increased interfacial development between dissolved NaOH and the polyester end groups, leaving less NaOH for side reactions. Certainly the higher molecular weight of the polyester samples with surfactant shown in Table 2 gives some validity to this hypothesis. All curves in Figure 6 indicated that none of the conditions tested deviated from Newtonian behavior. With the inclusion of water, a positive correlation was seen for the viscosity with surfactant concentration ($P < 0.0001$), whereas the R/W ratio had a negative influence ($P < 0.0001$).

Regarding torque measurements during water addition, the sudden drop noted previously without surfactant now became more common among the trial conditions, even without NaOH. In the absence of NaOH (Figure 7a–c at 0, 7.5, and 10% surfactant), the torque plots characteristically showed two drops with surfactant A. There are sharp torque drops at water mass fractions of 0.047 and 0.075 with $dT/dt = -0.145$ and -0.452 N·m/s, respectively, as seen in Figure 7b for 7.5% w/w surfactant A without NaOH. Subsequently, torque drops at mass fractions of 0.028 and 0.046 with $dT/dt = -0.0517$ and -0.38 N·m/s, respectively, were seen for 10% w/w surfactant A without NaOH (Figure 7c). Figure 7 indicates that the water mass fraction corresponding to the dramatic torque reduction changed in a notable manner from 0.02 to 0.01 with either increasing surfactant A content (up to 10% w/w) or NaOH content (up to 1.5% w/w) at 150 rpm. The dT/dt values were -0.191 and -0.22 N·m/s for 7.5% and 10% w/w surfactant A with 0.5% w/w NaOH content (Figure 7d,e), respectively, and -0.23 and -0.2 N·m/s for 7.5% and 10% w/w surfactant A with 1.5% w/w NaOH content (Figure 7f,g)), respectively. The drop in torque was sudden and significant for these cases in the presence of surfactant and when end group neutralization occurred. However, now at 100 rpm, sudden torque reductions were observed with dT/dt values of -0.25 and -0.29 N·m/s with 7.5% and 10% w/w surfactant A, respectively, at 1.5% w/w NaOH. The system change causing the sudden drop in the torque was less shear-dependent with surfactant A compared to the polyester melt containing only NaOH.

Because the torque value rose gradually after the initial dramatic drop and then stabilized over 20 min, each viscosity measurement was done only after that time period. That torque rise was small compared to the original drop but persistently occurred, lending credence to the belief that the dramatic torque drop was a significant indicator of morphological change in the system rather than being related to rapid and substantial chain degradation. Examples of the gradual torque rise can be seen in Figure 7f,g especially for the system with 1.5% w/w NaOH and either 7.5% or 10% w/w surfactant A.

Figure 8 indicates the temperature dependency of the system with surfactant A when including the 1.5% w/w NaOH content. The calculated Arrhenius activation energies were 49.0 ± 1.2, 45.5 ± 1.2, and 44.9 ± 1.2 kJ/mol for no water and R/W = 15 and 7, respectively, with 7.5% w/w surfactant A at the condition of 1.5% w/w NaOH (Figure 8a). On the other hand, Arrhenius activation energies of 53.2 ± 1.2, 51.0 ± 1.2, and 49.5 ± 1.2 kJ/mol were found for no water and R/W = 15 and 7, respectively, with 10% w/w surfactant A and 1.5% w/w NaOH (Figure 8b). Analysis was done for 150 rpm. The values have increased by 35% with 7.5% w/w surfactant and by 50% with 10% w/w surfactant, in comparison to conditions in the previous section

DOI: 10.1021/acs.iecr.5b00765
Ind. Eng. Chem. Res. 2015, 54, 5820–5829

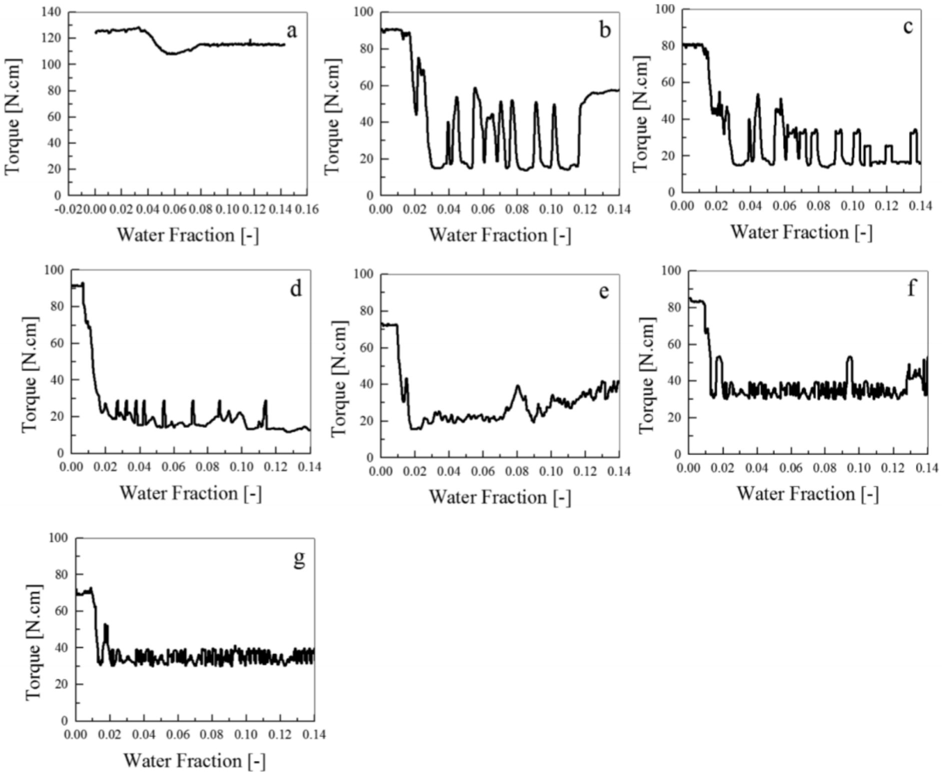

Figure 10. Surfactant B content effect on the torque reduction with/without NaOH at 150 rpm at 1.72 MPa with the addition of water: (a) 0% w/w NaOH/0% w/w surfactant B; (b) 0% w/w NaOH/7.5% w/w surfactant B; (c) 0% w/w NaOH/10% w/w surfactant B; (d) 0.5% w/w NaOH/7.5% w/w surfactant B; (e) 0.5% w/w NaOH/10% w/w surfactant B; (f) 1.5% w/w NaOH/7.5% w/w surfactant B; (g) 1.5% w/w NaOH/10% w/w surfactant B.

without surfactant. However, as noted in the previous section, the Arrhenius activation energy to flow decreased with increasing water content. The rise in the activation energy could be due to the fact that the surfactant did not dissolve completely in the system; however, no other chemical variable in this study has brought about such a large change. The result cannot be fully explained, although it may be related to the observation of Song et al.^{4} that a maximum in the viscosity exists for a polymer/water dispersion close to its phase inversion point.

3.4. Rheology of the Polymer/Water System with Surfactant B. Surfactant B is in its molten state as a low-molecular-weight oligomer during the process, and hence the viscosity of the system expectedly decreased with increasing content ($P = 0.0036$) when water was not present. This is displayed for both conditions of 0.5 and 1.5% w/w NaOH in parts a and b of Figure 9. Similar to the previous two cases above, the effect of the NaOH concentration remained insignificant ($P = 0.0618$) on the viscosity even when in the presence of surfactant B.

Statistical analysis of all results at 120 °C showed that surfactant B had no influence on the viscosity ($P = 0.0579$) when water was present at either R/W ratio (Figure 9c at 0.5% w/w NaOH and Figure 9d at 1.5% w/w NaOH). Moreover, the NaOH content ($P = 0.001$) and R/W ratio ($P < 0.0001$) had negative influences on the viscosity when surfactant B was present.

A plot of torque versus water fraction for samples containing surfactant B with the addition of water is shown in Figure 10. An abrupt torque reduction can be observed around a water fraction of 0.01 when surfactant B was used with NaOH (Figure 10d−g) and at a water fraction of 0.02 without NaOH (Figure 10b,c); these values are similar to the range of water fractions between 0.01 and 0.02 found with surfactant A. The calculated dT/dt values were −0.074 and −0.055 N.·m/s with 7.5 and 10% w/w surfactant B (without NaOH), respectively. Sharper drops of −0.103 and −0.106 N·m/s were, however, found with 7.5% and 10% w/w surfactant, respectively, when 0.5% w/w NaOH was included (Table 1 and Figure 10d,e). However, this was not replicated at 1.5% w/w NaOH, with dT/dt values of −0.033 to −0.029 N·m/s noted for surfactant concentrations of 7.5−10% w/w, respectively (Table 1 and Figure 10f,g). The magnitude of the dT/dt values for surfactant B was larger than that found with surfactant A, which was likely due to the fact that, being in a molten state, it offered a higher interfacial area with water upon mixing.

Another interesting phenomenon noted with the dramatic torque data were that the system appeared less stable with the

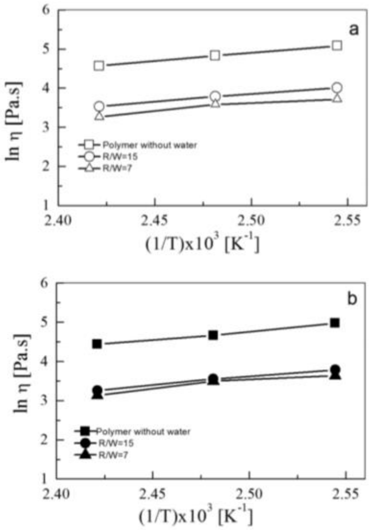

Figure 11. Temperature dependencies for (a) 7.5% w/w surfactant B and 1.5% w/w NaOH and (b) 10% w/w surfactant B and 1.5% w/w NaOH for different R/W ratios.

addition of water when surfactant B was used, as seen in Figure 10. The torque oscillated considerably, especially when surfactant B was present without NaOH, suggesting that the morphology was unstable at these conditions; such instability was not noted with surfactant A. Figure 10d showed that torque oscillations were also present for the condition with 7.5% w/w surfactant B and 0.5% w/w NaOH. At 10% w/w surfactant B, the system was now stable and the gradual torque rise after the drop was seen once again, as noted with surfactant A (Figure 10e). The torque response of the system left the belief that surfactant A produced a more stable morphology at a lower concentration compared to surfactant B.

Figure 11 displays the temperature dependency of the system when the surfactant B was used, again at 1.5% w/w NaOH content for comparison with the other two cases above. Arrhenius activation energies were 34.8 ± 1.5, 32.4 ± 1.5, and 30.6 ± 1.5 kJ/mol for no water and R/W = 15 and 7, respectively, with 7.5% w/w surfactant B and 1.5% w/w NaOH content (Figure 11a). On the other hand, Arrhenius activation energies were 35.9 ± 1.5, 34.4 ± 1.5 and 32.6 ± 1.5 kJ/mol for no water, R/W=15 and R/W=7, respectively with 10% w/w surfactant B and 1.5% w/w NaOH content (Figure 11b). As with the previous two cases, increasing the water content decreased the activation energy of the system. The barrier to flow was lowest when surfactant B was present, although only slightly lower compared to the case without surfactant, and its concentration had no influence. This was considered to be the plasticizing influence of a low-viscosity liquid (surfactant B) being added into the polyester. The fact that this surface-active species did not increase the activation energy similar to surfactant A may be related to the system instability mentioned above and our belief that it was a less effective surfactant for emulsifying the polyester.

4. CONCLUSION

Rheological analysis was used to study the emulsification mechanism of an aqueous polyester dispersion in a pressurized batch reactor by applying the Metzner−Otto approach. The transient response of the reactor torque sensor provided the most definitive information on the mixed polymer/water system because its morphology changed with the selected surface-active ingredients and process conditions. A rapid torque drop that could not be attributed to polymer degradation was believed to be indicative of a developed morphological flow field corresponding to an emulsion. The morphology was never created without surface-active ingredients; surface-active ingredients for this discussion included the use of NaOH for neutralization of the carboxylic acid end groups. The highest impeller speed tested, 150 rpm, was necessary to produce the morphology at the highest tested concentration of NaOH without surfactant but could be formed at a slower speed of 100 rpm when in the presence of a surfactant. The stability in the torque monitored during water addition led to a means of evaluating the suitability of surfactants for the dispersed system. In this regard, surfactant A (sodium dodecylbenzenesulfonate) was considered to produce a more stable morphology than surfactant B (a long-chain, linear primary carboxylic acid) based on the torque data.

■ AUTHOR INFORMATION

Corresponding Author

*Tel: (905) 525-9140 ext. 23213. E-mail: mthomps@mcmaster.ca.

Notes

The authors declare no competing financial interest.

■ ACKNOWLEDGMENTS

The authors thank the Xerox Corporation for their generous funding of this work as well as for the provision of the resin. Thanks to the Xerox Research Centre of Canada for their loan of the batch mixer for these trials. Furthermore, we wish to express our thanks to Mark Arnould at Xerox Webster who conducted the countless numbers of GPC tests to determine the molecular weights of our polymer samples.

■ REFERENCES

(1) Adeyeye, C. M.; Price, J. C. Development and evaluation of sustained release ibuprofen−wax microspheres. I. Effect of formulation variables on physical characteristics. *Pharm. Res.* **1991**, *8*, 1377.

(2) Adeyeye, C. M.; Price, J. C. Development and evaluation of sustained release ibuprofen−wax microspheres. II. In vitro dissolution studies. *Pharm. Res.* **1994**, *11*, 57.

(3) Bodmeier, R.; Wang, J.; Bhagwatwar, H. Process and formulation variables in the preparation of wax microparticles by melt dispersion technique for water insoluble drugs. *J. Microencapsulation* **1992**, *9*, 89.

(4) Song, D.; Zhang, W.; Gupta, R. K.; Melby, E. G. Role of Operating Conditions in Determining Droplet Size and Viscosity of Tackifier Emulsions Formed Via Phase Inversion. *AIChE J.* **2011**, *57* (1), 96.

(5) Akay, G.; Tong, L. Preparation of Colloidal Low-Density Polyethylene Latexes by Flow-Induced Phase Inversion Emulsification of Polymer Melt in Water. *J. Colloid Interface Sci.* **2001**, *239*, 342.

(6) Akay, G.; Tong, L.; Bakr, H. Preparation of ethylene vinyl acetate copolymer latex by flow induced phase inversion emulsification. *J. Mater. Sci.* **2002**, *37*, 4811.

(7) Hermoso, J.; Jofore, B. D.; Martinez-Boza, F. J.; Gallegos, C.; Hermoso.; et al. High Pressure Mixing Rheology of Drilling Fluids. *Ind. Eng. Chem. Res.* **2012**, *51*, 14399.

(8) Ulbrecht, J. J.; Carreau, P. J. Mixing of Viscous non-Newtonian Fluids. *Mixing of Liquids by Mechanical Agitation*; Gordon and Breach: New York, 1985; Chapter 4.

(9) Tatterson, G. B. *Fluid Mixing and Gas Dispersion in Agitated Tank*; McGraw-Hill: New York, 1991.

(10) Metzner, A. B.; Otto, R. E. Agitation of Non-Newtonian Fluids. *AIChE J.* **1957**, *3*, 3.

(11) Calderbank, P. H.; Moo-Young, M. B. The Power Characteristics of Agitators for the Mixing of Newtonian and non-Newtonian Fluids. *Trans. Inst. Chem. Eng.* **1961**, *39*, 337.

(12) Beckner, J. L.; Smith, J. M. Anchor Agitated System: Power Input with Newtonian and Pseudo-Plastic Fluids. *Trans. Inst. Chem. Eng.* **1966**, *44*, 224.

(13) Rieger, F.; Novak, V. Power Consumption of Agitators in Highly Viscous Non Newtonian Liquids. *Trans. Inst. Chem. Eng.* **1973**, *51*, 105.

(14) Tanguy, P. A.; Thibault, F.; Brito De la Fuente, E. A New Investigation of the Metzner Otto Concept for Anchor Mixing Impellers. *Can. J. Chem. Eng.* **1996**, *74*, 220.

(15) Bousmina, M.; Ait-Kadi, A.; Faisant, J. B. Determination of shear rate and viscosity from batch mixer data. *J. Rheol.* **1999**, *43* (2), 415.

(16) Santi, C. R.; Hage, E.; Correa, C. A.; Vlachopoulos, J. Torque Viscometry of Molten Polymers and Composites. *Appl. Rheol.* **2009**, *19*, 13148(1).

(17) Carreau, P. J.; Chhabra, R. P.; Cheng, J. Effect of Rheological Properties on Power Consumption with Helical Ribbon Agitators. *AIChE J.* **1993**, *39*, 1421.

(18) Bravo, V. L.; Hrymak, A. N.; Wright, J. D. Numerical simulation of pressure and velocity profiles in kneading elements of a co-rotating twin screw extruder. *Polym. Eng. Sci.* **2000**, *40* (2), 525.

(19) Li, T.; Manas-Zloczower, I. Flow field analysis of an intermeshing counterrotating twin screw extruder. *Polym. Eng. Sci.* **1994**, *34* (7), 551.

(20) Anne-Archard, D.; Marouche, M.; Boisson, H. C. Hydrodynamics and Metzner–Otto Correlation in Stirred Vessels for Yield Stress Fluids. *Chem. Eng. J.* **2006**, *125*, 15.

(21) Munari, A.; Fiorini, M.; Boisson, G.; Plati, F. J. Rheological behavior of poly(1,4-butylene isophthalate) containing sodium sulfonate groups. *Appl. Polym. Sci.* **1993**, *50*, 159.

(22) Weiss, R. A.; Fitzgerald, J. J.; Kim, D. Viscoelastic behavior of lightly sulfonated polystyrene ionomers. *Macromolecules* **1991**, *24*, 1071.

(23) Mishra, S.; Zope, V. S.; Goje, A. S. Kinetic and thermodynamic studies of depolymerisation of poly(ethylene terephthalate) by saponification reaction. *Polym. Int.* **2002**, *51*, 1310.

(24) East, G. C.; Rahman, M. Effect of applied stress on the alkaline hydrolysis of geotextile poly(ethylene terephthalate). Part 1: room temperature. *Polymer* **1999**, *40*, 2281.

(25) Wang, J. S.; Porter, R. S. On the viscosity-temperature behavior of polymer melts. *Rheol. Acta* **1995**, *34*, 496.

(26) Greener, J.; Gillmor, J. R.; Dally, R. C. Melt Rheology of a Class of Polyester Ionomers. *Macromolecules* **1993**, *26*, 6416.

(27) Hsieh, T. T.; Tiu, C.; Simon, G. P. Melt rheology of aliphatic hyperbranched polyesters with various molecular weights. *Polymer* **2001**, *42*, 1931.

DOI: 10.1021/acs.iecr.5b00765
Ind. Eng. Chem. Res. 2015, 54, 5820−5829

Chapter 3 Inline Rheological Behaviour of Dispersed Water in a Polyester Matrix With a Twin Screw Extruder

All experiments and data anlaysis in Chapter 3 were conducted by the thesis author. M. Arnould at Xerox Webster conducted GPC test to determine molecular weights of the polymer samples. A. Klymachyov and R. Sheppart did NMR and HPLC test in order to identfy the process modifier respectively. J. Pawlak and D. Lawton provided technical guidance during the project. This chapter is published in Willey Online Library, Polymer Engineering & Science—2017, DOI 10.1002/pen.24613. It is reprinted permission from John Wiley and Sons.

Inline Rheological Behavior of Dispersed Water in a Polyester Matrix With a Twin Screw Extruder

A. Goger,[1] **M.R. Thompson**,[1] **J.L. Pawlak**,[2] **M.A. Arnould**,[2] **A. Klymachyov**,[2] **R. Sheppard**,[2] **D.J.W. Lawton**[3]
[1] *Department of Chemical Engineering, McMaster University, Hamilton, Ontario, Canada*
[2] *Xerox Corporation, Rochester, New York*
[3] *Xerox Research Center of Canada, Mississauga, Ontario, Canada*

Solvent-free extrusion emulsification (SFEE) is a complex process using twin-screw extrusion to prepare solid-liquid dispersions of high viscosity polymers and has received little study to date on its inherent mechanisms. To gain rheological insights into the earliest stage of SFEE as the interfacial boundary between water and polymer grows, prior to phase inversion, an inline orifice-plate type viscometer is introduced to monitor transient behavior over a wide range of viscosities. The presented work examines rheological changes of a polyester-water system produced by varying two factors thought to significantly control the final state of the dispersion, specifically polar group contributions to surface energy and viscosity. A processing modifier was combined with the polyester to study the influence of these two factors. The inline viscometer revealed an abrupt transition in viscosity occurred with the developed state of water dispersion, confirming observations of a prior batch study. Analysis of the rheological response indicated that a higher polar surface energy contribution had the greatest influence on the state of this transition, and that a steeper transition was related to greater incorporation of water within the polyester matrix. POLYM. ENG. SCI., 00:000–000, 2017. © 2017 Society of Plastics Engineers

INTRODUCTION

Solid-liquid dispersions consisting of sub-micron polymer particles have many industrial applications such as adhesives, paints, or textile, and paper coatings. Conventional emulsification techniques are losing prevalence due to the high costs surrounding solvent recovery and increasingly stringent environmental regulations, especially pertaining to the health and safety of workers and the consumer. Exclusive use of water as an environmentally benign medium is preferred in green manufacturing processes. This article looks at aspects of a new green manufacturing process utilizing a conventional twin-screw extruder that is intent on producing an aqueous dispersion of high viscosity polymers internally by a top-down approach.

The top-down approach for preparing submicron polymer particles is generally considered when polymerization in water is implausible. However, mechanical top-down methods, like rotor-stator homogenization or milling, experience considerable difficulties in controlling the product particle size especially below the micron scale and hence, solvent emulsification is generally preferred as it is a phase-inversion technique [1–3]. In solvent emulsification, the solvent is responsible for lowering the system viscosity by dissolving the polymer, as well as acting as a surface-active agent. Particles are ultimately formed on dilution with water. Solvent-free emulsification is a less robust phase-inversion technique as it experiences greater difficulties in countering the high viscosity of many industrially interesting polymers (namely 1–1,000 Pa s) due to the absence of organic solvents, but is emerging to show its effectiveness with several viscous systems [4–9]. For example, Ashrafizadeh et al. [9] demonstrated the emulsification of crude oil by homogenization, which had a viscosity of 2.7 Pa·s, with water and no hazardous solvents at 25°C. They produced oil domains with a Sauter mean diameter varying between 8 and 25 μm among their samples. These are quite large domain sizes relative to standard emulsions but should be expected as the viscosity of the dispersed phase increases in such mechanical dispersion processes [10]. Song et al. [5] created a waterborne, pressure-sensitive adhesive with a multi-impeller batch mixer from rosin ester and partially hydrogenated wood rosin acid having a blend viscosity of 5 Pa·s from 43.3°C to 54.4°C. In their case, the mean particle size of the rosin emulsion varied between 0.6 and 1.5 μm for different processing conditions, smaller in their case by the better compatibility of rosin with water than crude oil. However, a closer example to this study would be the work of Akay et al. [6–8], who studied aqueous phase inversion in a batch mixer for different polymer melts with relatively high viscosities, including low density polyethylene which had a viscosity of approximately 50 Pa s. Moreover, the mean particle size changed between 1.03 and 4.19 μm for different content of hydrophobically modified water-soluble polymers. As the viscosity of the polymer intended to be emulsified increases, demands on the processing method to bring water uniformly into an oleophilic phase grow more difficult. For viscosities above 10 Pa s, a twin-screw extruder seems well suited as process equipment to the task of dispersion but its continuous nature introduces challenging constraints on emulsification since the available residence time for adequately mixing that may result in phase inversion is limited to seconds.

The use of a twin-screw extruder to emulsify polymers in the manner described above is referred to as *solvent-free extrusion emulsification* (SFEE) and was first patented by Abe et al. [11] in 1982. The SFEE process is exceedingly complicated and currently runs with a very narrow window of stable operation [12, 13], but understanding the mechanisms related to the process will permit improved processability. One of the most critical steps in the process is increasing the surface area between the polymer melt and water phases prior to phase inversion, through intensive mixing and appropriate chemistry. For Song et al. [5],

---

Additional Supporting Information may be found in the online version of this article.

Correspondence to: M.R. Thompson; e-mail: mthomps@mcmaster.ca

Contract grant sponsor: Xerox Corporation.
DOI 10.1002/pen.24613

base neutralization of the rosin acid promoted incorporation of water into the oleophilic matrix, leading to suitable conditions for phase inversion. For higher viscosity polymers like the polyester under study in this work, this neutralization reaction can produce chain degradation, which was not a point addressed in their study. In SFEE, this neutralization must occur simultaneously with incorporation of water to reduce the interfacial energy as the dispersion of water domains increases the interfacial area. In this study, the changes to molecular weight and generation of surface-active endgroups will be separated to understand which factor has a more significant influence on improved water dispersion within an oleophilic matrix.

The purpose of this article is to better understand this mechanism of water dispersion into a high viscosity polymer melt, which is prior to phase inversion in SFEE; emulsions will not be produced in this work as a result of its focus but presented in a future paper on SFEE. As mentioned above, improving the understanding of SFEE will be done by decoupling two factors which have been noted to occur during the initial water dispersion step, which are mixing and the polar group contributions to both surface energy and chain length reduction by utilizing a novel inline rheometer. The work builds on a previous study [14] that was a rheological study of the dispersion of water into a high viscosity molten polyester using a batch reactor.

MATERIALS AND METHODS

Material

A polyester synthesized from fumaric acid (FA) and dipropoxylated bisphenol A (pBPA) was provided by the Xerox Corporation (Webster, NY). The resin was a high flow grade (M_w=17081g/mol; M_W/M_N=4.2) with an acid number of 17.7 ± 1.7 mg/g KOH. Sodium hydroxide (NaOH) was purchased from Caledon Laboratories Ltd. (Georgetown, ON). Deionized water (>0.1 μS/cm^2) were used in the trials. Samples of the monomers, FA, and pBPA, were provided by Xerox Corporation to prepare a processing modifier resembling the polyester.

Processing Modifier Preparation

The modifier to adjust viscosity and interfacial properties of the polyester with water, was prepared by reacting the two monomers at a 1:1 molar stoichiometry for one hour at 180°C with 0.1 wt% catalyst (Fascat 4100; PMC Group, Mount Laurel, NJ). The resulting mixture of monomer and oligomer species ground but otherwise used without post-treatment was referred to as non-converted (NC) modifier in the study. The grade referred to as converted (C) modifier had any existing acid endgroup neutralized with 10 wt% $NaOH_{(aq)}$ for three hours at 60°C under agitation by an impeller at 300 rpm. The neutralized modifier was subsequently washed with deionized water until the pH of the wash water had dropped below 8. An acid number of zero was found on completion of the neutralization reaction. Both NC and C modifiers were used to lower the matrix viscosity in this study.

Extruder Setup

Extrusion trials were done with a 40 L/D, 27 mm Leistritz ZSE-HP co-rotating twin screw extruder (TSE) supplied by the American Leistritz Extruder Corporation (Somerville, NJ). The barrel temperature profile was kept constant at 95°C in every zone. The extruder was operated at a fixed screw speed of 300 rpm. The polyester flake and processing modifiers were manually blended and then fed at 8 kg/h by a DDSR20 gravimetric feeder (Brabender Technologie; Mississauga, Ontario). Water was fed to a zone 26 L/D upstream of the die with a 260D high pressure syringe pump (Teledyne Isco; Lincoln, NE); this offers a much longer mixing time than is normal for SFEE but ensures the greatest chances that the water will be fully incorporated on reaching the inline rheometer. An intensive mixing screw design was used as similar by Neubauer and Dunchus [15], though the actual design cannot be provided due to proprietary restrictions.

Inline Rheometer

The extruder die functioned as an inline rheometer in the study, based on an orifice plate flowmeter design. The main bore diameter of the die was 15 mm and included a 2 mm orifice plate midway along its length to increase the pressure difference, as seen in Fig. 1. The aim of the design was to partially restrict the exit of the polymer-water mixture so that it did not drool and to be able to accurately detect the pressure drop across the die for trials where high water content was used. For the present trials, the die was configured with two 21 MPa pressure transducers (model PT467E; Dynisco) at a distance of 17 mm either side of the orifice plate; both transducers were positioned to ensure that fully developed flow was being monitored A metal-sheathed, grounded K-type thermo couple was placed into the melt within 87 mm away from the orifice plate toward the die exit to take into account effects such as water cooling and viscous dissipation. The rheometer had an estimated measurement sensitivity to viscosities for a resin-to-water (*R*/*W*) ratio as low as 1.5 based on the 0.5% nameplate accuracy of the selected pressure transducers; this article will present the amount of water being added into the process as a resin-to-water ratio (*R*/*W*) rather than as a weight basis to be consistent with the industry to which the technology applies.

This inline rheometer was calibrated using the open-source numerical software package, OpenFOAM 2.0.1 (OpenCFD, Bracknell, UK), for the 3-D simulated environment shown in Fig. 1c. The flow domain of the die was meshed with 93,782 hexahedral elements using GAMBIT (Fluent Inc., Canonsburg, PA). Mass and momentum conservation equations were solved by the SIMPLE algorithm. A single-phase fluid of differing viscosities from 0.001–200 Pa s was approximated by solving the simulations with a power-law constitutive model with an index value of 0.96; the index value corresponded to the neat polyester as obtained from off-line parallel-plate and capillary rheometers [14]. A non-slip boundary condition was assumed valid at all die walls. The inlet of the die was set to 2.22×10^{-6} m^3/s and the outlet boundary was fixed at atmospheric pressure. Laminar steady shear flow under the isothermal conditions was used for the simulations.

Trial Procedure. Trials began by adding water at $R/W = 135$ (i.e., 0.74 wt%) to prevent the molten polyester from blocking the water injector. The polyester feedstock contained varying content (0, 0.5, 1.5, and 5 wt%) of either converted or non-converted modifier in a trial. The system was run for five

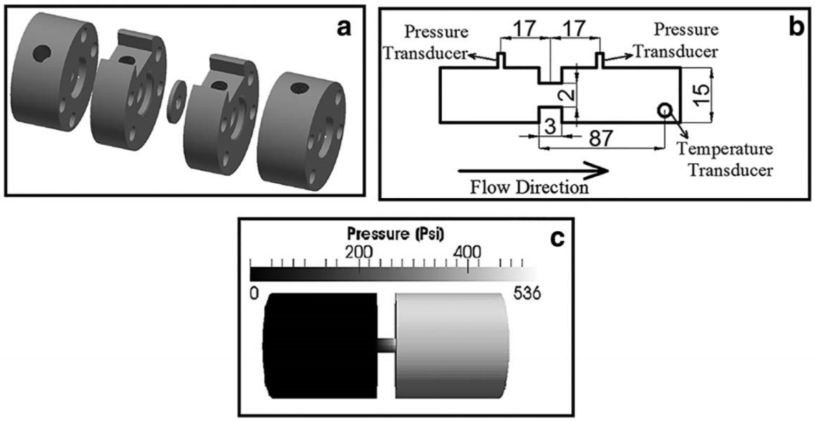

FIG. 1. (a) 3D view of customized die. (b) Dimensions of the customized die. (c) Pressure distribution in customized die at viscosity of 200 Pa s.*All dimensions are in mm.

minutes to reach steady conditions, at which point the fluctuations in monitored viscosity dropped well below ±4.5%. After the first five minutes, the rate of water addition was increased to $R/W = 5$.

The melt temperature was measured in the die and as a result, the inline apparent viscosity data were corrected to a comparable 100°C using an Arrhenius relationship with flow activation energy of 32.7 kJ/mol (determined by off-line rheometry). This was necessary as the melt temperature varied ±4°C for the different modifier conditions on account of viscous heat dissipation, making it necessary to standardize to a reference temperature for their comparison. Extrudate were collected for analysis after an additional eight minutes once steady-state conditions in the extruder had been confirmed by pressure and temperature measurements at the die. Most of the extrudate were dried under vacuum conditions at 60°C over night for characterizations. A small sample of the extrudate was not dried but rather immediately dispersed in water, as described below.

Offline Rheological Properties. Shear viscosities of the extruded polyester without water were measured in a parallel plate rheometer (ARES; TA Instruments, New Castle, DE) at 100°C, 110°C, 120°C, 130°C, and 140°C, respectively. The flow activation energy was determined based on an Arrhenius correlation to correct for viscous dissipation in the inline rheometer. In addition, complex viscosity curves of the dried extrudates containing different modifier types and contents were determined by an ARES parallel plate rheometer (TA Instruments, New Castle, DE) at 100°C. The diameter of the parallel plate was 25 mm and gap distance between plates was 1.5 mm. It was operated in oscillating mode over a frequency range of 0.1–100 rad/s at a strain of 18% (selected based on a strain sweep test).

NMR Spectroscopy

Weighted modifier was dissolved in a pyridine-deuterated chloroform solution containing a known amount of a perfluorinated version of BPA (Bisphenol AF) as an internal reference. To the mixture, 2-chloro-4,4,5,5-tetramethyl-1,3,2-dioxaphospholane (CTDP) was added as the phosphorus derivitizing agent. CTDP reacts quickly and quantitatively with both acid and hydroxyl groups, and through the use of Bisphenol AF as an internal standard, the amount of each specific acid and hydroxyl group can be determined [16]. Phosphorus-31(^{31}P) NMR measurements were performed using a Bruker AV-400 NMR spectrometer.

HPLC Spectroscopy

The samples were dissolved in methanol and filtered through 0.2 μm Teflon (PTFE) prior to analysis. The samples were analyzed by liquid chromatography (LC)/UV and LC/MS. The amount of pBPA plus FA/pBPA adduct were determined using an authentic sample of pBPA and assuming a similar response factor for the 1:1 adduct. The amount of pBPA was determined using LC/MS relative to the authentic standard. The amount of the 1:1 adduct was estimated as equal to the difference between the two methods.

LC/UV. 2 μL of each sample was injected onto the LC system where the components were separated on a 3 mm x 50 mm Hypersil ODS (3 μm) C-18 column using a 0.05% phosphoric acid/methanol gradient mobile phase with UV detection at 228 nm.

LC/MS. The samples were separated on a 2 × 30 mm Kinetex XB-C18 column at 300 μL/min using a gradient from 100% water to 100% methanol over 8 min on the Accela High Speed LC system interfaced to the Q-Exactive mass spectrometer. Data were collected using positive and negative mode electrospray ionization.

Gel Permeation Chromatography

Samples were prepared by dissolving approximately 5 mg modifiers or extrudate samples/mL in spectral grade $CHCl_3$ spiked with 0.1% (v/v) triethylamine (99% purity) followed by filtration through a 0.2 μm syringe filter (Whatman PTFE) into

2 mL sample vials. The samples were injected using an autoinjector onto a Polymer Labs GPC-50 System equipped with 2 × 5 µm PL Mixed Bed C GPC columns (300 × 7.5 mm) with a guard column and a Wyatt triple detection system (light scattering, viscometry and refractive index). Standard molecular weights were calculated using a 10-point polystyrene linear calibration and the absolute molecular weights were calculated using the triple detection data.

Scanning Electron Microscopy (SEM)

Morphology of the samples were evaluated using a Hitachi SU8000 scanning electron microscope (SEM). The accelerating voltage utilized was 2.0 kV. Samples were prepared by drying the extrudate samples out in a fume hood before mounting on a stage and sputter coated with platinum/palladium.

Thermal Properties

Thermal properties of dried polyester, extrudate samples, and neat modifiers were measured using a DSC Q200 differential scanning calorimeter (TA Instruments, New Castle, DE) with a heat-cool-heat cycle over a temperature range of 0°C–200°C for a heating/cooling rate of 10°C/min in an inert atmosphere (50 mL/min N_2). Glass transition temperature (T_g) and peak melting temperature (T_m) were determined from the thermograms using Universal Analysis V1.7V software (TA Instruments, New Castle, DE).

Particle Dispersion

To interpret dynamic viscosity changes seen in the trials as indicators of water incorporation into the polymer and hence the state of the polymer system in terms of readiness to emulsify, it was necessary to test for this possibility outside of the extruder; neither the extruder, screw design, nor die configuration were suitable for emulsification in this work as that was not the focus of the study. Approximately 3 grams of the extrudate was sampled at the die and immediately transferred to a 60°C heated water bath system fitted with a Polytron® PT 45/80 homogenizer (12 mm tip diameter). The sample was dispersed into 0.5 L of MilliQ water at 16,000 rpm over a three minutes period. Finally, 0.3 L of additional water was introduced to cool the dispersed extrudate samples before it was collected for particle size analysis. The premise to this test was that polymer samples containing thinner striated layers of water would disperse into smaller particles by homogenization. This assumes that the morphology of the polymer-water mixture demonstrates sufficiently slow stress relaxation that its state of mixedness changes little in the time taken to transfer samples from the die to the water bath.

Particle size distributions of the homogenized extrudate samples were measured with a Malvern Mastersizer 2000™ (Malvern, United Kingdom). It was capable of detecting particles in a range of 0.2–2000 µm. The mean particle size distributions were determined based on three replicate measurements ($n = 3$). The mean particle size (D_{50}) was used to represent the relatively tendency of the water-polyester extrudate to be dispersed into a greater amount of water.

Determination of Surface Energy

Ground and dried extrudate samples were hot pressed in a 5 × 5 × 0.5 cm mold under 2 metric tons for 2 min at 100°C. Surface energy values of the samples were estimated using the sessile drop contact angle method at room temperature with 1-bromonaphthalene (dispersive component $\delta^d = 42.517$ mJ/m^2, polar component $\delta^p = 0.283$ mJ/m^2) and glycerin ($\delta^d = 35.541$ mJ/m^2, $\delta^p = 25.359$ mJ/m^2). Dispersive and polar contributions to the total solid surface energy were calculated according to the Wu [17] method.

RESULTS AND DISCUSSION

Validation of Viscosity Calculations by the Die Rheometer

Neat molten polyester was extruded, without added water or modifier, at barrel/die temperatures of 100–140°C to measure its melt temperature and corresponding pressure drop across the inline rheometer. It is assumed that the Cox-Merz rule was applicable between the measurements in the offline rheometers and the die. Open source numerical software was used to simulate the custom build die for all viscosities of the neat polyester at different temperatures (200 Pa s and less) but also for neat water (0.001 Pa s) to calculate pressure drops. Calculated pressure drops and measured pressure drops across the orifice plate for the neat polyester at the different temperatures differed by less than 5%. Figure 2 compares the results obtained from the numerical simulations with experimental data from a parallel plate rheometer for the neat polyester. A semiempirical pressure drop-viscosity calibration curve, discussed below, is shown in the plot to closely fit to the experimental data.

Examining the system at fixed flow rate and different temperatures produced a range of viscosities for the calibration of the die. According to Bond [18] who examined the entrance pressure drop (P_e) for viscous fluid flow through an orifice plate flowmeter, a linear relationship exists between pressure drop and viscosity. Bond proposed the following equation:

$$P_e = \left(\frac{\mu Q}{R^3}\right) * \vartheta_3 \qquad (1)$$

where μ is the generalized Newtonian viscosity, Q is the volumetric flow rate, R is the radius of the orifice plate, and ϑ_3 is the dimensionless constant for a viscous fluid. A best-fit ($R^2 = 0.98$) semiempirical expression for apparent viscosity was determined with the inline rheometer based on measured

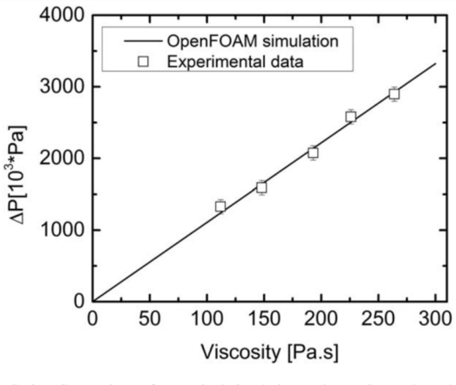

FIG. 2. Comparison of numerical simulation and experimental result.

TABLE 1. Content determination method and content of both NC and C modifier.

Component	Non-converted modifier (relative wt%)	Converted modifier (relative wt%)	Method
FA	7–9%	2–4%	NMR
pBPA (includes all oligomers)	25–30%	32–36%	HPLC
FA-pBPA	15–20%	30–40%	HPLC
pBPA-FA-pBPA	5–10%	1–3%	GPC
pBPA-FA-pBPA-FA-pBPA	6–8%	1–3%	GPC

pressure drop which assumes the validity of the linear correlation observed by Bond. That expression was found to be:

$$\eta = 8.65 * 10^{-5} \Delta P \qquad (2)$$

where ΔP (Pa) is the pressure difference between the two pressure transducers in the die and η is the apparent viscosity (Pa·s). This semiempirical model operates with less than 5% error for viscosities greater than 1 Pa·s. The error from the semiempirical model (*Eq. 2*) increases up to 40% when neat water was considered. The model was considered appropriate in the context of this study for converting a pressure difference into estimates of apparent viscosity since the lowest recorded viscosity was approximately 70 Pa·s.

Use of the inline rheometer and *Eq. 2* in this study is recognized to be based on several significant assumptions. First and foremost, it was assumed that the water-polyester mixtures remained morphologically similar across the orifice plate such that both pressure transducers were measuring flow conditions for the same fluid system. The similarity in individual pressure profiles at the two transducers during the tests suggests that the mixtures were adequately dispersed such that the extensional flow event across the orifice did not noticably affect the morphological state of the mixture; differences in the mixed state of a fluid are often denoted by attenuation of fluctuations in pressure for flow systems. Secondly, it is assumed that the water was adequately dispersed into the polyester such that the fluid flow resembled a single-phase system at all conditions studied; visual observations at the die exit showed no evidence of the water separating from the mixture. Goger et al. [14] previously measured the viscosity of this multiphase system in a batch reactor and found that a uniform distribution of water phase in polyester matrix can be assumed to exist for the polymer/water (i.e., multiple phase) system under the shear and pressurized environment.

Plasticizing Versus Surface Active Influence of the Modifier

The NC and C modifier produced in the study was analyzed by Gel Permeation Chromatography (GPC), NMR, and HPLC to determine their composition. The estimated ratio of monomer, dimer and larger species for the two clean modifiers are summarized in Table 1. The two modifiers consisted mostly of dipropoxylated bisphenol monomer (with the FA either sublimating or being washed away during cleaning) and dimer. Ideally, a modifier with a consistent degree of polymerization suitable for plasticization of the polyester was sought in the study to simplify the comparison between surface tension and viscosity effects on the dispersion process. Since the necessary quantity of modifier used in the study made it too difficult to terminate the reaction to produce exclusively a dimer or trimer, it is necessary to quantify the differences in plasticization between the two modifiers before examining their effects on the extrusion process.

Table 2 shows glass transition temperature (T_g) values for the dried extrudate samples blended with different modifier types and contents. The residual water content among the extruded samples in this analysis was consistent at 1.84 ± 0.07%, determined by a Mettler-Toledo HG63 moisture analyzer. In all cases, samples showed only a single T_g in their DSC thermograms, pointing to miscibility of the modifier in the polyester matrix. With increasing modifier content from 0 to 5 wt%, the T_g was reduced from 61°C to 54°C, respectively, with the NC modifier, and from 61°C to 58°C, respectively, for the C modifier. The decrease in T_g was considered to be a result of increased free volume within the polymer matrix by modifier inclusion. The change in free volume was calculated based on these T_g values for the different polyester blends, using the Flory-Fox method and are summarized in Fig. 3 to highlight the plasticizing effect of these modifiers [19, 20]. The free volume of the polymer was higher with the NC modifier compared to the C modifier for all three concentrations tested. GPC results of the polyester/modifier blends provided in Table 3 confirm that the NC modifier tended to slightly lower the number average molecular weight to a greater extent than the C modifier for 1.5 and 5 wt%. Overall, the NC modifier was a better plasticizer than the C modifier in polyester though ideally they should be equivalent, at least in this characterization where no water was present. The plasticization behavior of the differing modifiers blended into polyester was similarly reflected in the Newtonian melt viscosity curves measured by parallel plate rheometer, with the data included in Fig. 3.

Figure 4 depicts the change in apparent viscosity with respect to the different modifier type and its content blended into the polyester, as measured by the inline rheometer, for $R/W = 135$ (i.e., the minimum water condition used to prevent the injector from being blocked by melt). The plot includes for reference, the apparent viscosities of extruded neat polyester (when the injector was completely removed from the extruder) and the

TABLE 2. Glass transition temperature (T_g) and melting temperature (T_m) of dried extrudate samples and modifier, FA, and bisphenol A.

Sample name	T_g (°C)	T_m (°C)
Neat Polyester	61.3 ± 0.6	–
0.5 wt% non-converted (NC) modifier	60.8 ± 0.3	–
1.5 wt% non-converted (NC) modifier	59.1 ± 0.3	–
5 wt% non-converted (NC) modifier	54.0 ± 0.4	–
0.5 wt% converted (C) modifier	61.1 ± 0.4	–
1.5 wt% converted (C) modifier	60.0 ± 0.4	–
5 wt% converted (C) modifier	57.9 ± 0.3	–
Converted (C) modifier	–	130.8 ± 2.3
Non-converted (NC) modifier	–	136.1 ± 3.1
Bisphenol A	–	67.4 ± 0.4
Fumaric Acid[a]	–	287.0

NC, Non-converted; C, Converted.

[a] Vendor supplied value.

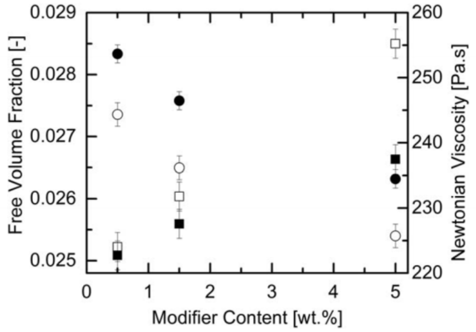

FIG. 3. Free volume fraction and Newtonian viscosity for different modifier types and contents. (□ Non-converted (NC) modifier for free volume fraction, ■ Converted (C) modifier for free volume fraction, ○ Non-converted (NC) modifier for Newtonian viscosity and ● Converted (C) modifier for Newtonian viscosity).

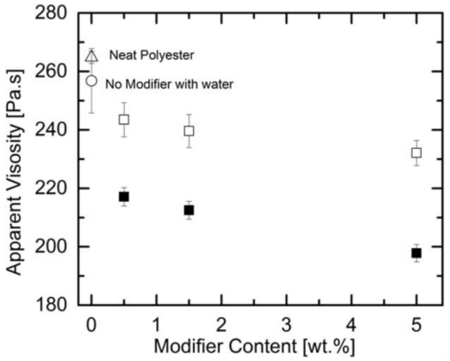

FIG. 4. Apparent viscosity for neat polyester without water, different modifier type and content at resin-to-water ratio (R/W) 135. (□ Non-converted (NC) modifier, ■ Converted (C) modifier, △ Neat polyester without water, ○ No modifier with water).

extruded neat polyester at $R/W = 135$, which were both higher than the modifier containing samples. The uncertainty in apparent viscosity (denoted by the included error bars representing one standard deviation) corresponding to the neat polyester at $R/W = 135$ (21 Pa s) was higher than the uncertainty when either NC or C modifier were present with water. This larger uncertainty was suggestive of poorer mixing between the neat polyester and the small amount of water being added, though no water was visible at the die exit or on the extrudate surface to suggest that the water was not at least being partially incorporated. The plot shows that the apparent viscosity decreased with increasing content of either NC or C modifier. For the NC modified blends, the reported apparent viscosity is similar to the parallel plate data reported in Fig. 3, confirming the accuracy of the inline device. The magnitude in apparent viscosity seen in Fig. 4 was always higher with the non-converted modifier compared to the converted modifier at equivalent concentration in the polyester, which is opposite to expectations based on the free volume and molecular weight of the blends but unlike those measurements the viscosity was determined in the presence of water.

While plasticization resulted from either NC or C modifier being used, as evident by the declining viscosity with increased modifier content, the affinity of the polyester blend for water was always significantly greater with the C modifier. Table 4 indicates that the polar surface energy contribution for the polymer/modifier blend significantly increased from 2.16 to 11.87 mN/m while the dispersive contribution was reduced from 41.2 to 30.56 mN/m, as the C modifier content was increased from 0 to 5 wt%. In comparison, the NC modifier content has a negligibly small effect on the polar versus dispersion contributions to the total surface energy. However, the total surface energy did not vary based on the type of modifier used. Based on this polar contribution, the acid groups of the NC modifier should have much lower affinity for water compared to the carboxylate of the C modifier. Therefore, even though the C modifier itself had a lesser plasticizing effect than the NC modifier, the apparent viscosity of the polyester blend with C modifier was lower than NC modifier at $R/W = 135$ due to improved dispersion of water into the former polymer matrix.

TABLE 3. Number average molecular weight for different modifier type and content.

Sample Name	M_n [g/mol]
Neat polyester	4158 ± 91
0.5 wt% non-converted (NC) modifier	4118 ± 76
1.5 wt% non-converted (NC) modifier	3960 ± 76
5 wt% non-converted (NC) modifier	3529 ± 76
0.5 wt% converted (C) modifier	4168 ± 76
1.5 wt% converted (C) modifier	4012 ± 76
5 wt% converted (C) modifier	3670 ± 76

Dispersion of Water into the Polyester/Modifier System

The addition of a larger amount of water into the molten polyester/modifier blend at $R/W = 5$ produced a significant change in apparent viscosity, as monitored by the inline rheometer, that was determined based on the type and content of

TABLE 4. Dispersive and polar contribution to total surface energy for different modifier type and content.

Sample name	Dispersive contribution (mN/m)	Polar contribution (mN/m)	Total surface energy (mN/m)
Neat polyester	41.2 ± 1.55	2.16 ± 0.46	43.36 ± 1.76
0.5 wt% non-converted (NC) modifier	41.05 ± 1.81	2.12 ± 0.38	43.17 ± 1.54
1.5 wt% non-converted (NC) modifier	40.67 ± 1.62	1.83 ± 0.42	42.50 ± 1.74
5 wt% non-converted (NC) modifier	40.57 ± 0.95	1.46 ± 0.53	41.93 ± 1.61
0.5 wt% converted (C) modifier	37.62 ± 1.15	5.54 ± 0.32	43.16 ± 1.73
1.5 wt% converted (C) modifier	33.41 ± 1.27	7.65 ± 0.41	41.06 ± 1.62
5 wt% converted (C) modifier	30.56 ± 1.35	11.87 ± 0.54	42.43 ± 1.59

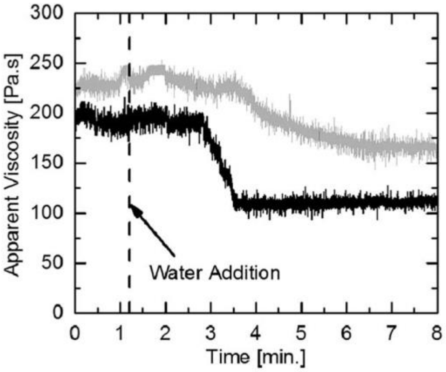

FIG. 5. Example graphs of viscosity versus time from inline rheometer for 0.5 wt%NC modifier and 5 wt% C modifier at *R*/*W* = 5. (−5 wt% C modifier, −5 wt% NC modifier).

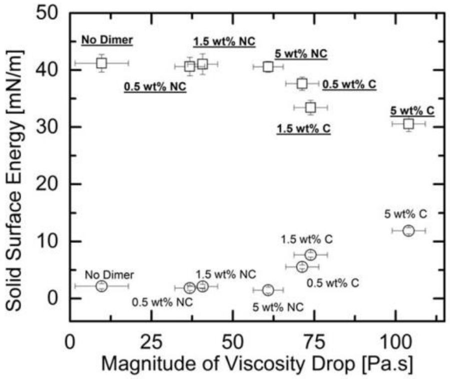

FIG. 6. Dispersive and polar contributions to total solid surface energy versus magnitude of viscosity drop. (☐ Dispersive contribution, ○ Polar contribution).

modifier included. Figure 5 illustrates a difference in apparent viscosity on a time basis after *R*/*W* was decreased from 135 to 5, with a gradual viscosity drop (5 wt% NC modifier) or rapid decline (5 wt% C modifier) shown based on the modifier type used. The plot demonstrates extremes in the transient behavior of the process that were seen once water was added to the process. Similar transient viscosity behavior has been reported by Akay et al. [7] while attempting to disperse water into a molten low density polyethylene containing a surfactant using a batch melt mixer. Our own published results with a batch system [14] reported on a rapid torque drop being observed as water was dispersed into the same molten polyester used in this study, though in that case, surfactants were included. Potential reasons to be considered for the decline are, as follows: (1) water hydrolysis, (2) mechanical degradation, or (3) morphological development of an immiscible polymer-water dispersion; hydrolytic and mechanical degradation are known issues with solvent free extrusion emulsification. Considering the possibilities of water hydrolysis or degradation, the chain length of the extruded polyester without modifier (M_n=4,156 ± 139 g/mol) changed little compared to the original (unprocessed) polyester (M_n=4,158 ± 91 g/mol), exhibiting a viscosity drop of only 7 ± 4 Pa s at *R*/*W* = 5. Comparatively, the viscosity dropped by 71.3 ± 5.1 Pa s for polyester with 0.5 wt% C modifier (M_n=4,168 ± 76 g/mol) and 40.7 ± 4.6 Pa s for polyester with 0.5 wt% NC modifier (M_n=4,118 ± 76 g/mol). The GPC results suggest that hydrolytic and mechanical degradation were both improbable causes of the aforementioned viscosity drop. It had been reported that hydrolytic degradation was not responsible for the rapid torque drops seen in our earlier studies in a pressurized batch reactor either [14]. In both that earlier batch work and in this study, morphological development of polymer-water blend was the considered explanation for the viscosity phenomenon being discussed.

The magnitude and slope of the apparent viscosity corresponding to this region of decline were used to quantify the phenomenon. It should be noted that slope of the horizontal line is assumed to be zero for the slope calculation. With NC modifier used in the polyester blend, the magnitude in viscosity drop (i.e., the difference in viscosity between the two plateau states) increased to 61 Pa s as modifier content increased to its highest loading (5 wt%) in the trials, as seen in Fig. 6. Conversely, the magnitude in viscosity drop was much larger with the C modifier blends, reaching 104 Pa s at the highest modifier loading (5 wt%). Moreover, Fig. 7 indicates that the viscosity drop became very abrupt, based on having the largest slope, with the highest C modifier content (i.e., 131 Pa s/min.) at *R*/*W* = 5. Comparatively, the slope of viscosity drop with NC modifier was less (reaching 46 Pa s/min at 5 wt%) representing a slower decline compared to the blends with C modifier. However, the viscosity drop was still sharper with NC modifier than found with the neat polyester (i.e., 5 Pa s/min) for the *R*/*W* = 5 condition.

The plots in Figs. 6 and 7 included surface energy contributions to reflect the significance of surface active agent on the transient viscosity behavior being observed by the inline rheometer. The samples with no modifier and NC modifier had similar surface energy contributions though showed increasing

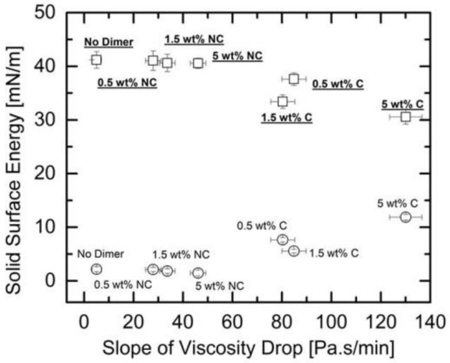

FIG. 7. Dispersive and polar contributions to total solid surface energy versus slope of viscosity drop. (☐ Dispersive contribution, ○ polar contribution).

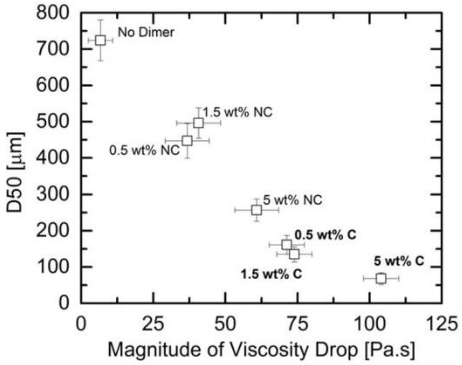

FIG. 8. Magnitude of viscosity drop versus D50 for various modifier types and contents.

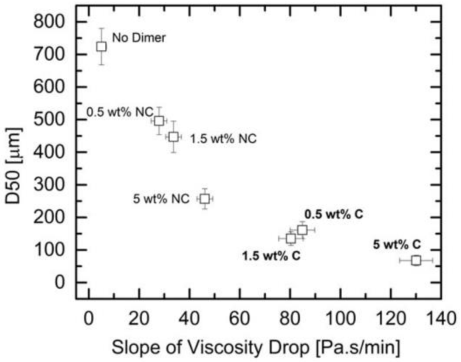

FIG. 9. Slope of viscosity drop versus D50 for various modifier types and contents.

magnitude and slope of the viscosity drop with increasing content, showing that plasticization had an influence on the transition. However, the plots better show that the magnitude and slope of the viscosity drop were significantly larger as the polar surface energy contribution increased, suggesting that this was a stronger effect on the transition even when we account for the difference in free volume afforded between the C and NC modifiers. The carboxylate ions of the C modifier would seem to be effective at the polymer-water interface in decreasing the interfacial tension [9, 21] such that water dispersed more rapidly in the process than solely relying on mechanical energy.

Homogenization of Extrudate Samples

To further affirm that the transient viscosity behavior noted by the inline rheometer in Figure 5 was an indicator of water being intimately dispersed within the polyester, as a prelude to emulsification, the extrudate samples were homogenized offline. A sample with a higher developed interfacial area of water and polymer should break down into smaller particles in an excess of water by homogenization. These particles will not resemble the proper emulsion ultimately sought by SFEE, but due to the absence of sufficient surfactant or water in the process, this approach seemed reasonable in seeking additional that the transient viscosity behavior was in fact indicating the morphological state of the polymer-water dispersion.

Figures 8 and 9 show the mean particle size diameter (D_{50}) plotted against the magnitude and the slope of the previously discussed viscosity drop, respectively, for the different types and contents of modifier. Homogenization and particle size measurement was conducted for both immediately extruded samples as well as extrudates stored for three days prior to the test. D_{50} of the stored extrudate samples was consistent at 940 ± 120 µm and did not vary based on the modifier type and content. The large particles, relative to those immediately homogenized, likely reflected water separation on storage. Figure 8 shows that D_{50} decreased for samples corresponding to an increasing magnitude for the viscosity drop. D_{50} for the blend with 5 wt% C modifier had decreased to 70 µm, while being quite large at 720 µm without modifier. Moreover, the content of C modifier in the polyester blend had a significant influence on D_{50}, greater than NC modifier, as seen in Figs. 8 and 9. The smaller particles obtained by homogenization for C modifier compare to NC modifier fits with the hypothesis that a higher interfacial area between polymer and water was being produced and detected within the extruder when the C modifier was used. It was therefore with reasonable confidence to infer that the viscosity drop detected by the inline viscometer could be considered as related to the state of water dispersion in polyester matrix, for the dispersion zone of SFEE. Having this process-related indicator will make it easier to test formulation and operational factors related to SFEE modeling in future studies.

Morphology of the Water Dispersed into Polyester

Finally, the morphology of the extruded polyester-water dispersion at $R/W = 5$ was examined. Stratified polyester fibrils are indicated with white arrows in the SEM image shown in Fig. 10. In the polymer blend field, the morphology of a dispersed phase follows a well-known, three step mechanism starting from lamellas, to fibrils, and finally transformed into droplets [22]. This eventual droplet transformation requires a prolonged period of time for high viscosity ratios [22]. It seems that a stratified lamella structure occurred in the polyester-water system produced in the extruder, but in the dispersion stage, the water

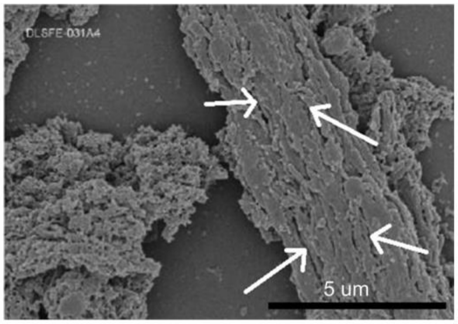

FIG. 10. Stratification of polyester domain by water at resin-to-water (R/W) ratio 5:1 in TSE.

failed to complete the first transformative step of forming fibrils due to the excessively high viscosity ratio between the polyester and water.

CONCLUSIONS

The new inline rheological measurement technique was developed with the validation of 3D numerical software OpenFOAM, as well as conventional parallel plate and capillary rheometers. It has been shown that this dynamic technique can be used to detect viscosity changes, which are related to the state of dispersion of water into a polyester matrix. The water forms stratified lamella-like structure in the polymer as proper physiochemical conditions arise. Recognizing the relationship between the transient viscosity behavior and the developed state of dispersion, this inline rheometer will be an invaluable tool in modeling the SFEE process. Changes in the SFEE process related to matrix molecular weight and the content of a surface active modifier were separated in the study to understand which factor had a greater effect on water dispersion in the polyester matrix; these two factors change simultaneously in the SFEE process normally and create a challenging system to control. Without surprise, higher polar surface energy contributions were most important but the relevance of lower viscosity implies that some chain degradation in the actual SFEE process is important.

Supporting Information related to the strain sweep for the parallel plate measurements is available for this article and is accessible for authorized users.

ACKNOWLEDMENT

The authors wish to thank the Xerox Corporation for their generous funding of this work as well as for the provision of the resin.

REFERENCES

1. M. Trotta, F. Debernardi, and O. Caputo, *Int. J. Pharm.*, **247**, 153 (2003).
2. H. Hamishehkar, J. Enami, A.R. Najafabadi, K. Glani, M. Minaiyan, H. Mahdavi, and A. Nokhodchi, *Colloids Surfaces B: Biointerfaces*, **74**, 340 (2009).
3. S.N. Sani, N.G. Das, and S.K. Das, *J. Microencapsulation*, **26**, 556 (2009).
4. M.A. Norato, L.L. Tavlarides, and C. Tsouris, *Can J. Chem. Eng.*, **76**, 486 (1998).
5. D. Song, W. Zhang, R.K. Gupta, and E.G. Melby, *AIChE J.*, **57**, 96 (2011).
6. G. Akay, *Chem. Eng. Sci.*, **53**, 203 (1998).
7. G. Akay and L. Tong, *J. Colloid Interface Sci.*, **239**, 342 (2001).
8. G. Akay, L. Tong, H. Bakr, R.A. Choudhery, K. Murray, and J. Watkins, *J. Mater. Sci.*, **37**, 4811 (2002).
9. S.N. Ashrafizadeh, E. Motaee, and V. Hoshyargar, *J. Petrol. Sci. Eng.*, **86**, 137 (2012).
10. W.D. Pandolfe, *J. Dispersion Sci. Technol.*, **2**, 459 (1981).
11. K. Abe, M. Tsuruoka, S. Kiriyama, and K. Nakamori, U.S. Patent, 4320041 A (1982).
12. J. Chung, C.M. Cheng, S.M. Malachowski, E.D. Godshall and J.L. Pearson, U.S. Patent, 9052625 B2 (2014).
13. K. Zhou, G. Sacripante, and E. Zwartz, U.S. Patent, 20070141494 A1 (2007).
14. A. Goger, M.R. Thompson, J.L. Pawlak, and D.J.W. Lawton, *Ind. Eng. Chem. Res.*, **54**, 5820 (2015).
15. A.C.P. Neubauer, and N.W. Dunchus, U.S. Patent, 20120238681 A1 (2016).
16. A. Spyros, *J. Appl. Polym. Sci.*, **83**, 1635 (2002).
17. S. Wu, *J. Polym. Sci. Part C: Polym. Symp.*, **34**, 19 (1971).
18. W.N. Bond, *Proc. Phys. Soc. Lond.*, **34**, 139 (1921).
19. M. Bakar and F. Djaider, *J. Thermoplast. Compos. Mater.*, **20**, 53 (2007).
20. T.G. Fox and P.J. Floory, *J. Appl. Phys.*, **21**, 581 (1950).
21. S. Acevedo, X. Gutierrez, and H. Rivas, *J. Colloid Interface Sci.*, **242**, 230 (2001).
22. S.C. Jana and M. Sau, *Polymer*, **45**, 1665 (2004).

Supporting Information for Chapter 3

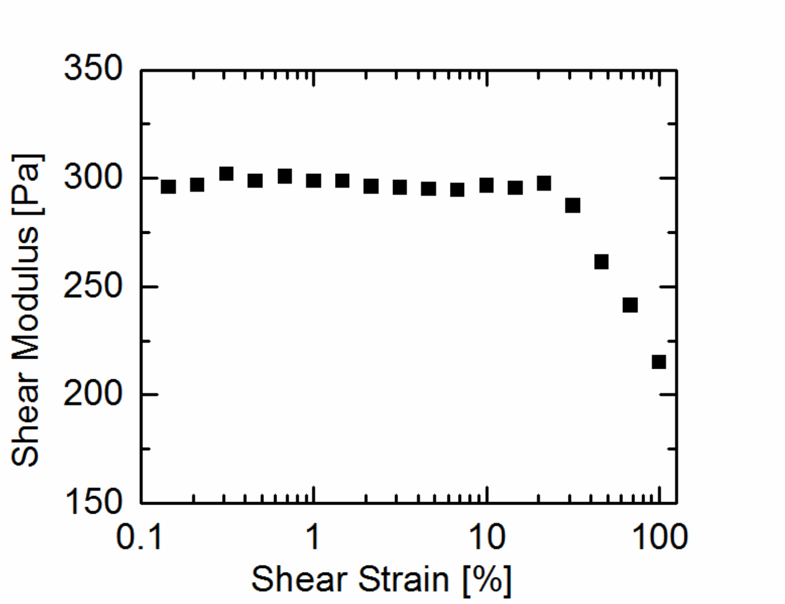

Supplementary Figure 2 The curve between shear modulus and shear strain for neat polyester at 100ºC.

Chapter 4 Solvent-Free Polymer Emulsification inside a Twin Screw Extruder

All experiments and data anlaysis in chapter 4 were conducted by the thesis author. M. Arnould at Xerox Webster conducted GPC test to determine molecular weights of the polymer samples. J. Pawlak and D. Lawton provided technical guidance during the project. This chapter is submited to AIChE Journal on 15 May 2017.

Solvent-Free Polymer Emulsification Inside A Twin Screw Extruder

A. Goger[1], M.R. Thompson[1*], J.L. Pawlak[2], M.A. Arnould[2], D.J.W. Lawton[3]

ABSTRACT

Solvent-free extrusion emulsification (SFEE) is new technique for a twin screw extruder to prepare sub-micron sized particles (100-500 nm) without using hazardous solvents. The particle size is reliant upon the thickness of striated lamellae, which can be monitored rheologically based on the viscosity change occurring at the SFEE process. The lamellae coarsening rate is predominantly affected by the interfacial energy of the system when a surfactant is added but shows stronger dependency on viscosity change when interfacial growth between the polymer and water phases is solely determined by the end-groups conversion into carboxylate species. For this latter case, the dissolution of the sodium hydroxide species and the kinetics of end-groups conversion prove to be rate-limiting phenomena to generating thinner striated lamellae. Additionally, the ionic strength of the system is notably important to the viscosity response and particle size produced, particularly when surfactant is not added.

KEYWORDS: Phase Inversion Emulsification, Mixing, Twin Screw Extruder, Inline Rheometer

INTRODUCTION

Solid-liquid dispersions consisting of sub-micron polymer particles have many applications such as adhesives, coatings or pharmaceutics. Conventional emulsification techniques are losing prevalence due to the high costs surrounding solvent recovery and increasingly stringent environmental regulations, especially pertaining to the health & safety of workers and consumers. Exclusive use of water as an environmentally benign medium is preferred in green manufacturing processes. This paper looks at aspects of a new green manufacturing process with a twin-screw extruder that is intent upon internally producing an aqueous dispersion by a top-down approach with high viscosity polymers.

A top-down approach for preparing submicron polymer particles is generally considered when polymerization in water is implausible or other components need to be incorporated in the particle that are sensitive to reactions. However, mechanical top-down methods, like milling, experience considerable difficulties in controlling the product particle size, especially below a micron. Solvent emulsification is preferred as a method under this approach since greater control over particle size is achieved, and the energy input is lower than mechanical methods.[1–3] In solvent emulsification, the solvent is responsible for lowering the system viscosity by dissolving the polymer, as well as acting as a surface-active agent. Particles are ultimately formed upon dilution of the polymer solution with water. Solvent-free emulsification is a less robust phase-inversion technique as it experiences greater difficulties in countering the high viscosities of many industrially interesting polymers (namely 1-1000 Pa-s), largely due to the absence of organic solvents. However, it is becoming increasingly apparent that solvent-free emulsification is effective with several moderately viscous systems.[4–9] Ashrafizadeh and Hashyargar[9] demonstrated the emulsification of crude oil, which had a viscosity of 2.7 Pa·s, with water and no hazardous solvents, by homogenization at 25ºC. They produced oil domains with a Sauter mean diameter varying between 8 µm to 25 µm among their samples. These domains are quite large in size relative to standard emulsions, but should be expected as the viscosity of the dispersed phase increases in such mechanical dispersion processes.[10] Song et al.[5] created a waterborne, pressure-sensitive adhesive with a multi-impeller batch mixer from rosin ester and partially hydrogenated wood rosin acid, having a blend viscosity of 5 Pa·s in the temperature range of 43 ºC to 54 ºC. In their case, the mean particle size of the rosin emulsion varied between 0.6 µm to 1.5 µm for different processing conditions; the improved compatibility of the rosin with water compared to the earlier example with crude oil resulted in a smaller particle size. However, a much closer example of this solvent-free process to the present study is found in the work of Akay et al.[6–8], who studied the aqueous phase inversion of different polymer melts with high viscosities in a batch mixer, including low density polyethylene which had a viscosity of approximately 50 Pa-s. Moreover, the mean particle size changed between 1.03 µm to 4.19 µm for differing content of hydrophobically modified water-soluble polymers (HMWSPs).[7] For none of these examples was a continuous system like a twin-screw extruder used, even though for viscosities above 10 Pa-s, this machine is well suited to the task of dispersion. The continuous nature of the twin-screw extruder introduces challenging constraints on emulsification since there are few locations for water to be added to the polymer melt and the available residence time for adequate mixing such viscously disparate fluids is limited to only a few seconds.

The use of a twin-screw extruder to emulsify polymers in the manner described above is referred to as *solvent-free extrusion emulsification* (SFEE). The SFEE process is complicated by the number of variables to which the process is sensitive, resulting in a very narrow window of stable operation,[11,12] but understanding the mechanisms of the process should permit improved processability. The SFEE process takes the twin screw extruder and divides it into three processing zones. The first zone is the standard *melting zone,* where polymers and possibly surface active agents are mixed into a homogenous molten phase; other ingredients could be incorporated into the polymer phase as well at this point such as colorants and fillers but were not used in this study. The second is the *dispersion zone* where a small weight fraction of water is first injected and mixed into the polymer. Finally, the last zone of the extruder is for *dilution* where the final, much higher, weight fraction of water is injected to create the desired oil-in-water (O/W) type emulsion prior to the melt solidifying.

The purpose of this paper is to gain understanding of the mechanism in the dispersion zone by examining the influences of different chemical factors on the ability to create an aqueous polyester dispersion by SFEE. The goal is to improve the robustness of the process in order to consistently obtain product with a final particle size in the order of 100 nm. The variables of study included the manner by which sodium hydroxide (NaOH) was added as well as NaOH content, NaCl concentration, resin-to-water (R/W) ratio, and surfactant content. These variables were chosen due to their known strong influence on successful emulsification whereas other important factors related to process temperature, material viscosity and screw design will be present in a future study. The effects of these variables on the dispersion zone of SFEE were quantify during processing by a novel inline rheometer introduced in a previous study[13] along with several off-line analysis methods.

MATERIALS AND METHODS

Material

A polyester synthesized from fumaric acid (FA) and dipropoxylated bisphenol A (pBPA) was provided by the Xerox Corporation (Webster, NY). The high viscosity resin was a high flow grade (M_w=17081 g/mol; M_W/M_N=4.2) with an acid number of 17.7±1.7 mg KOH /g sample. Sodium hydroxide (NaOH) and sodium chloride (NaCl) pellets were purchased from Caledon Laboratories Ltd. (Georgetown, ON). The NaOH was ground and sieved to a desired particle size to increase dissolution (i.e. 850 µm-1180µm). Deionized water (>0.1µS/cm^2) was used in the trials. Sodium dodecylbenzenesulfonate (SDBS) was obtained from Sigma-Aldrich (Toronto, ON) having a melting temperature of 300 °C, 348 g/mol molar mass, and a 1 g/cm^3 solid density. A 0.1 M potassium hydroxide (KOH) stock solution was purchased from Sigma-Aldrich (Toronto, ON). Methylene ethylene ketone (MEK) was purchased from VWR International (Toronto, ON).

Extruder Setup

Extrusion trials were done with a 40 L/D, 27 mm Leistritz ZSE-HP co-rotating twin-screw extruder (TSE) (American Leistritz Extruder Corporation; Somerville, NJ). The barrel of the TSE was designed to have two sampling ports at zone 5 (20 to 24 L/D) and zone 7 (28 to 32 L/D), downstream of the feed port (zone 0). The barrel temperature profile was kept constant at 95ºC in every zone. The extruder was operated at a fixed screw speed of 300 rpm. The polyester was fed into the extruder at 8 kg/h via a DDSR20 gravimetric feeder (Brabender Technologie Inc; Mississauga, Ontario); the feed included solid particles of NaOH and/or SDBS when required by trial conditions. The first addition of water was injected at zone 3 (14 L/D downstream from the feed port); this water contained dissolved NaOH if the test conditions required 'solution NaOH' else it was pure water. The second, larger amount of water added at zone 7 was always pure water but was only added when required by conditions in the trials (as discussed below). In both cases, a 260D high pressure syringe pump (Teledyne Isco Inc.; Lincoln, NE) was used for precise feeding of the water streams. An intensive mixing screw design was used similar to the one by Neubauer et al.[14]

Inline Rheometer

A custom-designed extruder die was used as an inline rheometer for the study, modeled on an orifice plate flow-meter design. Goger et al.[15] validated this rheometer for the measurement of apparent viscosity for the polyester-water mixture. The main bore diameter of the die was 15 mm and included a 2 mm orifice plate mid-way along its length to increase the pressure difference (as well as minimize free water draining from the extruder). The pressure drop across the orifice plate spanning 17 mm was measured using Dynisco model PT467E pressure transducers. The measured pressure drop was converted into an apparent viscosity by the same method stated by Goger et al.[15] A K-type thermocouple was immersed into the melt at a distance of 87 mm downstream of the orifice plate towards die exit, which was beneficial to considering the effects of water cooling and viscous dissipation on the calculation of viscosity.

Trials Procedures

Trials began by adding small amounts of water at R/W_1=135 (i.e. 0.74 wt. %) in order to prevent the molten polyester from blocking the injectors while baseline conditions were established for the inline rheometer; R/W stands for resin-to-water ratio on a weight basis whereas W_1 refers to the total water present provided at the first injection port. Once a steady baseline was recorded, R/W_1 was changed according to experimental conditions. The variables of study for the mixture were NaOH content (0.5 wt.% and 1 wt.%), form of NaOH added (as ground solid particles entering the extruder with the resin or as an aqueous solution injected at the first water injection port). Added surfactant content (SDBS; 0 wt.% or 7.5 wt.%) and resin-to-water$_1$ ratio (R/W_1=5 and 3.5) were controlled at the gravimetric feeder and the first injector site, respectively. The variables of study are listed in Table 4-1.

Table 4-1Experimental parameter used in this study.

NaOH addition method	[-]	Solid vs. Solution
Surfactant content	[wt.%]	0 vs. 7.5
Resin-to-water-ratio (R/W_1)	[-]	5 vs. 3.5
NaOH content	[wt.%]	0.5 vs. 1
NaCl content	[ppm]	4 x10^4, 6 x10^4 and 8 x10^4

Procedure 1

The extruder ran for five minutes to establish a steady baseline condition, which was determined when fluctuations in the apparent viscosity measured by the inline rheometer dropped below ±4.5%. Subsequently, the rate of water addition at the first injection port (zone 3) was increased to produce an R/W_1 ratio of 5 or 3.5, while the injector at the second injection port (zone 7) was not used. With no water added at the second port, the total resin-to-water ratio (R/W_T) of the exiting material was the same as at the first port (i.e. $R/W_T = R/W_1$). This mode of operation (Mode 1) admittedly creates a longer mixing length for the first instance of injected water than the normal SFEE process (i.e. Mode 2) and so studies the best mixed water dispersion based on the formulation, but provided stable measurements at the inline rheometer; subsequent studies under Procedure 2 (below) will identify the state of mixing along the mixing length such that the differences to the normal SFEE will be identified. Inline apparent viscosity data was collected for five minutes while in this mode of operation. After viscosity measurements and sampling were completed under Mode 1, water was now added at the second injector (zone 7) while the rate of water addition at zone 3 remained unchanged such that Mode 2 produced a fixed $R/W_T = 1.3$. Operating in Mode 1 extruded material that resembled a plastic extrudate with the water well incorporated, while Mode 2 create a milky-looking emulsion at the exit.

Under Mode 1, samples (~20 g) of the plastic extrudate at the exit were sampled and quenched in cold water to preserve its morphology. Under Mode 2, the resultant emulsion was collected from the end of the extruder for three minutes. Collected emulsions were cooled down by dispersed into a beaker holding 200 mL of water.

Melt temperature of the polymer/water system was measured at the die during the trial and used to correct the apparent viscosity data to conditions at 100 ºC by use of an Arrhenius shift factor with flow activation energy of 32.7 kJ/mol (determined by off-line rheometry).[15] This normalized correction was necessary for comparative purposes since the melt temperature varied ±4 ºC for the different trial conditions due to viscous dissipation.

Procedure 2

The extruder was run for five minutes to reach steady baseline conditions and then the water at the first port was adjusted to $R/W_1=5$ or $R/W_1=3.5$ for an additional five minutes till steady conditions were again established, similar to Procedure 1 under Mode 1. At the end of this time, a plastic extrudate sample was collected at the die exit and quenched in cold water. The TSE was stopped immediately afterwards and all zones were crash cooled to 40ºC. While the TSE zones were cooling to 40ºC, the port covers at zones 5 and 7 were opened. On average, it required 1.8±0.2 min to cool the barrel zones from 95ºC to 40ºC and open the two aforementioned covers. Samples were collected from the openings at zones 5 and 7 as well as the die for chemical analysis. All of the collected samples were dried under vacuum for 18 hours at 60ºC. In this trial, it is assumed that neither degradation nor end group conversion occurred once the extruder stopped since the system was being quickly cooled below the glass transition temperature of polyester (T_g =59.6ºC as measured by differential scanning calorimetry).

Residence Time Distribution (RTD)

The residence time corresponding to samples at the barrel zones 5, 7 and the die exit were evaluated by measuring the residence time distribution (RTD). To determine the RTD of the solvent-free extrusion emulsification process, one gram of graphite powder was fed into the extruder as a pseudo dirac pulse similar to the method published by Mu and Thompson[16] and Li et al.[17] Clear acrylic port plugs, comparable in design to the metal versions supplied with the extruder, were installed in the ports of barrel zones 5 and 7 to observe the flow inside the TSE. Color intensity data was recorded as a function of time from high resolution digital video looking down on the longitudinal axis of the TSE. Adobe Photoshop CS4 software (Adobe Systems Inc.; San Jose, CA, USA) was used to analyze individual frames of the videos for color intensity. Color intensity was considered to have a linear relationship with respect to concentration of the graphite powder in the image. In this study, the mean residence time (MRT) was defined as the average time that the material spends until reaching the position where the video was collected. Selected conditions were repeated three times (n=3) to determine the measurement uncertainty.

Particle Dispersion

Particle size distributions of emulsions sampled from the TSE were measured with a Malvern Mastersizer 2000^{TM} (Malvern, United Kingdom). It was capable of detecting particles in a range of 0.1-2000 µm. The mean particle size distributions were determined based on three replicate measurements in a water medium (n=3).

Gel Permeation Chromatography (GPC)

Samples were prepared by dissolving approximately 5 mg polymer/mL in spectral grade $CHCl_3$ spiked with 0.1% (v/v) triethylamine (99% purity) followed by filtration through a 0.2 µm syringe filter (Whatman PTFE) into 2 mL sample vials. The samples were injected using an auto-injector onto a Polymer Labs GPC-50 System equipped with 2 x 5 µm PL Mixed Bed C GPC columns (300 x 7.5 mm) with a guard column and a Wyatt triple detection system (light scattering, viscometry and refractive index). Standard molecular weights were calculated using a 10-point polystyrene linear calibration and the absolute molecular weights were calculated using the triple detection data. This analysis was performed at the Xerox Corporation (Webster, NY).

Colorimetric Titration

The Acid Number (AN) was determined using the standard method ASTM-D974. The method required 2 g of dried sample to be added to 100 mL titration solvent (methyl ethyl ketone) and 0.5 mg of p-naphtholbenzein indicator. The solution was titrated with a standardized potassium hydroxide (KOH) solution in isopropanol (Sigma-Aldrich, 0.1 N certified standard).

Degradation Ratio (DR) and Neutralization Ratio (NR) Calculation

The degradation ratio (DR) and neutralization ratio (NR) were used to quantify the extent of chain length breakages and end group conversion of samples collected at Zone 5 (i.e. 16 L/D away from the die), Zone 7 and the die exit. DR is calculated based on changes in the number-average molecular weight (M_n) reported by GPC between dried extrudate and unprocessed virgin polyester samples, as shown in Equation 4.1. NR is calculated based on the ratio between the acid number (AN) of a dried extrudate sample and the theoretical AN of unconverted polyester, as stated in Equation 4.2. The theoretical AN value was based on the measured AN of the virgin polyester but adjusted to include an estimate of newly-created carboxylic acid end group due to chain scission assuming one new acid group per scission.

$$DR = \left(1 - \frac{M_{n\ extrudate}}{M_{n\ vigin}}\right) * 100 \tag{4.1}$$

$$NR = \left(1 - \frac{AN_{extrudate}}{AN_{theoretical}}\right) * 100 \tag{4.2}$$

Surface Tension Measurement

Dried polyester was molded into a 5 x 5 x 0.5 cm specimen after hot pressing with 2 metric tons force for two minutes at 100ºC. Sessile drop (i.e. ~5µl) contact angle values were found at room temperature for 1-bromonaphthalene (dispersive component δ^d=42.517 mJ/m^2, polar component δ^p=0.283 mJ/m^2) and glycerin (δ^d=35.541 mJ/m^2, δ^p=25.359 mJ/m^2). The surface energy of polyester was calculated by using the Wu[18] method. Values were corrected to 100 ^{o}C based on the finding Gokel[19] that surface energies of most chemicals decreases with temperature at -0.1 mN/m/ºC. Interfacial tension using Young's equation was estimated by measuring the contact angle via sessile drop method of water with differing polyester-surface active agent polymer blends.

Scanning Electron Microscopy (SEM)

Morphology of the emulsions was evaluated using a scanning electron microscope (SEM) (JEOL JSM-6610V; JEOL USA, Peabody, MA). Samples for the SEM were prepared by the following method: (i) 3 mL of extrudate emulsion was diluted in 30 mL isopropyl alcohol, (ii) 3 mL of diluted emulsion are dispersed onto a 25 mm diameter metal plate to evaporate in fume-hood for 1 hour, and then (iii) the evaporated samples were sputtered with gold (Sputter coater S150B, West Sussex, United Kingdom). The accelerating voltage was 20kV.

Statistical Analysis

Experimental factors, mentioned in Table 4-1, were evaluated using Design Expert 7.1 (State-Ease Inc., Minneapolis, MN) under a general factorial statistical design.

RESULTS AND DISCUSSION

The dispersion zone of the SFEE process is primarily under study in this work. The zone is considered to exist between the first and second water injection zones in the extruder. Some surfactant is generally added but to minimize the cost and possible negative aspects of its inclusion in final products, the carboxylic acid endgroups of the polyester are purposefully converted into carboxylates by reaction with NaOH. The NaOH can be added to the extruder as solid granules with the polyester feedstock, or in solution at the first injection port. Our preliminary findings (data not provided) have never found evidence that the NaOH, if added as a solid, begins endgroup conversion or chain degradation, until in the presence of water. This means that several changes occur in the dispersion zone simultaneously, including endgroup conversion, hydrolysis of the polyester as a side-reaction, and the development of a favourable water-polyester morphology in preparation of spontaneous phase inversion once an excess of water is added at the second injection port.

The variables under study in this paper examine the interplay of endgroup conversion, hydrolysis and addition of surfactant on the developed water-polymer morphology in the dispersion zone.[20,21] The window of operations for this process is quite narrow, with the condition selected found to be most suitable to produce emulsions, making the challenge to understand the mechanism and widen the processing window.

Emulsification by Twin Screw Extrusion

The dispersion stage of SFEE is discussed in general terms in this section, with subsequent sections giving detailed coverage of the mechanisms involved for the emulsion system with and without SDBS and examining the influence of ionic strength on emulsification.

Representative viscosity profiles measured by the inline rheometer under Procedure 1/Mode 1 are seen in Figure 4-1, showing a step-like rise or decline in viscosity occurring over several seconds or minutes after the water at the first injection port increased from $R/W_1=135$ to either $R/W_1=5$ or $R/W_1=3.5$. It should be pointed out that the extrudate from the die appears as molten plastic under Mode 1 and will only generate particles under Mode 2. A rise in viscosity is rare for SFEE if emulsification occurs. The tendency for apparent viscosity to decrease or increase in this study, similar to the changes seen in the figure, corresponded to:

(i) Formulations with SDBS surfactant always resulted in a decrease in apparent viscosity.

(ii) Formulations with a high sodium hydroxide content (no SDBS) resulted in a small positive step changing whereas low sodium hydroxide content produced a negative step change in apparent viscosity.

(iii) Increasing the ionic strength of the system by addition of NaCl promoted an increase in apparent viscosity.

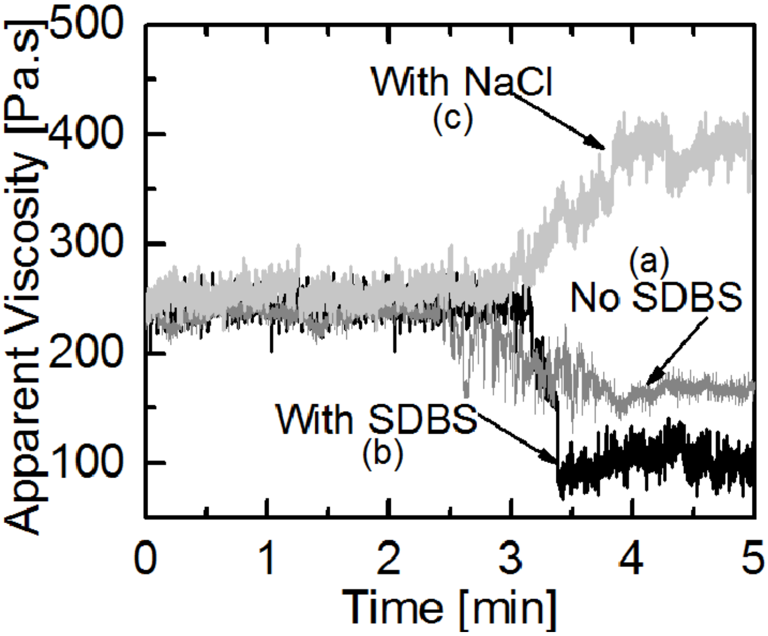

Figure 4-1 Example of apparent viscosity changes measured by the inline rheometer. ((a) 1 wt.% aqueous NaOH solution-No SDBS-R/W1=3.5 without NaCl, (b) 1wt.% solid NaOH-7.5wt.% SDBS-R/W1=3.5 without NaCl, (c) 1wt.% aqueous NaOH solution-No SDBS-R/W1=3.5 with 8 x104 ppm NaCl.)

The state of mixing developed in the dispersion zone is represented by this transient rheological response that is measured at the die soon after water begins to be added at the first injection port in significant quantities. It is quantified by the magnitude of the apparent viscosity change (Δη) reflecting the degree of water dispersion into the polymer, and by the slope of the apparent viscosity change (Δη/Δt) corresponding to the kinetics of the mixing process and progression of reactions. Positive values for Δη and Δη/Δt indicate a rise in apparent viscosity over time while negative values correspond to a decline. Previous studies found that a more abrupt decline in viscosity corresponded to a higher likelihood that the polymer-water mixture would produce smaller particles, though in that case, the mixture was taken from the extruder and mechanical dispersed by a bench top homogenizer and so the relationship was purely attributed to SFEE;[15] the same transient rheological behaviour has been reported in a batch emulsification processes for the same polymer-water system.[6,13] For the present study where emulsified particles are now being collected directly from the extruder, under Procedure 1/Mode 2, we can see this behaviour once again demonstrated in Figure 4-2 without surfactant addition (0 wt.% SDBS) and in Figure 4-3 with surfactant addition (7.5 wt.% SDBS). These two figures plot mean particle size (D_{50}) in relation to the state of mixing in the dispersion zone given by Δη/Δt; selected data is given in Table 4-2 to observe the influence of SDBS on the state of mixing. Only the derivative was used in the plots, though the same trend with particle size is seen for Δη.

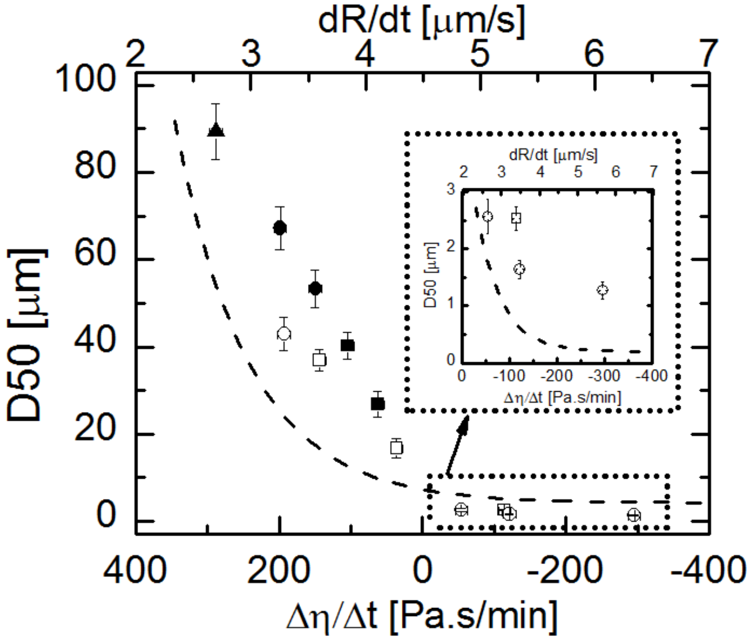

Figure 4-2 Slope of viscosity changes (Δη/Δt) vs. mean particle diameter (D50) without surfactant. (☐ Solid NaOH addition, ○ Aqueous NaOH solution addition, ■4 x104 ppm NaCl addition, ● 6 x104 ppm NaCl addition, and ▲ 8x104 ppm NaCl addition).

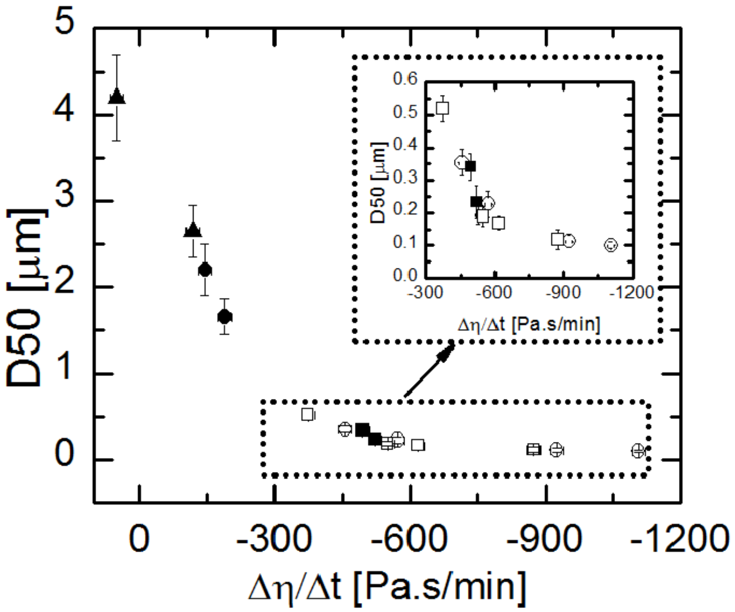

Figure 4-3 Slope of viscosity changes (Δη/Δt) vs. mean particle diameter (D50) with surfactant. (□Solid NaOH addition, ○ Aqueous NaOH solution addition, ■ 4 x10^4 ppm NaCl addition, ●6 x10^4 ppm NaCl addition, and ▲ 8 x10^4 ppm NaCl addition).

In both Figures 4-2 and 4-3, there appeared to be an inverse relationship for mean particle size of the emulsified polyester with Δη/Δt, though that trend was much sharper for systems including SDBS. Two SEM micrographs in Figure 4-4(a) and 4-4(b) show representative particles produced with increasingly negative Δη/Δt, and both appear as nearly spherical with little distortion in shape. Conversely, the micrograph in Figure 4-4(c) shows larger particles corresponding to a positive Δη/Δt (i.e. elevated ionic strength condition) that now exhibit tails or fibrils suggestive of a less well developed mixed state prior to particle formation (by dilution at the second injection port) and possibly the influence of shear deformation on the particle as it solidified. The vials included in figure show similar stable emulsions being created at all three conditions. However, SFEE is not boundless and emulsions were not possible in this study for the conditions of 1 wt.% NaOH (solid addition) at R/W_1=5 without SDBS nor at 1wt.% NaOH (aqueous solution) with a high content of NaCl (6x10^4 ppm and 8x10^4 ppm) at R/W_1=3.5 without SDBS.

Table 4-2 Magnitude and slope of viscosity changes for different experimental conditions.

		Magnitude of viscosity changes ($\Delta\eta$) [Pa-s]	Slope of viscosity changes ($\Delta\eta/\Delta t$) [Pa-s/min.]
WITHOUT SDBS at R/W_1=3.5 with 1 wt.% NaOH	Solid NaOH without NaCl	-77±6	-114±9
	Solution NaOH without NaCl	-112±6	-121±8
	Solution NaOH at 4x10^4 ppm NaCl	113±6	149±8
	Solution NaOH at 6 x10^4 ppm NaCl	143±6	198±8
	Solution NaOH at 8 x10^4 ppm NaCl	188±6	288±8
WITH SDBS at R/W_1=3.5 with 1 wt.% NaOH	Solid NaOH without NaCl	-172±6	-616 ±12
	Solution NaOH without NaCl	-187±5	-1106±11
	Solution NaOH at 4 x10^4 ppm NaCl	-121±5	-875±11
	Solution NaOH at 6 x10^4 ppm NaCl	-97±5	-521±11
	Solution NaOH at 8 x10^4 ppm NaCl	Unstable	Unstable

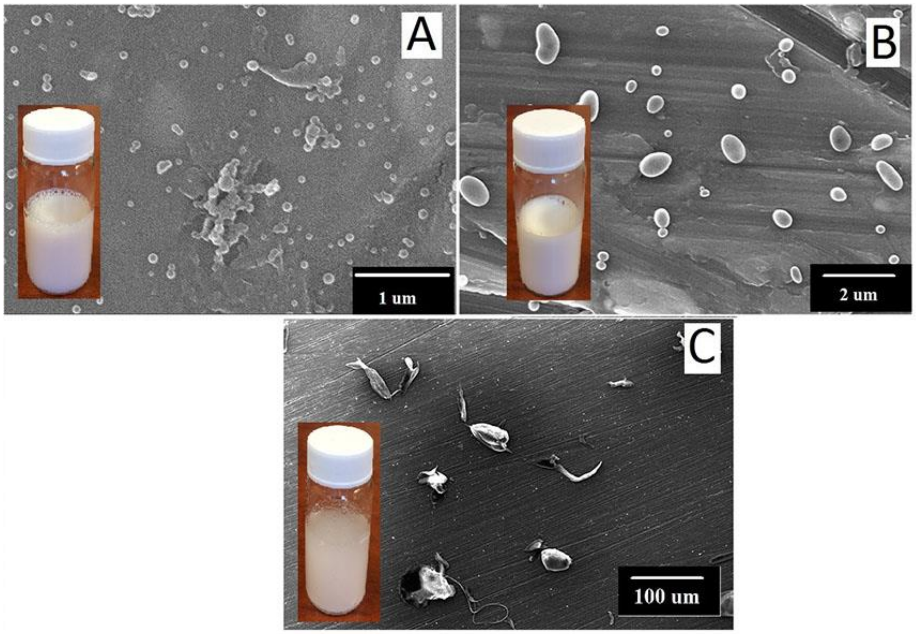

Figure 4-4 SEM pictures of emulsions. Image (a): 1 wt.% aqueous NaOH solution-7.5wt.% SDBS-R/W1=3.5 without NaCl. Image (b): 0.5 wt.% aqueous NaOH solution-No SDBS-R/W1=3.5 without NaCl. Image (c): 1 wt.% aqueous NaOH solution- No SDBS-R/W1=3.5 with 4 x104 ppm NaCl addition. *Vials are showing the milky-like emulsion created inside the extruder.

Analysis of the experimental design is summarized in Table 4-3 showing that the concentration of SDBS surfactant (P=0.0003) and resin-to-water (R/W_1) ratio (P=0.02) are the most significant parameters affecting Δη. Conversely, all tested parameter significantly affected Δη/Δt, except NaOH content (P=0.2).

The inclusion of NaOH in the SFEE process to promote end group conversion will have the unintended consequence of catalyzing hydrolytic degradation of the polyester.[13,15] Both chain length breakages and end group conversion are considered to be important simultaneously occurring phenomena in the dispersion zone of the SFEE process. Figure 4-5 show DR (in plots a,b) and NR (in plots c,d) versus mean residence time corresponding to the locations of Zone 5, Zone 7 and the die exit for cases without SDBS added; mean residence time is measured from the feed opening (t=0). Figure 4-6 show DR (plots a,b) and NR (plots c,d) with fixed inclusion of 7.5 wt.% SDBS. The samples in these plots were collected under Procedure 2, which is exactly the same as Procedure 1/Mode 1 for which the online rheological data was collected. The plots (a,b) show degradation always occurs in the process but that chain length is not significantly altered past Zone 5, with minor changes noted up to Zone 7 for the condition with 1 wt.% solid NaOH.

Table 4-3 Significances of parameters on viscosity changes and mean particle diameter without NaCl addition.

PARAMETERS	Magnitude of viscosity changes ($\Delta\eta$) [Pa.s]	Slope of viscosity changes ($\Delta\eta/\Delta t$) [Pa.s/min]	Mean Diameter (D_{50}) [μm]
NaOH feeding type	p value:0.2	p value:0.003	p value:0.4
Surfactant content	p value:0.0003	p value:<0.0001	p value:0.01
Resin-to-water$_1$ ratio(R/W$_1$)	p value:0.02	p value:0.003	p value:0.07
NaOH content	p value:0.8	p value:0.2	p value:0.3

The analysis given in Table 4-4 shows that the method of NaOH addition ($P<0.0001$), R/W_1 ratio ($P=0.01$), surfactant content ($P=0.02$) and NaOH content ($P<0.0001$) were all strongly significant parameters affecting the degradation ratio (DR). Higher DR values are seen with higher NaOH content, but also DR is always higher when solid NaOH addition was used in comparison to the solution approach (49% higher without SDBS and 35% higher with SDBS). There might be two main reasons for the solids affecting the extent of degradation more, which are: (i) polyester hydrolysis is highly dependent on pH and the highly localized pools of dispersed water contacting these solid particles of NaOH will predictably produce an extremely high pH in that region; and (ii) the local temperature rise during the dissolution of solid NaOH in water may initiate thermal degradation as a participating reaction. The former reason was felt to be reinforced by the fact that DR was notably larger for $R/W_1=5$ versus $R/W_1=3.5$ where water would be more localized due to the lower amount present. It is also notable in the figure that lower R/W_1 produced a lower mean residence time by ~ 0.2 min on account of the higher total flow rate. In comparison, to the results with no SDBS added, the DR for cases with SDBS is always ~46% higher (except for the case of low solid NaOH content at Zone 5). This small rise in degradation may have occurred because SDBS more readily allowed water migration into polyester matrix, which allowed for earlier and greater hydrolysis.

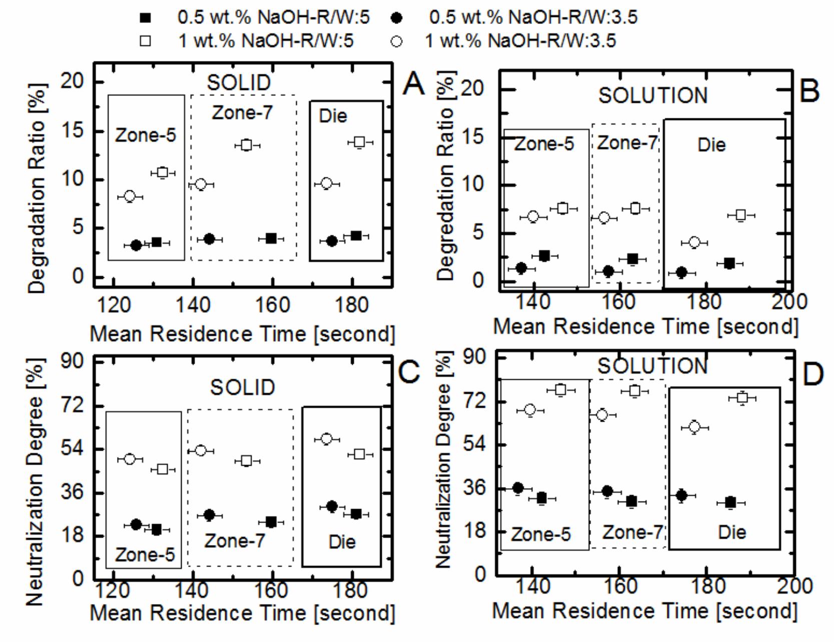

Figure 4-5 Degradation ratio (DR) and neutralization ratio (NR) vs. mean residence time without surfactant. Plot (a): Degradation ratio (DR) vs. mean residence time for solid NaOH addition. Plot (b): Degradation ratio (DR) vs. mean residence time for aqueous NaOH solution addition. Plot (c): Neutralization ratio (NR) vs. mean residence time for solid NaOH addition. Plot (d): Neutralization ratio (NR) vs. mean residence time for aqueous NaOH solution addition.

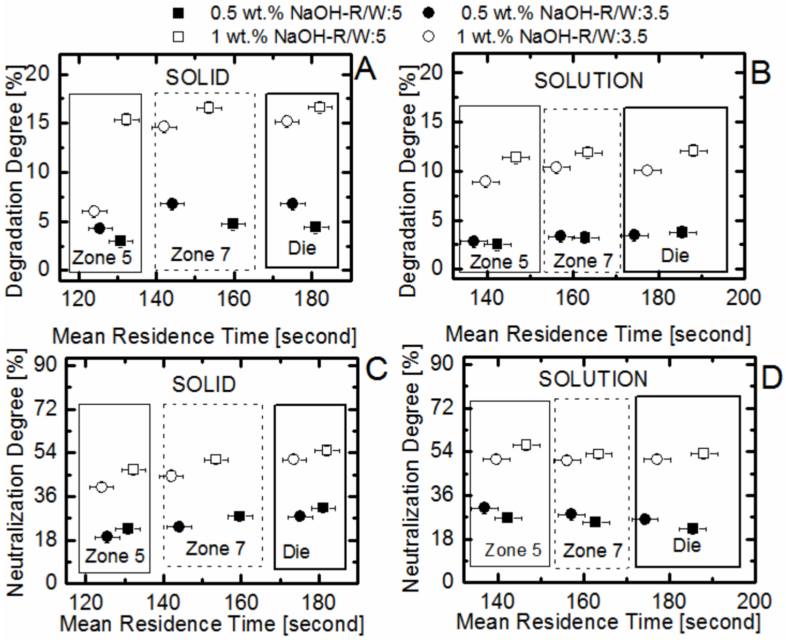

Figure 4-6 Degradation ratio (DR) and neutralization ratio (NR) vs. mean residence time with surfactant. Plot (a): Degradation ratio (DR) vs. mean residence time for solid NaOH addition. Plot (b): Degradation ratio (DR) vs. mean residence time for aqueous NaOH solution addition. Plot (c): Neutralization ratio (NR) vs. mean residence time for solid NaOH addition. Plot (d): Neutralization ratio (NR) vs. mean residence time for aqueous NaOH solution addition.

The number of endgroups converted (NR), corrected for new chain ends generated by degradation in each zone, change predominately between Zone 3 to Zone 5; endgroup conversion only proceeded once in the presence of water[13]. Corrected NR values were ~12% lower for the cases with SDBS (Figure 4-6) compared to tests without SDBS (Figure 4-5) and took noticeably longer in residence time to reach their maximum value along the screw. The difference is related to the higher chain degradation occurring with SDBS present. Due to dissolution kinetics, NR shows a minor increase past Zone 5 for the solid NaOH cases indicating endgroups are slowly and continual converted. In general, the NR and DR results are showing that chemical contributions to the rheological behaviour measured at the die (under Procedure 1/Mode 1) should be considered similar to those at Zone 7 where particles are produced when operating under Procedure 1/Mode 2. NR was always higher when aqueous NaOH solution was used (34% higher without SDBS and 12% higher with SDBS), but a significant contribution to the difference is the lower number of newly-created carboxylic acid end group for the solution cases during degradation. As expected, higher NaOH content by either addition methods produced higher NR, and the R/W_1 ratio had no effect. The statistical analysis in Table 4-4 notes that the method of NaOH addition ($P=0.004$), surfactant content ($P<0.0001$) and NaOH content ($P<0.0001$) are significant parameters affecting the neutralization ratio (NR) while R/W_1 is insignificant ($P=0.4$).

Table 4-4 Significances of parameters on degradation ratio (DR) and neutralization ratio (NR).

PARAMETERS	Degradation ratio (DR) [%]	Neutralization ratio (NR) [%]
Method of NaOH addition	p value:<0.0001	p value:0.004
Surfactant (SDBS) content	p value:0.02	p value:<0.0001
Resin-to-water ratio (R/W_1)	p value:0.01	p value:0.4
NaOH content	p value:<0.0001	p value:<0.0001

Influence of Endgroup Conversion in the Absence of SDBS

The discussion in this section is specific to the emulsion system consisting of polyester with only its converted carboxylate endgroups acting as surface active species, and where emulsification was conducted without the addition of NaCl to adjust ionic strength.

Looking back at Figure 4-2 in more detail, the largest particles produced by SFEE in the case without surfactant (or salt) was D_{50}=36.9±2.5 μm (Procedure 1/Mode 2) corresponding to $\Delta\eta/\Delta t$=144±8.7 Pa-s/min (measured under Procedure 1/Mode 1) for the condition with high solid NaOH content (1 wt.%) and high resin-to-water ratio in the dispersion zone (R/W_1=5). A similar particle (D_{50}=42.6±3.2 μm) was produced for the same chemistry but using NaOH in solution. Particle size is seen to be decreasing with lower NaOH content, which is unexpected since less converted endgroups are formed (i.e. NR) to stabilize the emulsion. The higher ionic strength of the system with high NaOH concentration will be examined in the section on NaCl as the cause for the positive viscosity change and larger particles. The smallest particle size in the figure without addition of surfactant was D_{50} =1.3±0.2 μm for the conditions of low NaOH content (0.5 wt.% added by solution) and R/W_1=3.5. In general, these particles were far too large for the goals of this work.

Viscosity and particle size of the process are thought related to the developing morphology of the polymer-water mixture prior to inversion. The mentioned morphology appears as striated lamellae in previously reported SEM micrographs.[15,21] The morphology is reminiscent of those found with co-continuous polymer blends.[22,23]

Zumbrunnen and Inamdar[24] stated that the co-continuous structure of polymer blends can be formed even at very low concentrations of the dispersed component by chaotic mixing which is certainly similar to the present polymer-water system. Veenstra et al.[22] proposed a coarsening rate for lamella development of co-continuous polymer blends depending upon their interfacial tension and viscosity that seems to reflect the trend seen in Figure 4-2; the viscosity of an emulsifying system is often considered to inversely influence interfacial area growth per unit volume.[9,24] The model of Veenstra for the rate of lamellae coarsening (dR/dt) is given as:

$$\frac{dR}{dt} = \frac{c\sigma}{\eta} \tag{4.3}$$

where σ is the interfacial tension between the two mixed phases, η is the viscosity of the blend, and c is a dimensionless constant. Both Potschke and Paul[23] and Veenstra et al.[22] mentioned that model agreement with data was best when c=0.03, which was hence chosen for our calculations. The interfacial tension used to calculate dR/dt was estimated based on surface energy values given in Table 4-5 while blend viscosity was equated to the measured apparent viscosity by inline rheometer at steady conditions (Procedure 1/Mode 1, well after the transient step response discussed above). A plot of the coarsening rate predicted by Equation 3 for each test condition versus experimentally measured particle size is included in Figures 4-2. The same inverse relationship between dR/dt versus D_{50} is seen that is notable for $\Delta\eta/\Delta t$ versus D_{50}. A higher dR/dt is suggestive of a thinner striated lamella structure occurring for the same span of time inside the extruder. Based on these finding, a relationship between particle size and thinner lamellae is assumed in the following discussion, and so also is the assumption that $\Delta\eta/\Delta t$ reflects dR/dt.

Table 4-5 Surface tensions that were used in coarsening rate (dR/dt) calculations.

		Surface Tension [mN/m]
	Neat polyester	43.3±0.7
WITHOUT SDBS	0.5 wt. % solid NaOH*	40.2±0.7
	0.5 wt. % solution NaOH*	38.2±0.7
	1 wt. % solid NaOH*	36.9±0.7
	1 wt. % solution NaOH*	35.1.1±0.7
WITH SDBS	Polyester with SDBS*	20.6±0.7
	0.5 wt. % solid NaOH*	19.4±0.7
	0.5 wt. % solution NaOH*	19.1±0.7
	1 wt. % solid NaOH*	18.7±0.7
	1 wt. % solution NaOH*	18.2±0.7

Operating with lower R/W_1 (P=0.07) is seen in Figure 4-2 to produce thinner striated lamellae in SFEE on account of the greater amount of water present. This relies upon an acceptable affinity between the two phases, which is not sufficient in the present case without SDBS to produce nanosized particles. Most distinctive from the data in the figure is a trend showing smaller particles being more consistently produced with NaOH added as a solution compared to its solids form. The statistical analysis in Table 4-3 does not show this effect as significant due to the strong influence of SDBS on particle size, but re-analysis of data without SDBS shows that the addition method becomes more significant (P=0.06) while other parameter remain in similar significance level. dR/dt varies between 3.5 µm/s and 7.1µm/s for conditions producing the largest to smallest nominal particle size for aqueous NaOH addition, while a slower rate between 2.3 µm/s to 4.9 µm/s is predicted with solid NaOH addition. The main factor influencing the difference in particle, based on the dR/dt calculation, was viscosity whereas little change in surface energy was found. Since the system viscosity is a reflection of lamellae generation in the dispersion zone of the extruder, the effect of addition method appears to reflect a system dependency affecting mixing (at least while SDBS is not present). This points to NaOH dissolution in water being a rate-limiting step compared to mixing in the interfacial area generation when solids are used, at least when considering the short time for endgroup conversion between Zone 3 and Zone 7 (estimated to be ~45 s). Between those two ports, it is hypothesized that the interfacial tension between the two phases must decline sufficiently to aid the shear and elongational stresses such that lamellae thickness is minimized prior to dilution and phase inversion. If mixing is less effective in the early regions of the dispersion zone due to delayed conversion of endgroups, for example, then interfacial are growth will similarly be less effective and larger particles should be expected as a result. Conversely, when NaOH is immediately available to neutralize carboxylic acid end groups by solution addition, mixing becomes the rate-limiting step in the mechanism and greater interfacial area is thought to be produced based on the smaller particles generated.

Influence of the SDBS Surfactant

The discussion in this section is specific to the emulsion system consisting of two surface active species, namely the carboxylate endgroups of polyester and SDBS, and where emulsification was conducted without the addition of NaCl to adjust ionic strength.

Examining the results in Figure 4-3 more closely, the largest particle size is D_{50}=0.52±0.04 μm corresponding to the smallest negative $\Delta\eta/\Delta t$ = -373±12 Pa-s/min for the case with 1 wt.% solid NaOH addition and R/W_1=5; the viscosity change is always negative with SDBS present. The smallest particle size is D_{50} =0.10±0.02μm corresponding to 1 wt.% NaOH by aqueous solution and R/W_1=3.5, which corresponds to the steepest negative slope of -1106±10 Pa-s/min. These particle sizes are much more consistent with the targeted size sought for this process.

The effect of NaOH content is not significant on D_{50} in the present case (P=0.3). There is little difference in converted endgroup (12% higher NR for the solution case) based on addition method but NR was 90% higher at 1 wt.% NaOH compared to 0.5 wt.%. D_{50} is smaller with lower R/W_1 similar to the cases without SDBS. SDBS content (P=0.01) was the only significant effect on D_{50} while R/W_1 ratio (P=0.07) was found to have lesser significance. Table 4-5 indicates that the surface energy is dramatically lower when SDBS is present. The surface activity of only endgroup conversion was apparently inadequate to form sufficiently thin striated lamella for the targeted particle size of this study. Comparatively, the concentration of surface active functional groups is 0.08 mol/kg at 1 wt.% NaOH solution without SDBS and yet reaches 0.3 mol/kg when SDBS is included with NaOH. This means that there was ~375% more surface active agent to assist interfacial area growth between the polymer and water phases when SDBS is present. The coarsening rate (dR/dt) is not shown in the figure since the contact angle between a solid surface of polyester containing SDBS and a droplet of water was too low to distinguish from zero. Finally, it is noted in the presented data that the transient change in apparent viscosity with SDBS is always negative for both NaOH addition methods, indicating a reduced sensitivity on ionic strength unlike the results without SDBS.

Examining the Influence of Ionic Strength by NaCl Addition

The discussion in this section is specific to the emulsion systems with or without SDBS, and where emulsification was conducted with the addition of NaCl to adjust ionic strength. The trials were intended to differentiate the effect of Na^+ from surface active groups on apparent viscosity changes and final emulsion particle size to better understand the larger particles and positive $\Delta\eta/\Delta t$ seen in the non-SDBS cases.

Dissolved NaCl was added at 4, 6 or 8 x10^4 ppm (resin basis) in the aqueous media entering at the first injector site. Any higher salt concentration and the SFEE process became very unstable with no emulsion possible for a transient viscosity change greater than $\Delta\eta/\Delta t$=301 Pa-s/min. Only the aqueous NaOH solution addition approach at R/W_1= 3.5 was tested for these experiments. Filled data points in Figure 4-2 and Figure 4-3 highlight the results for these conditions. Particle size reached up to D_{50}=89.4±6.4 μm with $\Delta\eta/\Delta t$=288±10 Pa-s/min for the case without SDBS for 1 wt.% NaOH with 8 x10^4 ppm NaCl, as seen in Figure 4-2. The $\Delta\eta/\Delta t$ was always positive without SDBS. On the other hand, for cases with SDBS the largest particle size was D_{50}=4.2±0.5 μm at 0.5 wt.% NaOH with $\Delta\eta/\Delta t$=51±6 Pa-s/min with 8 x10^4 ppm NaCl, as shown in Figure 4-3. The added salt increased the system viscosity but only one case with SDBS produced a positive $\Delta\eta/\Delta t$. SDBS diminished the influence of the salt despite the fact that it contributed more Na^+ ions to the system.

The increased viscosity and thicker striated lamellae structure found with NaCl is attributed to a low energy barrier to agglomeration and generation of insoluble sodium carboxylate due to a ‘ionic caging’ phenomena, based on the findings of others.[9,25–27] According to Ashrafizadeh et al.[9] who employed NaCl to differentiate the effects of Na^+ versus their surface active CO_3^{-2} on the emulsification of heavy crude oil in water, the added salt increased interfacial tension by the creation of insoluble salts of sodium carboxylate. The high ionic strength impeded dissociation of the carboxylate species, caging the functional groups, despite being present in a water medium. Zhang et al.[25] and Tawari et al.[26] observed the same effect for their studies of an aqueous dispersion of laponite particles with sorbitan oleate which became gel-like and the system viscosity dramatically increased as NaCl concentration was varied up to 20mM. They reported a notably lower energy barrier to agglomeration due to increased insoluble salts on the surfaces of their particles. Similarly, Suksamranchit and Sirivat[27] found higher aggregation of an ionic surfactant-polymer emulsion was promoted with salt addition due to a decrease in electron repulsion between the ionic surfactant head groups. Put into context with the present study, the higher interfacial energy of the non-SDBS, endgroup converted polyester-water system was more sensitive to the build-up of Na^+ from local high concentrations of NaOH such that the increased tendency to agglomerate thickened the lamellae and increased the system viscosity in much the same manner as these other studies.

CONCLUSION

A completely novel green process referred to as solvent-free-extrusion-emulsification (SFEE) is studied to better understand the effects of chemical parameters on its mechanism. It is shown that a transient rheological behaviour observed upon commencing water addition is a strong indicator of the striated lamella morphology to be developed by SFEE with the presented chemistry. The results and a related model on lamellae coarsening point to the lamellae thickness generated in dispersion region as being related to the final particle size after inversion. In order to obtain thinner lamellae, mixing favours the inclusion of a surfactant over solely depending on endgroup conversion to rapidly lower the interfacial tension between the polyester and water. When solely reliant upon polymer endgroups to favor interfacial growth between the polymer and water phases, the results show that the manner of NaOH addition can significantly affect lamellae thickness. Solid addition of NaOH becomes a rate-limiting step to morphology development because dissolution is comparable in timescale to the mixing time of the dispersion zone. Finally, the ionic strength of the system will notably affect the process in the absence of SDBS, which can be described as a caging effect that impeded dissociation of the functional group, raising the interfacial energy while lowering the activation energy to agglomeration of the striated lamellae.

ACKNOWLEDGMENTS

The authors thank to Dr. Robert H. Pelton for equipment use in his lab and Xerox Corporation for the provision of the resin. This study is supported by funds from Xerox

Corporation. The authors would also like to thank Canadian Centre for Electron Microscopy for using their facility.

REFERENCES

1. Trotta M, Debernardi F, Caputo O. Preparation of solid lipid nanoparticles by a solvent emulsification-diffusion technique. *Int J Pharm*. 2003;257(1-2):153-160.

2. Hamishehkar H, Emami J, Najafabadi AR, et al. The effect of formulation variables on the characteristics of insulin-loaded poly(lactic-co-glycolic acid) microspheres prepared by a single phase oil in oil solvent evaporation method. *Colloids Surf B Biointerfaces*. 2009;74(1):340-349.

3. Sani SN, Das NG, Das SK. Effect of microfluidization parameters on the physical properties of PEG-PLGA nanoparticles prepared using high pressure microfluidization. *J Microencapsul*. 2009;26(6):556-561.

4. Norato MA, Tavlarides LL, Tsouris C. Phase inversion studies in liquid-liquid dispersions. *Can J Chem Eng*. 1998;76(3):486-494.

5. Song D, Zhang W, Gupta RK, Melby EG. Role of operating conditions in determining droplet size and viscosity of tackifier emulsions formed via phase inversion. *AIChE J*. 2011;57(1):96-106.

6. Akay G. Flow-induced phase inversion in the intensive processing of concentrated emulsions. *Chem Eng Sci*. 1998;53(2):203-223.

7. Akay G, Tong L. Polymer dispersion preparation by flow induced phase inversion emulsification Part 1 The effect of silica on emulsification and dispersion characteristics. *Journal of Material Scinece.* 2000;5:3699-3709.

8. Akay G, Tong L, Bakr H, Paints ICI, Sl S. Preparation of ethylene vinyl acetate copolymer latex by flow induced. 2002;7:4811-4818.

9. Ashrafizadeh SN, Motaee E, Hoshyargar V. Emulsification of heavy crude oil in water by natural surfactants. *J Pet Sci Eng*. 2012;86:137-143.

10. Pandolfe WD. Effect of Dispersed and Continuous Phase Viscosity on Droplet Size of Emulsions Generated by Homogenization. *J Dispers Sci Technol*. 1981;2(4):459-474.

11. Chung JT, Cheng CM, Malachowski SM, Godshall ED, Pearson JL, inventors; Xerox Corporation, assignee. Method of continuously forming an aqueous colorant dispersion using a screw extruder. US9052625 B2. 2015.

12. Zhou K, Qiu SS, Moffat KA, Sacripante GG, inventors; Xerox Corporation, assignee. Solvent-free phase inversion process for producing resin emulsions. US20090208864 A1. 2009.

13. Goger A, Thompson MR, Pawlak JL, Lawton DJW. In situ rheological measurement of an aqueous polyester dispersion during emulsification. *Ind Eng Chem Res*. 2015;54(21):5820-5829.

14. Neubauer AC, Dunchus NW, inventors; Union Carbide Chemicals and Plastic Technology, assignee. Extuder Screw. US9278473 B2. 2016.

15. Goger A, Thompson MR, Pawlak JL, et al. Inline Rheological Behaviour of Dispersed Water in a Polyester Matrix with a Twin Screw Extruder. *Polym Eng Sci*. 2017; doi: 10.1002/pen.24613.

16. Mu B, Thompson MR. Examining the mechanics of granulation with a hot melt binder in a twin-screw extruder. *Chem Eng Sci*. 2012;81:46-56.

17. Liu Y, Thompson MR, O'Donnell KP, Grasman NS. Effect of temperature on the wetting behavior of hydroxypropyl methylcellulose in a twin-screw granulator. *Powder Technol*. 2016;302:63-74.

18. Wu S. Calculation of interfacial tension in polymer systems. *J Polym Sci Part C Polym Symp*. 2007;34(1):19-30.

19. Gokel GW. *Dean's Handbook of Organic Chemistry (2nd Edition).* McGraw-Hill, 2004.

20. Goger A, Thompson MR, Pawlak JL, Lawton DJ. Dynamic Rheological Measurements of Aqueous Polyester Dispersion in Batch Reactor and Twin Screw Extruder. *Society of Plastics Engineers (ANTEC)*; 2016:710-714.

21. Lawton DJW, Thompson MR, Faucher S. Morphological Development of Latex Particles in a Solvent-Free Extrusion Process. *Society of Plastics Engineers (ANTEC)*; 2014:1169-1174.

22. Veenstra H, Van Dam J, Posthuma De Boer A. On the coarsening of co-continuous morphologies in polymer blends: Effect of interfacial tension, viscosity and physical cross-links. *Polymer*. 2000;41(8):3037-3045.

23. Pötschke P, Paul DR. Formation of Co-continuous Structures in Melt-Mixed Immiscible Polymer Blends. *J Macromol Sci Part C Polym Rev*. 2003;43(1):87-141.

24. Otsubo Y, Prud'homme R. Effect of drop size distribution on the flow behavior of oil-in-water emulsions. *Rheol Acta 33 303-306*. 1994;306:303-306.

25. Zhang J, Li L, Wang J, Sun H, Xu J, Sun D. Double Inversion of Emulsions Induced by Salt Concentration. *Langmuir*. 2012;28(17):6769-6775.

26. Tawari SL, Koch DL, Cohen C. Electrical Double-Layer Effects on the Brownian Diffusivity and Aggregation Rate of Laponite Clay Particles. *J Colloid Interface Sci*. 2001;240(1):54-66.

27. Suksamranchit S, Sirivat A. Influence of ionic strength on complex formation between poly(ethylene oxide) and cationic surfactant and turbulent wall shear stress in aqueous solution. *Chem Eng J*. 2007;128(1):11-20.

Supporting Information for Chapter 4

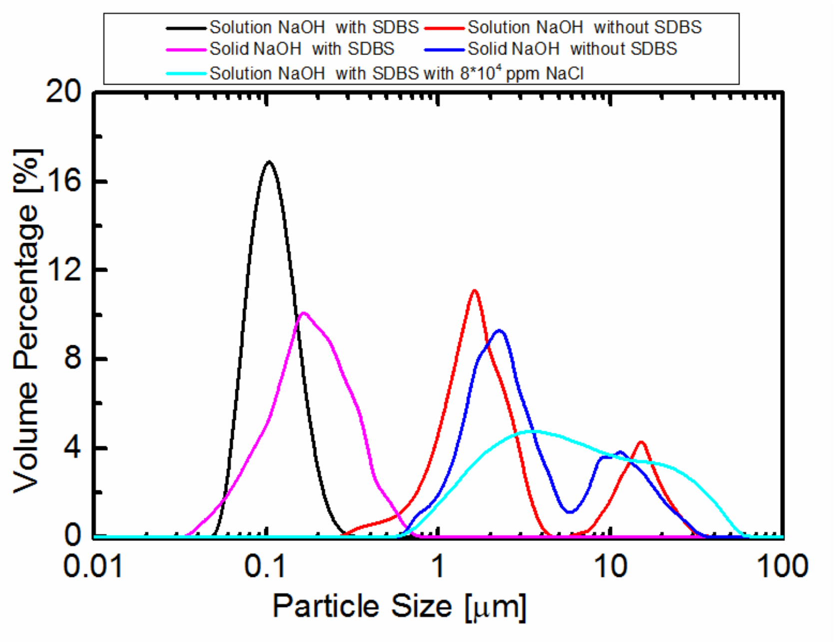

Supplementary Figure 4-1 Examples of particle size distribution of emulsion at 1 wt.% NaOH for different chemical contents.

Supplementary Table 4-1 Degradation ratio (DR), corrected neutralization ratio and uncorrected neutralization ratio with corresponded mean particle diameter (D_{50}) at Zone 7 of extruder.

	Sample Name	**Degradation Ratio [%]**	**Corrected Neutralization Ratio[%]**	**Uncorrected Neutralization Ratio [%]**	**D_{50} [μm]**
NO SDBS	Solid 0.5 wt.% NaOH-R/W:5	4.0	23.9	24.8	36.9
	Solid 0.5 wt.% NaOH-R/W:3.5	3.9	26.6	27.7	16.7
	Solid 1 wt.% NaOH-R/W:5	13.7	49.2	55.8	-
	Solid 1 wt.% NaOH-R/W:3.5	9.5	53.5	58.6	2.53
	Solution 0.5 wt.% NaOH-R/W:5	2.6	30.6	31.3	2.56
	Solution 0.5 wt.% NaOH-R/W:3.5	1.4	34.6	34.9	1.27
	Solution 1 wt.% NaOH-R/W:5	7.8	76.4	82.2	42.9
	Solution 1 wt.% NaOH-R/W:3.5	6.9	66.4	70.8	1.64
WITH SDBS	Solid 0.5 wt.% NaOH-R/W:5	5.7	27.8	29.1	2.21
	Solid 0.5 wt.% NaOH-R/W:3.5	6.9	23.6	25.2	1.63
	Solid 1 wt.% NaOH-R/W:5	16.7	51.2	59.6	0.52
	Solid 1 wt.% NaOH-R/W:3.5	14.8	44.4	50.9	0.17
	Solution 0.5 wt.% NaOH-R/W:5	3.6	25.1	25.9	0.35
	Solution 0.5 wt.% NaOH-R/W:3.5	3.3	28.1	29.0	0.11
	Solution 1 wt.% NaOH-R/W:5	11.9	53.1	59.4	0.22
	Solution 1 wt.% NaOH-R/W:3.5	10.4	50.4	55.6	0.10

Chapter 5 The Effect of Polymer Viscosity on Solvent-Free Polymer Emulsification inside a Twin Screw Extruder Part I: Molecular Structure

In chapter 5, all experiments and data anlaysis were conducted by the thesis author. M. Arnould at Xerox Webster conducted NMR test to determine molecular weights of the polymer samples. J. Pawlak and D. Lawton provided technical guidance on the project. The manuscript version of this chapter is being prepared for publication in 2017.

The Effect of Polymer Viscosity On Solvent-Free Polymer Emulsification Inside A Twin Screw Extruder Part I: Molecular Structure

A. Goger[1], M.R. Thompson[1*], J.L. Pawlak[2], M.A. Arnould[2], D.J.W. Lawton[3]

ABSTRACT

A new continuous emulsification technique known as solvent-free extrusion emulsification (SFEE) was recently introduced to prepare sub-micron particles (100-500 nm) from high viscosity polymers (100-1000 Pa.s) with a twin screw extruder. The present study examined the influence of matrix viscosity on its dispersion mechanism using crosslinked polyester as a viscosity modifier. The investigation used an inline rheometer for transient and steady state measurements of system viscosity, and offline characterizations including soxhlet extraction, colorimetric titration, and particle size analysis. Though it remained possible to produce particles close to their target size of 100-200 nm, particle size was notably increased by varying the matrix viscosity from 250 Pa.s for neat polyester up to 630 Pa.s with added modifier. The results point to thicker striated lamellae from less effective mixing prior to phase inversion when the matrix viscosity increases without a corresponding increase in surface active species. The study included a preliminary investigation on the screw configuration, revealing that a longer mixing zone for dispersing the water into the polyester was beneficial to forming smaller particles.

KEYWORDS: Mixing, matrix phase viscosity, twin screw extruder, solvent-free extrusion emulsification

INTRODUCTION

Methods of emulsification are used to prepare solid-liquid polymer dispersions for numerous products, such as adhesives, coatings and pharmaceutics. A new continuous emulsification technique is studied in this paper, previously introduced as solvent-free extrusion emulsification (SFEE)[1,2] suited to preparing solid-liquid dispersions from high viscosity polymers without the need for hazardous solvents. The technique is uniquely targeted to polymers in the range of 10-1000 Pa.s as the polymer must first flow as a bulk melt inside the extruder prior to phase inversion with water. A selection of literature studies are summarized in Table 5-1 to highlight the influence that viscosity has on phase inversion in regards to final particle size, covering range from 0.0007 Pa.s to 50 Pa.s[3–11]. Li et al.[3] were able to produce nano-sized particles between 40-200nm for very low polymer viscosities (i.e. 0.003 Pa.s-0.4 Pa.s), working at ambient temperatures with an agitator. Brooks and Richmond[4] found that their particle size increased from 13 µm to 99 µm as polymer viscosity rose from 0.0007 to 0.2 Pa.s, similarly working at room temperature with a rotor-stator device. In more recent studies by Ashrafizadeh et al.[7] and Song et al.[8], the viscosity range of their studied polymers reached 2 Pa.s and only micron sized particles were produced in those cases. The closest studies in terms of viscosity to SFEE were conducted by Akay et al.[9–11] who used a flow-induced phase inversion technique to prepare particles of 1-4 µm from polyethylenes with viscosities in the range of 50 Pa.s at 120ºC in an energy intensive batch shear mixer. The list in Table 5-1 demonstrates that batch processes show increased difficulty in producing nano-sized emulsified particles as the viscosity of the bulk matrix approaches 1 Pa.s and as a result, commonly require solvents to overcome this limitation.

Table 5-1 Polymer viscosity range used in literature in phase inversion process.

References	**Polymer Viscosity**	**Emulsion Particle Size**	**Processing Temperature**	**Device**
Li et al.[3]	0.003-0.040Pa.s	40-200nm	Ambient	Agitator
Brooks and Richmond[4]	0.0007 Pa.s	13 µm	Ambient	Rotor-Stator Device
	0.05 Pa.s	60 µm		
	0.1 Pa.s	64 µm		
	0.2 Pa.s	99 µm		
Zerfa et al.[5]	0.013mPa.s	3-70 µm	Ambient	Paddle-Type Agitator
Fernandez et al.[6]	-	0.6-10 µm	80ºC	Homogenizer
Ashrafizadeh et al.[7]	2.7 Pa.s	8-25 µm	25ºC	Homogenizer
Song et al.[8]	5 Pa.s	0.6-1.5 µm	43-54ºC	Multi-Type Impeller
Akay and Tong[9]	50 Pa.s	1.03-4.19 µm	120ºC	Haake® Mixer
Goger et al.[2]	200 Pa.s	~0.15µm	95ºC	Twin Screw Extruder (TSE)

Compared to traditional emulsification methods, SFEE is attractive to industry[12–15] for its effective handling of high viscosity polymers, capable of producing sub-micron particles in the range of 100 nm in a water medium without the need of undesirable solvents. The process takes place in a twin screw extruder within three distinct regions that are shown in Figure 5-1 as the: (i) *Melt-mixing zone* where polymers are plasticated and mixed with other ingredients into a bulk melt phase; (ii) *Dispersion* zone where the first water addition occurs and is mixed into the melt phase; and (iii) *Dilution zone* where a second, much larger amount of water is added to initiate phase inversion and subsequently solidify the generated particles. The challenge to utilizing the method and scaling its output to industrial needs, is understanding its sensitivity to a broad range of material and process variables, few of which have received study to date.

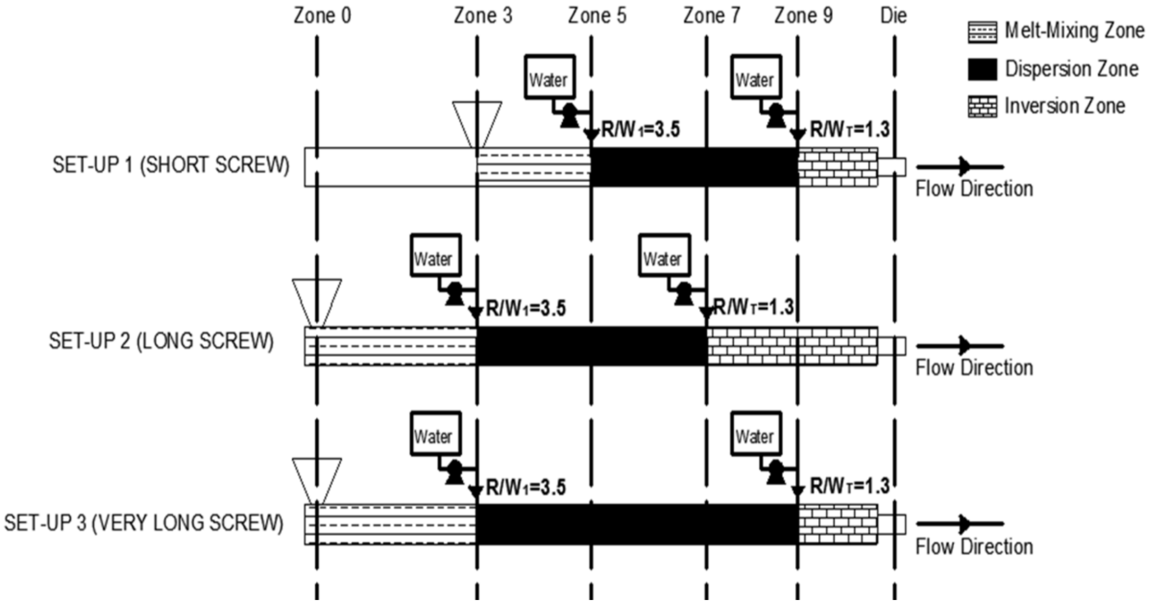

Figure 5-1 Drawing of extruder set-ups used in this study. a: Set-Up 1 (Short Screw), b: Set-Up 2 (Long Screw), c: Set-Up 3 (Very Long Screw).

A previously published study examined the role of surface active species on generated particle size[1] but in the presence of hydrolytic degradation, questions arose regarding the role of matrix viscosity on SFEE. For SFEE, variation of matrix viscosity without significantly affecting other variables that control particle generation such as interfacial energy can be accomplished either be altering the molecular structure of the polymer or varying the barrel temperature. In the present paper, polymer viscosity was adjusted by crosslinking, whereas the influence of system temperature will be examined in a following study.

The purpose of this paper is to elicit a better understanding of the mechanism within the dispersion zone of SFEE, building on previous work, and to begin to gain insight into particle solidification in the following dilution zone of the extruder. The two main variables of study were polymer viscosity and screw configuration, while other important parameters related to surface energy were adjusted to perturb the system.

MATERIALS AND METHODS

Material

The polyester provided by the Xerox Corporation (Webster, NY) was classified as a high flow grade (M_W=17081 g/mol; M_W/M_N=4.2) with acid number of 17.7±1.7 mg/g KOH. Sodium hydroxide pellets (NaOH) (Caledon Laboratories Ltd.; Georgetown, Ontario) were ground and sieved, using only particles in the order of 850-1180 μm to improve their dissolution. Sodium dodecyl benzenesulfonate (SDBS) [melting point 300ºC, molar mass 348.48 g/mol and solid density 1g/cm^3] was purchased from Sigma-Aldrich (Toronto, Ontario). Deionized water (>0.1 μS/cm^2) was used in all experiments. Benzoyl peroxide (BPO) was purchased from Sigma-Aldrich (Toronto, Ontario) for crosslinking to produce the process modifier.

Processing Modifier (PM) Preparation

A process modifier (PM) was synthesized to be added to the neat polyester as a means of increasing matrix viscosity. It was prepared by reacting the neat polyester and benzoyl peroxide (BPO) inside a Rheomix 3000 batch mixer (Haake, Germany) operating at 50 rpm. Firstly, 200 g polyester was melted at 90ºC for 5 min followed by mixing in 2.5 wt.% BPO over an additional 5 min, keeping the melt below 105ºC which is the decomposition temperature of the peroxide according to Han et al.[16] Subsequently, the mixture was reacted by increasing the mixer temperature to 110ºC and continuing to mix for another 15 min. The torque of the mixer reached a plateau value of 46.3±1.4 Nm after 13.7±0.2 min once at 110ºC. Lastly, the mixer temperature was increased to 120ºC for 5 min in order to ensure consumption of all unreacted BPO. The mixer was returned to 110ºC with a measured torque value of 45.8±1.2 Nm, confirming completion of the reaction. The process modifier was ground into 3 mm granules and stored.

General Process Setup

SFEE trials were done with a 40 L/D, 27 mm Leistritz ZSE-HP co-rotating twin-screw extruder (TSE) (American Leistritz Extruder Corporation; Somerville, NJ). Two high pressure syringe pumps (Teledyne Isco; Lincoln, NE) were used to inject water into the TSE. The first water injection into the process occurred at Zone 3 or Zone 5, as shown in Figure 5-1, depending on the screw configuration while the second injection location varied between Zone 7 or Zone 9. Details on how the injection locations were used are provided in a following section. Solids were fed at 8 kg/h by DDSR20 gravimetric feeder (Brabender Technologie Inc.; Mississauga, Ontario) to the feed port, which shown in the figure was positioned at Zone 0 or Zone 3.

The water temperature inside pumps for the first and second water injection locations was controlled by an Isotemp™ heating bath (ThermoFisher Scientific Inc.;

Waltham, MA) in order to reasonably maintain a constant temperature difference (ΔT = 90 ^{o}C) between the incoming water and polymer melt within the extruder; this was more important to a later study to be published on varying barrel temperature but it was consistently applied in the present case as well due to differences in viscous energy dissipation between experimental conditions. The melt temperature at the first water injection location was measured with a K-type thermocouple to control this temperature differential, with the measured values (prior to water addition) shown in Table 5-2 for differing amounts of process modifier added to the polyester.

Table 5-2 Barrel, melt and water temperature for different operating conditions.

Barrel Temperature	Melt Temperature	Water Temperature
[ºC]	[ºC]	[ºC]
110 (with 0 wt% PM)	124±0.4	34
110 (with 9 wt% PM)	127±0.6	37
110 (with 27 wt% PM)	134±0.4	44

The barrel temperatures are kept constant at 110ºC from zone 0 (0-4 L/D) to zone 9 (36-40 L/D) along the extruder. The extruder screw speed was 300 rpm for all trials with aggressive mixing screw design like the one by Neubauer et al.[17] Sketches in Figure 5-1 show the three extruder set-ups used in this study to vary mixing in the dispersion zone, and are described below. The configurations were intended to further probe the mechanism in the dispersion zone, building upon earlier studies.[1,2] The configurations were also used to gain some preliminary insights into solidification within the dilution zone, though future studies will examine the section in greater detail.

Set-up 1

In this extruder configuration, the feed port for solids was located at Zone 3 (12 to 16 L/D) shortening the overall process length. The first amount of water was injected at Zone 5 (20 to 24 L/D), the second addition of water was pumped into the TSE at Zone 9 (36 to 40 L/D) immediately before the die. The configuration is shown in Figure 5-1(a) and is referred to as the "short screw". The dispersion zone in this configuration was normal in length to the standard configuration[2] but eliminated the dilution zone after the second water injection location where the dispersed polymer phase is normally allowed to solidify prior to exit. The screw design allows direct sampling of the polymer immediately upon phase inversion, and in comparison highlights phenomena in the dilution zone when results were compared to those from Set-up 2.

Set-up 2

This extruder configuration was identical in length and arrangement to the standard configuration for SFEE.[2] The gravimetric feeder and feed port for solids were located at Zone 0 (0 to 4 L/D). The first water addition location was found at Zone 3(12 to 16 L/D) while the second water injection location was placed at Zone 7 (28 to 32 L/D), as drawn in Figure 5-1(b). This configuration is referred to as the "long screw".

Set-up 3

In this extruder configuration, the gravimetric feeder and feed port were found at Zone 0 (0 to 4 L/D) while the first water injection location is placed at Zone 3 (12 to 16 L/D) and the second water injection location is located at Zone 9 (36 to 40 L/D), as shown in Figure 5-1(c). This configuration was referred to as the "very long screw" and used in order to examine the effect of mixing length on the dispersion zone of SFEE while once again eliminating the dilution zone past the second water injector compared to Set-up 2. Only conditions with SDBS were studied in this configuration since its use was intended to focus on improving the process rather than the more detailed study of the dispersion zone mechanisms done with the other two set-ups.

Inline Rheometer

A custom-built inline rheometer based on an orifice plate flow-meter design was used as the extruder die for inline measurement of apparent viscosity of polyester-water mixture. The inline rheometer was validated in an earlier study, being used to measure steady state viscosity as well as transient rheological behaviors of the SFEE process.[1] It has been shown to provide valuable insights into the dispersion mechanism related to morphological development of the polyester-water mixture prior to phase inversion in the extruder,[2] but first noted in a batch reactor.[18] The diameter of the die is 15 mm, though its flow is obstructed by a 2 mm orifice plate midway along its length in order to generate as well resolved pressure drop and to also minimize water potentially draining from the extruder rather than extruded under drag forces. Two PT467E pressure transducers (Dynisco; Franklin, MA) measured the pressure drop across the orifice plate as a distance of 17 mm before and after the obstruction. A K-type thermocouple (located 87 mm between the orifice plate and die exit) was used to measure the exiting fluid temperature. The exit temperature was used to correct viscosities measured at the die to a comparable value at a reference temperature of 100 ^{o}C, compensating for the influences of water cooling and viscous dissipation based on the conditions of study. The temperature shift in viscosity values was done using an Arrhenius approximation with flow activation energy of 32.7 kJ/mol obtained by offline rheometer.[18]

Trial Procedure

The variables of the study included, SDBS content, method of NaOH addition, PM content and extruder configuration. The solids added by gravimetric feeder included polyester flake that was dry blended with processing modifier (0, 9 or 27 wt.%), and SDBS (0, 7.5 wt.%) based on experimental condition. The NaOH content was fixed at 1 wt.% but introduced as either ground solids to be added with the polyester or as an aqueous solution at the first water injector location. The variable list is included in Table 5-3, showing all levels tested under each factor. The latter two variables are newly considered for their influence on the dispersion zone compared to previous studies.

Table 5-3 Variables were used in this study.

SDBS Content [wt.%]	NaOH Addition Type [-]	Extruder Configuration [-]	Polyester Matrix Viscosity [Pa.s]
0	Solid	Short Screw	251
7.5	Solution	Long Screw	374
		Very Long Screw	624

Under normal operations, after five minutes running the extruder to record a steady baseline condition by the rheometer, the resin-to-water at the first water injection location (R/W_1) was set to 3.5 while the second injector was not used. This mode of operation is denoted as *Mode 1* in the discussions to examine the rheological behaviour in the polymer-water mixture prior to phase inversion. After collecting inline rheometer data over five minutes of operation, water was now added at the second water injection location to increase the total resin-to-water ratio (R/W_T) to 1.3. This mode of operation is called *Mode 2*, producing a milky-looking emulsion at the exit. The only rheological data collected during this mode of operation was used in the emulsion stability trials. The procedure was explained in more detail in a previous study.[2] While running in Mode 1, approximately 20 g of the plastic-looking extrudate was collected at the end of die exit and quickly quenched in cold water to preserve the morphology. Collected samples were dried over 18 h at 60 ^{o}C under vacuum and stored for endgroup titration. While running in Mode 2, approximately 50 ml of the milky emulsion was collected at the end of die and rapidly cooled further by dispersing into a beaker containing 200 mL pure water at room temperature.

Particle Characterization

The particle size distribution of prepared polymer particles with sizes under 1µm were obtained by laser light scattering using a Brookhaven 90Plus (Long Island, NY) which used a 35 mW laser source of 600 nm wavelength configured at an angle of 90º. For particle size distributions above 1µm, measurements were done with a MasterSizer 2000^{TM} (Malvern, United Kingdom) which has a detection range of 0.1 to 2000 µm. All testing was done with three replicas in a water medium. Span of the distribution was calculated according to Eq. (5.1):

$$Span = \frac{D_{90} - D_{10}}{D_{50}} \tag{5.1}$$

where D_{50} is the mean diameter of the particle population, D_{90} corresponding to the size where 90% of the distribution lies below and D_{10} corresponds to the particle size below which 10% of the population lies.

Colorimetric Titration

The method used to calculate acid number (AN) followed ASTM-D974. Methyl ethyl ketone (MEK) (50 mL) was used to dissolve 1 g of a dried sample with the addition of 0.5 mg p-naphtholbenzein indicator. The solution was constantly stirred while being titrated with a 0.1 N potassium hydroxide (KOH) solution in isopropanol (Sigma-Aldrich, certified standard).

Offline Rheology

Viscosity of the neat polyester, cross-linked PM, and melt extruded polyester-PM mixtures (9 wt.% and 27 wt.%) were determined in an ARES parallel plate rheometer (TA Instrument; New Castle, DE) using 25 mm diameter plates and a 1.5 mm gap distance. The offline rheometer was conducted at oscillating mode over a frequency range of 0.1 to 100 rad/s at a strain rate of 5% (determined with strain sweep test).

Gel Content Measurement

The gel content of the cross-linked polyester was determined by Soxhlet extraction with MEK at 100ºC for 24 h. Approximately 1 g of sample, ground to a 20 Mesh size, was tested each time in a glass fiber 603G Whatman® thimble. After extraction, the thimble filled with residual material was dried for 24 h at 60ºC under vacuum. The gel content was calculated based on the ratio between dry weights of the sample before and after extraction.

NMR Spectroscopy

Weighed process modifier or neat resin was dispersed in a pyridine-deuterated chloroform solution containing a known amount of a perfluorinated version of BPA (Bisphenol AF) as an internal reference. To the mixture, 2-chloro-4,4,5,5-tetramethyl-1,3,2-dioxaphospholane (CTDP) was added as the phosphorus derivitizing agent. CTDP reacts quickly and quantitatively with both acid and hydroxyl groups, and through the use of Bisphenol AF as an internal standard, the amount of each specific acid and hydroxyl group can be determined.[19] Phosphorus-31(^{31}P) NMR measurements were performed using a Bruker AV-400 NMR spectrometer.

Statistical Analysis

A general factorial statistical design based on the factors in Table 5-3 was applied in this study. The significance level was determined based on P-values determined using Design Expert 7.1 (State-Ease Inc., Minneapolis, MN). In addition, regression analysis was done for the two experimental responses of rheological changes and mean particle diameter. The coefficients of C_1 and C_2 were obtained for the different matrix viscosities to gauge the relative impact of viscosity on these two rheological responses. The regression equation is shown as,

$$d_{50} = C_1\left(\frac{\Delta\eta}{\Delta t}\right) + C_2(\lambda) \qquad (5.2)$$

where d_{50} is normalized mean particle diameter, $\Delta\eta/\Delta t$ is the slope of apparent viscosity change, and λ is the relative viscosity. Relative viscosity (λ) was calculate as the ratio between the polyester-water mixture at R/W_1=3.5 versus the matrix viscosity without water (both values determined by the inline rheometer). d_{50} was calculated by using mean D50 and standard deviation of D_{50} of all experiments.

RESULTS AND DISCUSSION

The dispersion zone (i.e. the zone between first and second water injection locations) was primarily under study but this work also includes for the first time, preliminary analysis of phenomena in the dilution zone (i.e. region after the second water injection location). The three variants in screw design were selected for this purpose; however, the influence of viscosity was considered the major variable of study. Varying viscosity by changes in molecular structure was ideally accomplished with no change in the number of convertible endgroups since the carboxylate groups they form within the process would otherwise affect the surface activity of the resin with respect to water; interfacial energy and viscosity were shown in a previous paper[2] to govern the developed lamellae morphology controlling final particle formation in SFEE. Hence, an unobscured study of viscosity on particle properties needed to be done with minimal influence on aspects that would simultaneously change surface energy of the resin. In this regards, creating a crosslinked polyester as an additive for the matrix was considered the best approach. The initial discussions below characterize the process modifier created and its impact when added to the neat polyester before examining the effect of matrix viscosity on the SFEE process.

Characteristics of Process Modifier (PM) and Processed Resins

Offline complex viscosity curves at 110 °C are shown in Figure 5-2 for the PM collected from the batch mixer in comparison to extruded samples of mixtures containing 9 wt.% or 27 wt.% PM blended with the neat polyester (without water, NaOH or surfactant present). The PM exhibited significant shear thinning behaviour with a power-law index of 0.49 due to crosslinking, quite different from the near Newtonian behavior of the neat polyester. The extruded neat polyester and the two polyester/PM blends were found to have power-law indices of 0.98, 0.89 and, 0.82, respectively. The two polyester blends with 9 wt.% and 27 wt.% PM show viscosities of 364 Pa.s and 624 Pa.s, respectively at the average shear rate inside the die (previously calculated[1] and shown as a dashed line in the figure), showing a distinctive rise relative to 251 Pa.s for the neat resin.

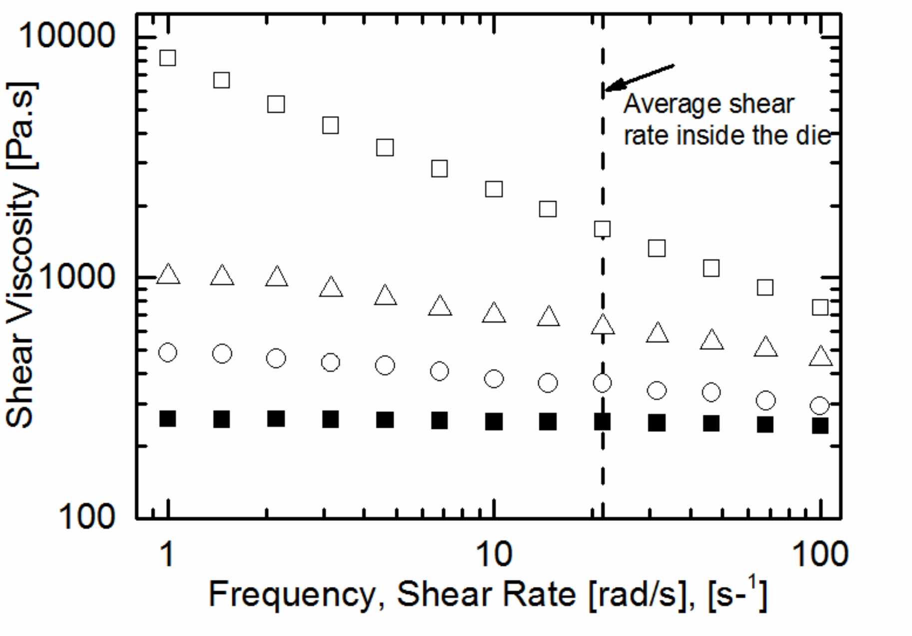

Figure 5-2 Viscosity curves for the processing modifier (PM) and different polyester/PM mixtures at 110°C (■ 0 wt.% PM, ○ 9wt.%PM, △27 wt%.PM, □100 wt.% PM)

Acid number (AN) was used to estimate endgroup content in the study. No AN value was possible for PM by titration due to dissolution problems in MEK solvent. The titration results in Figure 5-3 show that AN changed slightly for the differing PM contents, increasing by 15% with 27 wt.% PM added. For comparison, the acid number was similarly assessed for neat polyester and PM by ^{31}P NMR, finding AN of the former to be 15.9 mg KOH/g sample and little change for the latter at 16 mg KOH/g. Due to known dissolution issues with crosslinked polymers, both techniques possess some error in their quantification, but it was felt the results were generally showing an insignificant increase in endgroups by PM addition as a viscosity enhancer. Included in Figure 5-3, the gel content of the mixtures rose to 7.1% and 16.3% for 9 wt.% and 27 wt.% PM in the polyester, respectively while PM itself exhibited a 56.9% gel content. It might be possible that these gels hindered SFEE in producing a narrower particle size distribution by constraining some particles to be larger in size, but no trend between span and PM content was found to consider this as a concern in the study.

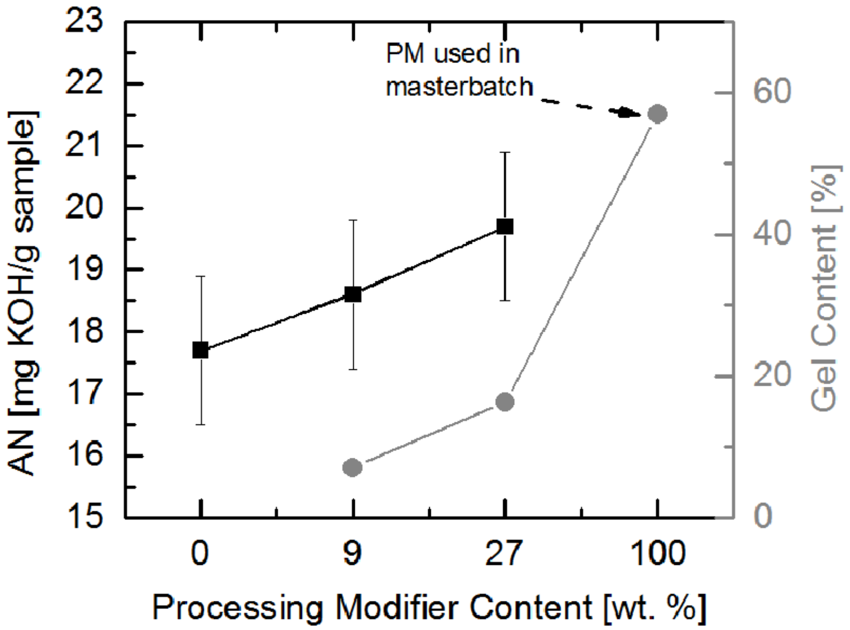

Figure 5-3 Acid number (AN) and gel content for different PM content. (■ AN, ● Gel Content). Neat processing modifier (PM) is shown with a dashed arrow.

Effect of Surfactant

To minimize the SDBS content necessary for SFEE and to increase the system robustness, it is normal part of the process that some fraction of the carboxylic acid endgroups are converted *in situ* to carboxylates. Ideally, complete conversion would benefit SFEE but then the extent of hydrolysis becomes an uncontrollable side-reaction. The extent of conversion is stated by the neutralization ratio (NR), which is the percent of initial endgroups converted based on the measured acid number; difficulties experienced with molecular weight characterization of the samples containing gels prevent correcting this value chain breakages during the process. Figure 5-4 shows the determined NR plotted against matrix viscosity for the cases without and with SDBS as well as for both methods of NaOH addition in the short screw configuration. The results show no effect of matrix viscosity on the extent of endgroup conversion, validating the intent of using PM to modify viscosity in the study. The constant neutralization ratio indicates that interfacial energy between the polyester and water can be reasonably considered to be constant relative to changes in matrix viscosity. Notably, other variables were influential though, with NR lower in value with the inclusion of SDBS or use of solid NaOH in the process; the influence of these two variables on NR is consistent with earlier reported finding.[2]

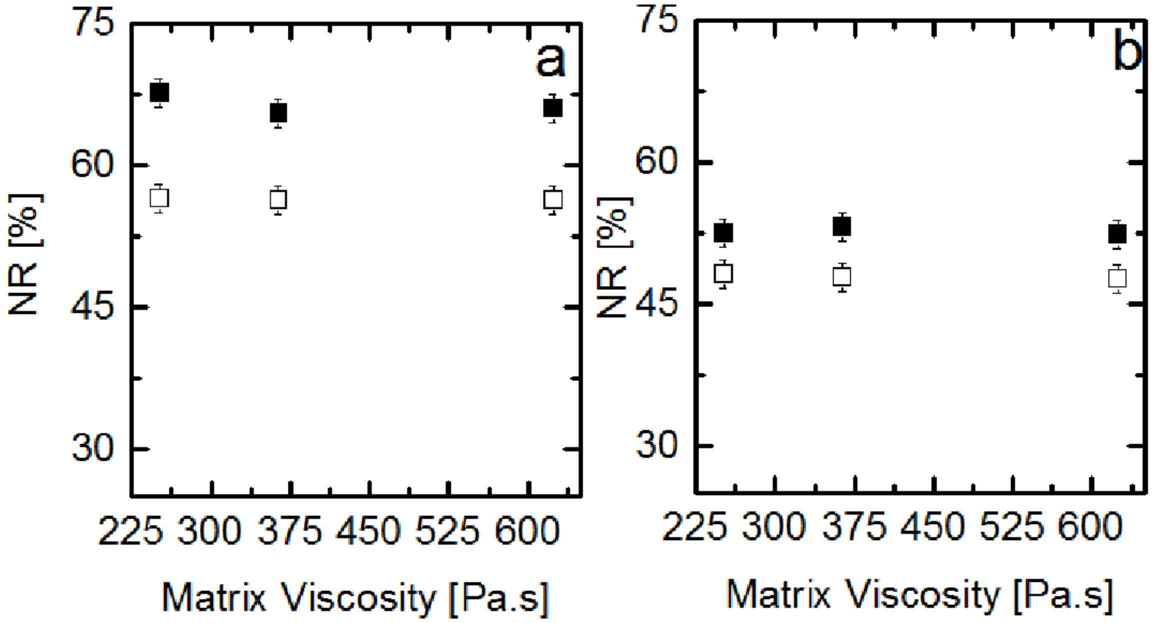

Figure 5-4 Neutralization ratios (NR) for different polyester matrix viscosities with short screw. (a) Without SDBS (b) With SDBS. (■ Solution NaOH, □ Solid NaOH)

The generation and thinning of striated lamellae of polyester with respect to water are considered to be the dominant mechanism in the dispersion zone of SFEE[20] and the kinetics of lamellae thinning can be expressed by the slope of changing apparent viscosity[1,2] ($\Delta\eta/\Delta t$). Goger et al.[1] found that this transient rheological response occurring as water first enters the dispersion zone, is related to the kinetics of water incorporation in the polyester and can be a good predictor of the final particle size. A more rapid drop in apparent viscosity (i.e. larger negative slope) occurs with more favourable polymer-water association, correlating strongly with smaller particle generation.[1,2] The relative viscosity will similarly decline in value, $\lambda<1$, with more favorable water incorporation into the polyester matrix. Figure 5-5 illustrates the trend for $\Delta\eta/\Delta t$ and λ (measured under Mode 1 operations with short screw) versus mean particle diameter (D_{50}) (based on samples collected under Mode 2 conditions with long screw) for cases with varying SDBS content and method of NaOH addition. Plot (a) and (c) show similar trends to earlier findings,[1,2] with a lower $\Delta\eta/\Delta t$ (i.e. larger negative slope) corresponded to smaller particle sizes and the fact that sub-micron particles could only be produced with the inclusion of SDBS. Plot (b) finds that relative viscosity varied between $\lambda=0.69$ (solid NaOH) and $\lambda=1.22$ (solution NaOH) addition without addition of SDBS, compared to more significantly reduced values between $\lambda=0.52$ (solid NaOH) and $\lambda=0.42$ (solution NaOH) when SDBS was included. The relative viscosities show that prior to phase inversion, the viscosity of the polymer-water mixture remained well above 100 Pa.s and possibly exceeded the viscosity of the neat polyester for the solution NaOH case, which has been attributed to undesirable associations between the lamellae.[2] It is interesting to note that that the method of NaOH addition had opposite effects in the plots depending on whether SDBS was present. It may explained with earlier findings[2] that low interfacial energy of the SDBS, polyester-water mixture was not sensitive to the build-up of $Na+$ from local high concentrations of NaOH such that the increased tendency to agglomerate thickened the lamellae and increased the system viscosity. Reported P-values for significance are given in Table 5-4, showing that both inclusion of SDBS and matrix viscosity significantly affected $\Delta\eta/\Delta t$ ($P<0.0001$) and λ ($P<0.0001$).

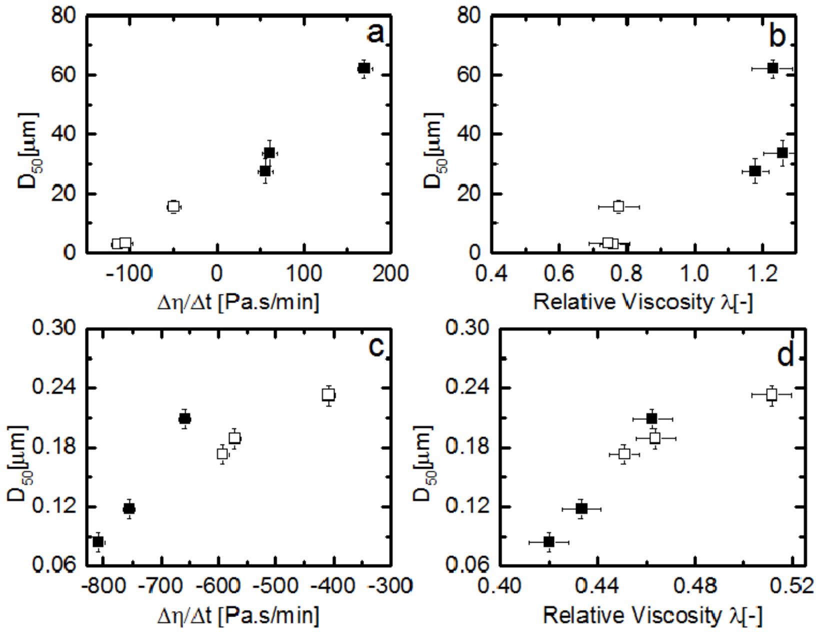

Figure 5-5 Effect of slope of viscosity changes (Δη/Δt) and relative viscosity (λ) of short screw set-up on mean particle diameter (D50) of long screw set-up (a) Δη/Δt without SDBS (b) λ without SDBS (c) Δη/Δt with SDBS (d) λ with SDBS. (■Solution NaOH, □ Solid NaOH)

Table 5-4 Significances of parameters on rheological properties.

Parameters	Δη/Δt [Pa.s/min]	λ [-]
Surfactant Content	p value<0.0001	p value<0.0001
NaOH Addition Type	p value=0.006	p value=0.1
Polyester Matrix Viscosity	p value<0.0001	p value<0.0001
Screw Type [short vs. very long screw]	p value=0.03	p value=0.008

To highlight the effect of matrix viscosity on these two rheological measures of the dispersion mechanism, Table 5-5 summarizes the regression coefficients fitting the effects of $\Delta\eta/\Delta t$ and λ on normalized d_{50} based on the viscosity of the polyester; the model fit was acceptable in each case with R^2 of 0.92, 0.90 and 0.95 for matrix viscosities of 251 Pa.s, 374 Pa.s and 624 Pa.s, respectively. Particle sizes produced by SFEE appeared tolerant to a small increase in matrix viscosity progressing from 251 Pa.s for the neat resin to 374 Pa.s at 9 wt.% PM, with the coefficients for both $\Delta\eta/\Delta t$ (C_1=0.002) and λ (C_2=1.8) unaffected. However, raising the matrix viscosity to 624 Pa.s, both coefficients increased by a factor of five to C_1=0.01 and C_2=9.5 indicating the process now had greater difficulties in generating smaller particles. The kinetics for water incorporation became substantially slower suggesting poorer transmission of stresses between the polymer and water phases during mixing in the dispersion zone as matrix viscosity increased, resulting in thicker striated lamellae by the end of the zone. This effect was made more obvious with the inclusion of SDBS, where the concentration of surface active functional groups was 375% higher than without SDBS, such that interfacial area growth became more favourable.

Table 5-5 Coefficients of regression analysis for different matrix viscosities.

Matrix Viscosity (Pa.s)	C_1 [-]	C_2 [-]
251	0.0023	1.8
364	0.0024	1.8
624	0.0117	9.5

The data in Figure 5-5 shows that the process with SDBS was able to maintain better stress transmission between the phases during mixing, producing much smaller $\Delta\eta/\Delta t$ and λ, and little difference in their values between 251 Pa.s to 374 Pa.s. Based on the model of Veenstra[21] for rate change of lamella thickness, solid surface energy needed to increase 32% and 59% for 374 Pa.s and 624 Pa.s in compensation of the viscous forces hindering lamellae thinning. Figure 5-6 highlights the influence that matrix viscosity had on dispersion mechanism by plotting emulsified particle size, without and with SDBS for the long screw configuration. The delayed effect of increasing matrix viscosity on generating larger particles mentioned above by inclusion of additional surface active species in the process is well demonstrated in these plots. The data indicates that particle size of the emulsified polymer increased linearly within the range of matrix viscosities studied, though the SDBS cases suggest a possible non-linear relationship if the range of viscosities increased. According to Salager et al.,[22] conditions producing a stable Q/W emulsion by catastrophic phase inversion diminished in their allowable variance as the oleophilic phase viscosity increased, and completely vanished above 0.5 Pa.s in their case. The span of the particle size distribution was unaffected by matrix viscosity yet varied from 2.5±0.2 in the absence of SDBS, to 0.21±0.04 when SDBS was included; the state of mixing in the process became more uniform when SDBS was used.

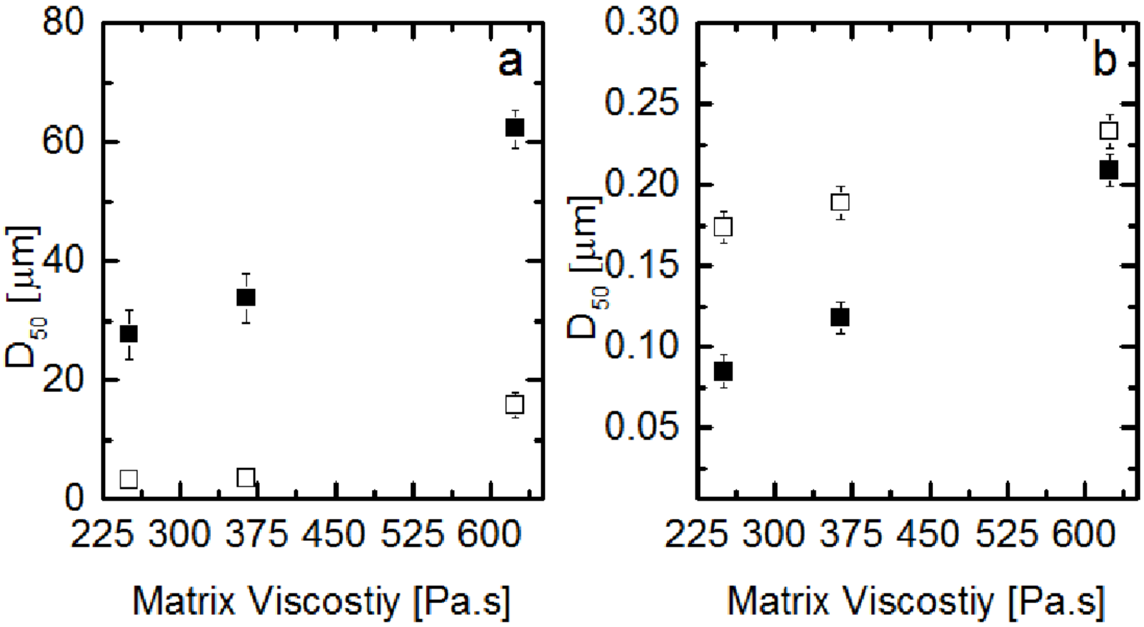

Figure 5-6 Influence of matrix viscosity on mean particle diameter (D_{50}) for long screw set-up. (a) without surfactant. (b) with surfactant.(■Solution NaOH, □ Solid NaOH)

Effect of Dispersion Length

The previous section indicated declining effectiveness of mixing water into the polymer as matrix viscosity increased, but in that case for a fixed dispersion zone length. Increasing surface active species in the system allowed a broader range of viscosities to produce the same particle sizes yet one can speculate that increasing the mixing length might further broaden the robustness of the process. To test this hypothesis, the effect of dispersion length was evaluated based on NR, inline rheological changes and D_{50} of the prepared emulsions, looking at conditions using solid NaOH addition and SDBS included between the short and very long screw. The rheological data collected under Mode 1 was being compared in this case with particles collected under Mode 2 operation from the same screw configuration. In plot (a) and (b) of Figure 5-7, it is seen that $\Delta\eta/\Delta t$ and λ

increased with increasing matrix viscosity for both short and very long screw due to the fact that rate changes of lamella thickness was predominantly affected by interfacial tension with SDBS being present. Both rheological responses (i.e. Δη/Δt and λ) decreased as dispersion length increased, showing beneficial lamellae thinning with increasing mixing time. However, the longer dispersion zone did not affect the robustness seen in the shorter screw configuration, with similar Δη/Δt and λ between 251-364 Pa.s and a large increase at 624 Pa.s seen in both setups.

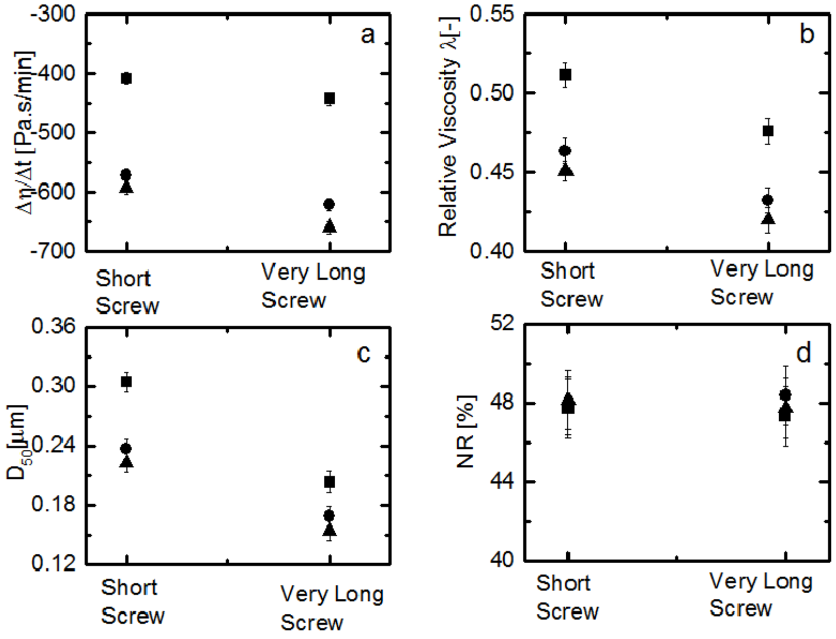

Figure 5-7 The effect of dispersion zone length on the SFEE in the inclusion of surfactant with solid NaOH. (a) Slope of viscosity changes (Δη/Δt) (b) Relative viscosity (λ) (c) Mean particle diameter (D_{50}) (d) Neutralization ratio (NR).(▲251 Pa.s, ●374 Pa.s, ■624 Pa.s)

The particle size results in Plot (c) confirm the improved mixing state for lamellae generation with a longer dispersion length by showing significantly smaller particles produced on the very long screw. Notable in the plot is the similar particle size at 624

Pa.s compared to those produced at the other viscosities on the very long screw, which neither rheological response above would have predicted. Finally, Plot (d) shows that end group conversion was not affected by the length of the dispersion zone; earlier reported finding[2] show that the conversion reaction occurs relatively rapidly and NR values rarely change past the second barrel zone after when water was added (i.e. Zone 7).

Effect of Dilution Zone

In this section, some insight was sought into particle solidification and coalescence phenomenon within the dilution zone of SFEE by examining results between the different screw configurations. Only results under Mode 2 operational conditions are reported, for cases using solid NaOH and SDBS. Figure 5-8 compares particle size from the short screw (which has a negligible dilution zone) and the long screw (which has the same dispersion zone as the short screw but two zones (Zones 7-9) after the second injection location to cool the particles. Temperature of the added water at the second injection site varied according to Table 5-2 based on the matrix viscosity but was always maintained well below the glass transition temperature of the polyester. Interestingly, the particle size data shows that D_{50} increased noticeably when the short screw is used compare to long screw, even though the dispersion zones were equivalent. The reason may be that the absence of dilution zone limits the heat transfer between polyester-water mixture and water which delays the onset of phase inversion.

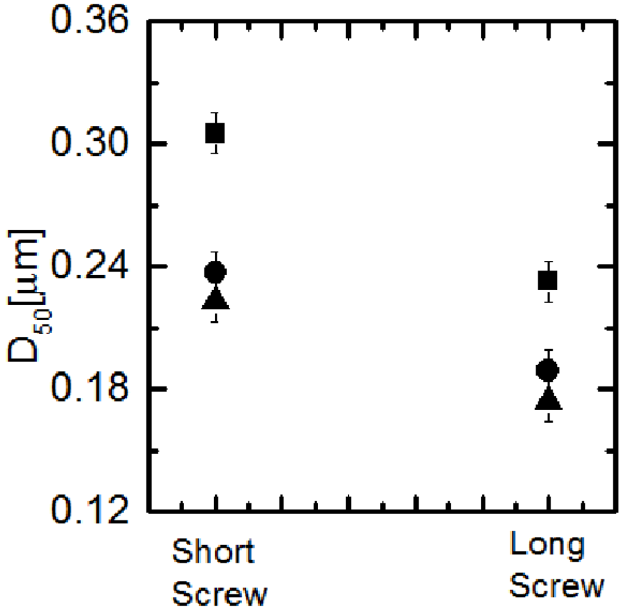

Figure 5-8 Effect of dilution zone in SFEE on mean particle diameter (D50) in the inclusion of surfactant with solid NaOH. (▲251 Pa.s,   374 Pa.s,   624 Pa.s)

Emulsion Stability in the Dilution Zone

The prior sections studied the mechanisms of SFEE while this section specifically evaluates its processability. The apparent viscosity of emulsion after the second water addition ($R/W_T = 1.3$) was typically in the range of 25 Pa.s regardless of the screw configuration or matrix viscosity used. Stability of created emulsions in SFEE was categorized based on inline rheological analysis where: (i) “Very Stable” corresponded to fluctuations in the apparent viscosity that were less than 10%; (ii) “Stable” where fluctuations varied between 10 % and 60%; and (iii) “Not Stable” where fluctuations in apparent viscosity exceed more than 60%. Table 5-6 summarizes stability of the process for the different screw configurations and formulations considered throughout the study. In the absence of SDBS, most cases were unstable with only matrix viscosities of 251Pa.s and 374 Pa.s for the solid NaOH cases displayed stability. These stable cases corresponded to the smallest particles without SDBS being used, below 3.6µm. On the other hand, the process was considered very stable in operation under most conditions with SDBS used except with the highest polyester matrix viscosity that only showed stable processability. The cases with matrix viscosity of 624 Pa.s that showed only stable operations were noted to produce the largest particles for all three screw types with SDBS present.

Table 5-6 Emulsion stability in dilution zone for different screw type and chemical contents.

Sample Name		**Screw Type**	**Viscosity Fluctuation Level**
SOLUTION NaOH- 251 Pa.s	No SDBS	Short Screw	NOT STABLE
SOLUTION NaOH- 374 Pa.s		Short Screw	NOT STABLE
SOLUTION NaOH- 624 Pa.s		Short Screw	NOT STABLE
SOLID NaOH- 251 Pa.s		Short Screw	STABLE
SOLID NaOH- 374 Pa.s		Short Screw	STABLE
SOLID NaOH- 624 Pa.s		Short Screw	NOT STABLE
SOLUTION NaOH- 251 Pa.s		Long Screw	NOT STABLE
SOLUTION NaOH- 374 Pa.s		Long Screw	NOT STABLE
SOLUTION NaOH- 624 Pa.s		Long Screw	NOT STABLE
SOLID NaOH- 251 Pa.s		Long Screw	STABLE
SOLID NaOH- 374 Pa.s		Long Screw	STABLE
SOLID NaOH- 624 Pa.s		Long Screw	NOT STABLE
SOLUTION NaOH- 251 Pa.s	With SDBS	Short Screw	VERY STABLE
SOLUTION NaOH- 374 Pa.s		Short Screw	VERY STABLE
SOLUTION NaOH- 624 Pa.s		Short Screw	VERY STABLE
SOLID NaOH- 251 Pa.s		Short Screw	VERY STABLE
SOLID NaOH- 374 Pa.s		Short Screw	VERY STABLE
SOLID NaOH- 624 Pa.s		Short Screw	STABLE
SOLUTION NaOH- 251 Pa.s		Long Screw	VERY STABLE
SOLUTION NaOH- 374 Pa.s		Long Screw	VERY STABLE
SOLUTION NaOH- 624 Pa.s		Long Screw	VERY STABLE
SOLID NaOH- 251 Pa.s		Long Screw	VERY STABLE
SOLID NaOH- 374 Pa.s		Long Screw	VERY STABLE
SOLID NaOH- 624 Pa.s		Long Screw	STABLE
SOLUTION NaOH- 251 Pa.s		Very Long Screw	VERY STABLE
SOLUTION NaOH- 374 Pa.s		Very Long Screw	VERY STABLE
SOLUTION NaOH- 624 Pa.s		Very Long Screw	VERY STABLE
SOLID NaOH- 251 Pa.s		Very Long Screw	VERY STABLE
SOLID NaOH- 374 Pa.s		Very Long Screw	VERY STABLE
SOLID NaOH- 624 Pa.s		Very Long Screw	STABLE

CONCLUSION

The influence of matrix viscosity for a polymer being emulsified by SFEE was studied to better understand its role in the mechanism of lamellae thinning within the dispersion zone of the process. Increasing matrix viscosity was found to slow the kinetics of water incorporation and lower the degree to which water became dispersed in the polyester matrix, which resulted in increasing mean particle size of the generated emulsion. Process stability was notably lower at the highest matrix viscosity studied. Sub-micron particles could not be created in the absence of surfactant despite consistent neutralization of the carboxylic acid endgroup irrespective of matrix viscosity. Increasing the content of surface active species, however, delayed particle enlargement to higher viscosities. A longer dispersion zone provided more time for incorporation between polyester and water, favouring an apparent increases in the rate of lamella thinning and decreasing emulsified particles size.

REFERENCES

1. Goger A, Thompson MR, Pawlak JL, et al. On-line Rheological Behaviour of Dispersed Water in a Polyester Matrix with a Twin Screw Extruder. *Polym Eng Sci*. 2017.
2. Goger A, Thompson MR, Pawlak JL, Arnauld MA, Lawton DJW. Solvent-Free Polymer Emulsification Inside a Twin Screw Extruder. *AIChE J*. Submitted on 2017.
3. Li Y, Zhang Z, Yuan Q, Liang H, Vriesekoop F. Process optimization and stability of d-limonene nanoemulsions prepared by catastrophic phase inversion method. *J Food Eng*. 2013;119(3):419-424.

4. Brooks BW, Richmond HN. Phase inversion in non-ionic surfactant—oil—water systems—III. The effect of the oil-phase viscosity on catastrophic inversion and the relationship between the drop sizes present before and after catastrophic inversion. *Chem Eng Sci*. 1994;49(11):1843-1853.
5. Zerfa M, Sajjadi S, Brooks BW. Phase behaviour of polymer emulsions during the phase inversion process in the presence of non-ionic surfactants. *Colloids Surf Physicochem Eng Asp*. 2001;178(1–3):41-48.
6. Fernandez P, André V, Rieger J, Kühnle A. Nano-emulsion formation by emulsion phase inversion. *Colloids Surf Physicochem Eng Asp*. 2004;251(1–3):53-58.
7. Ashrafizadeh SN, Motaee E, Hoshyargar V. Emulsification of heavy crude oil in water by natural surfactants. *J Pet Sci Eng*. 2012;86:137-143.
8. Song D, Zhang W, Gupta RK, Melby EG. Role of operating conditions in determining droplet size and viscosity of tackifier emulsions formed via phase inversion. *AIChE J*. 2011;57(1):96-106.
9. Akay G, Tong L. Preparation of Colloidal Low-Density Polyethylene Latexes by Flow-Induced Phase Inversion Emulsification of Polymer Melt in Water. *Journal of Colloid and Interface Science* 2001;239:342-357.
10. Akay G. Flow-induced phase inversion in the intensive processing of concentrated emulsions. *Chem Eng Sci*. 1998;53(2):203-223.
11. Akay G, Tong L. Polymer dispersion preparation by flow induced phase inversion emulsification Part 1 The effect of silica on emulsification and dispersion characteristics. *Journal of Material Scinece*. 2000;5:3699-3709.
12. Abe K, Tsuruoka M, Kiriyama S, Nakamori K, inventors; Mitsubishi Petrochemical Company, assignee. Aqueous dispersion of olefin resins and continuous process for preparing thereof. US432004 1982.

13. Chung JT, Cheng CM, Malachowski SM, Godshall ED, Pearson JL, inventors; Xerox Corporation, assignee. Method of continuously forming an aqueous colorant dispersion using a screw extruder. US9052625 B2 2015.

14. Zhou K, Qiu SS, Moffat KA, Sacripante GG, inventors; Xerox Corporation, assignee. Solvent-free phase inversion process for producing resin emulsions. US20090208864 A1 2009.

15. Warner GL, Leng DE, inventors; Dow Chemical Company, assignee. Continuous process for preparing aqueous polymer microsuspensions. US 4123403 A 1978.

16. Han C, Ran X, Su X, Zhang K, Liu N, Dong L. Effect of peroxide crosslinking on thermal and mechanical properties of poly(ε-caprolactone). *Polym Int*. 2007;56(5):593-600.

17. Neubauer AC, Dunchus NW, inventors; Union Carbide Chemicals and Plastics Technology, assignee. Extruder Screw. US9278473 B2. 2016.

18. Goger A, Thompson MR, Pawlak JL, Lawton DJW. In situ rheological measurement of an aqueous polyester dispersion during emulsification. *Ind Eng Chem Res*. 2015;54(21):5820-5829.

19. Spyros A. Quantitative determination of the distribution of free hydroxylic and carboxylic groups in unsaturated polyester and alkyd resins by 31P-NMR spectroscopy. *J Appl Polym Sci*. 2002;83(8):1635-1642.

20. Lawton DJW, Thompson MR, Faucher S. Morphological Development of Latex Particles in a Solvent-Free Extrusion Process. *Society of Plastics Engineers (ANTEC)*. 2014;1169-1174.

21. Veenstra H, Van Dam J, Posthuma De Boer A. On the coarsening of co-continuous morphologies in polymer blends: Effect of interfacial tension, viscosity and physical cross-links. *Polymer*. 2000;41(8):3037-3045.

22. Salager JL, Lopéz-Castellanos G, Miaña-Pérez M. Surfactant-Oil-Water Systems Near the Affinity Inversion: Part Vi: Emulsions Hith Viscous Hydrocarbons. *J Dispers Sci Technol*. 1990;11(4):397-407.

Chapter 6 Conclusion Remarks

This thesis has focused on devising a mechanistic explanation of solvent-free extrusion emulsification (SFEE) which is used to create submicron polymer particles. The measurement of inline rheological behaviour has served as an invaluable tool to understand the mixed state of the multi-phase (polymer-water-surface active agent) system. The effects of chemical compositions and TSE mechanical design on SFEE process mechanism are explained. The overall objectives stated in this work have been achieved.

6.1. Key Findings and Contributions

Specific conclusions arising from this research are summarized below.

1. A new inline rheological measurement technique was developed with the validation by 3D numerical software OpenFOAM, as well as conventional parallel plate and capillary rheometers. It has been shown that this dynamic technique can be used to detect transient rheological events, which are considered to be related to the state of water dispersion in a polyester matrix.
2. Changes in the SFEE process related to matrix molecular weight and the content of a surface active modifier were separated in the study to understand which factor had a greater effect on water dispersion in the polyester matrix. Typically matrix molecular weight and surface active modifier content change simultaneously in the SFEE process and create a challenging system to control. Polar surface energy

contributions were found to be most important but the relevance of lower viscosity implies that some chain degradation in the actual SFEE process is beneficial.

3. With the presented chemistry, it was shown that a transient rheological behaviour observed upon commencing water addition was a strong indicator of the striated lamella morphology to be developed by SFEE. This finding was related to lamellae coarsening, where lamellae thickness generated in the dispersion region predicts the final particle size after inversion. In order to obtain thinner lamellae, the inclusion of a surfactant during mixing was favoured versus solely depending on endgroup conversion to salt groups to rapidly lower the interfacial tension between the polyester and water.
4. When solely reliant upon polymer endgroups to favour interfacial growth between the polymer and water phases, the results showed that the method of NaOH addition significantly affected lamellae thickness. The addition of solid NaOH becomes a rate-limiting step to morphology development because dissolution is comparable in timescale to the mixing time of the dispersion zone.
5. In the absence of SDBS, the ionic strength of the system will notably affect the process. This can be described as a caging effect that impedes dissociation of the functional group, raising the interfacial energy while lowering the activation energy to agglomeration of the striated lamellae.
6. It is reported that sub-micron particles cannot be created in the absence of surfactant (i.e. SDBS).

7. Increasing the polyester viscosity by molecular modification resulted in slower coarsening kinetics ($\Delta\eta/\Delta t$) and lower water dispersion degree (λ) for the striated-lamella structure of polyester-water mixture produced larger mean particle diameter (D_{50}) especially with the inclusion of SDBS.
8. A longer mixing time in the dispersion zone of SFEE allows thinner lamella morphology capable of developing the emulsification sought in preparation of smaller particle in the following dilution zone of SFEE.

6.2. Future Works

In order to provide more mechanistic explanations related to SFEE process, further experimental studies should be carried out. This work should focus on the process behaviour at the inversion zone of SFEE after the second water addition. The coalescence ad aggregation phenomenon should be evaluated in the SFEE process.

A two-phase numerical model is recommended to investigate the contributions of mechanical/chemical mechanisms for lamellae growth in the dispersion zone of SFEE and later a particle-fluid model to study the dynamics of the process during the cooling of particles in the dilution zone. This model can incorporate interfacial tuning to accommodate different surfactant/polymer scenarios inside the extruder.

It is believed that studying different ratios of different surfactant types (i.e. anionic, non-ionic) could be very beneficial in order to optimize the amount of surfactant needed to create submicron polymer particles.

Finally, developing aqueous dispersions from different polymers which represent a more sustainable feedstock, such as recycled polyester from bottle reclaim, as well as bioplastics like polylactic acid would be interesting.